ARCHIVES OF ACOUSTICS
21, 3, 227–229 (1996)

THE CONFERENCE NOISE CONTROL 95

Foreword

The 10th International Conference on Protection Against Noise NOISE CONTROL 95 was held in Warsaw on June, 20–22nd, 1995. The conference was arranged by the Acoustic Committee of the Polish Academy of Sciences, the Polish Acoustic Society and the Central Institute for Labour Protection by co-operation with the Department of Mechanics and Vibroacoustics of the Academy of Mining and Metallurgy and the Department of Acoustics of the Building Research Institute in Warsaw.

The conference was patronized by

— the vice-Premier and the Chairman of the State Committee for Scientific Research (KBN)

— the Minister of Labour and Social Policy

— the Minister of Space Economy and Building Industry

— the Minister of Environment Protection, Natural Resources and Forestry

— the Minister of Industry and Trade

The guiding subject of the NOISE CONTROL 95 conference was

Noise as a threat to the civilization

The conference NOISE CONTROL was held for the tenth time in Poland. It has been organized for several dozen years in Warsaw and Kraków, beeing inititated for the most part by Professor Stefan Czarnecki who died in 1982. It should be emphasized that the NOISE CONTROL conferences belong to those organized in Poland that are permanently indicated in the international diary of scientific congresses and conferences. It was not mere chance that the Central Institute for Labour Protection was chosen as the right location for the present conference. In that institution, that has a 45 years old tradition, there has been from the very beginning the Department of Acoustics. Nowadays, the Department of Acoustics of the Central Institute for Labour Protection is a centre dealing with the problems of protection against noise and vibrations, mainly in the labour environment, that has found approval not only in Poland, but also world-wide. Here, at the Institute for Labour Protection, worked Professor Czesław Puzyna who, in co-operation with Professor

Stefan Czarnecki, was a precoursor in developing modern methods of limiting noise in Poland.

159 participants from Poland nad 9 other countries took part in the conference. The following planary lectures were given:

1. I. Malecki, Z. Engel, A. Lipowczan, J. Sadowski
   Problems of Noise Control in Poland in the Way to European Integration
2. D. Augustyńska
   European Directives and Standards for Vibroacoustic Protection
3. A. Cops
   Sound Intensity: State-of-the Art in Noise Control of Buildings
4. K. Kido
   Active Control or Passive Control?
5. A. Rakowski
   Noise as Music

Beside the plenary session, there were 11 other sessions, including a poster one, in those 55 papers were presented; the topics were divided into 5 groups:

1. Fundamental Problems	17 contributions
2. Noise in Industry	16 contributions
3. Noise in the Environment	6 contributions
4. Measurements and Analysis	10 contributions
5. Active Methods	6 contributions

Poster sessions are a tradition of the polish conferences on protection against noise. In the plenary session, a few minutes were given to each author of a poster for the introduction in the problems of its paper. The large interest for the poster session, as well as the long discussions in front of the posters, justify the arrangement of those sessions.

During the conference, there was also a round-table session devoted to the laws of protection against noise. Special attention was paid to the imperfection of polish regulations concerning the protection against noise and vibrations. The law on environment protection from 1980 and the corresponding executory regulations, in those many errors have been indicated, were judged with particular criticism. The idea of a special law on the protection against noise was recalled. An appropriate project already exists. The lack of reliable regulations makes the estimation of the threat for the environment by noise, e.g. by aviation noise, difficult. The participants formulated a number of demands that, after a thorough analysis by the Acoustic Committee of the Polish Academy of Sciences, will be handed over to the authorities.

A valuable supplement to the conference was the exhibition of measuring equipment and materials, sound absorbing fabrications and structures.

In the conference conclusions, the usefulness of those meetings was emphasized. The noise in the humans life and labour environment is a public imminence that brings about undesired social and economic consequences. The first ones consist in the fact that milions of people in Poland are exposed to noise of the level A exceeding 60 dB; the health effects are obviously negative, the hearing ability becomes

irreversibly reduced, the risk of traffic and industrial accidents increase. The negative economic consequences is the lowered working capacity, increasing number of sick-leaves, the accelerated waste of machines and equipment and a hindrance in the export of the latters because the international standards are not met.

The noise threat is typified by a multitude of sources and by some univesality, expecially in large cities and in the industry. The most arduous sources of noise are communication routs and objects; this is of particular importance at the beginning of new superhighway- and national road-buildings, as well as in the modernization of airports.

In this issue of the Archives of Acoustics, there are published a few papers presented at the conference NOISE CONTROL 95.

Z. Engel

ARCHIVES OF ACOUSTICS
21, 3, 231–254 (1996)

SOUND INTENSITY: STATE-OF-THE ART IN NOISE CONTROL OF BUILDINGS

A. COPS

Laboratory for Acoustics and Thermal Physics, Department of Physics,
Katholieke Universiteit Leuven, Celestijnenlaan 200D, B-3001 Leuven-Heverlee, Belgium

This paper summarizes the progress that has been made in the application of sound intensity techniques related to the research of sound transmission loss in building acoustics. The modern development of sound intensity instruments began with the discovery of the fast Fourier transform and with the develpoment of techniques for filtering electrical signals using digital techniques. It was only after these techniques became well established, that instruments and procedures for the determination of sound intensity became available for laboratory and in situ measurements. Applications for these instruments and procedures quickly followed and are still pursued today. In this paper some of these developments are discussed, with emphasis on those directly related to sound transmission loss in buildings.

1. Introduction

Trends in developing new room acoustic predictions and design techniques consist in utilizing mathematical modelling and computer calculations. The process requires an extensive knowledge of the acoustic parameters related to the sound field generated from the source side, the propagation path and the sound field at the receiver side. This can be obtained by theoretical modelling, but in many cases it is more significant to obtain this information experimentally and, therefore, precision measurement techniques have become a crucial component of the design and prediction process.

Until recently the only acoustical quantity that could be measured accurately was the sound pressure, and from this, other acoustical quantities could be calculated. The scientific interest to get more accurate information on sound insulation for example by scanning overall surfaces, required that other acoustical quantities needed to be measured. The development of the Fast Fourier Transform analyzer, the introduction and perfection of digital electronic technology and the improvement of acoustic transducers permitted the construction of reliable sound intensity meters and other valuable equipment for laboratory and in situ measurements.

The ability to obtain acoustic power flow from nearfield measurements in receiving rooms, substantially expands our capability to study all details of the sound

radiation from complex building structures, in order to study the details of sound propagation in spaces with complex boundaries and to perfect the measurement of the acoustical properties of structures. Using computational technique, sound field maps of acoustic intensity vectors and waveforms, as well as acoustic holography repesentations, can be obtained.

2. Sound intensity

The sound intensity, its measurements and applications, has been the common factor in one of the most remarkable progresses in acoustical engineering in the last 15 years. This has also been the case in building acoustics research, and that for several reasons.

First the increased availability of computing power together with advanced graphic representation have enabled us to show sound intensity fields. Examples of the flow pattern of the sound power radiated from a violoncello measured by the sound intensity technique and from iso-normal intensity contour distributions in the

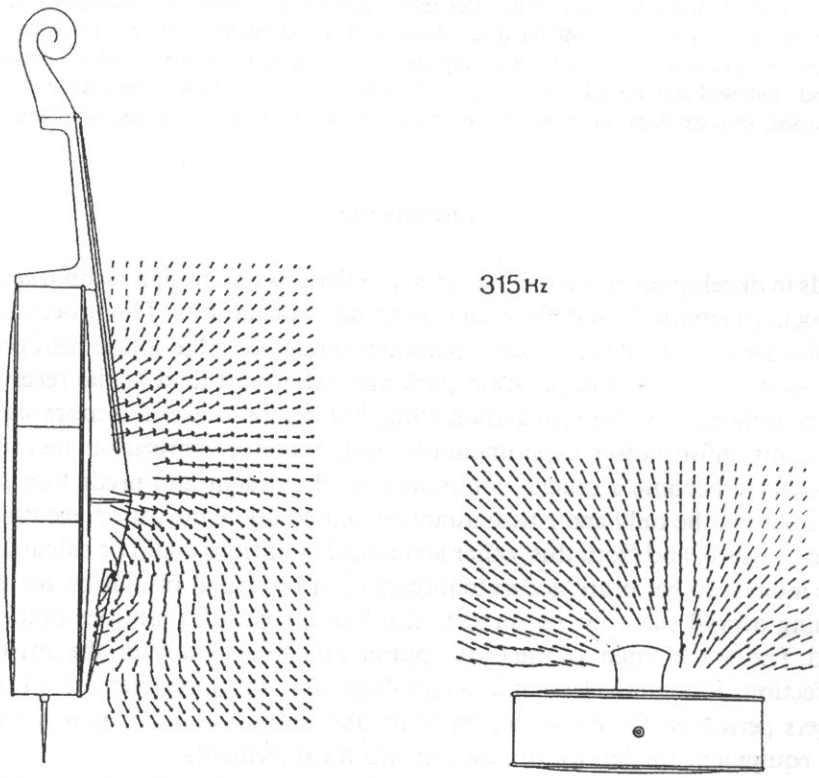

Fig. 1. Flow pattern of the sound power radiated from a violoncello measured by the sound intensity technique [1].

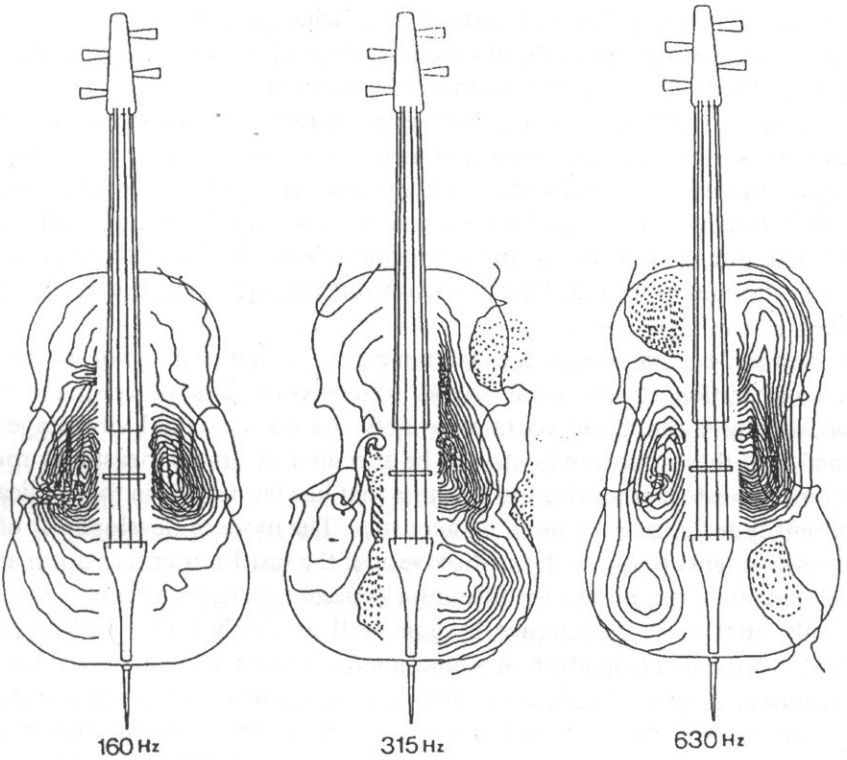

Fig. 2. Iso-normal intensity contour distributions in the field of a violoncello (Full lines: positive, broken lines: negative) [1].

field of a violoncello are given in Fig. 1 and Fig. 2 [1]. This has led to a better understanding of the sound field radiated from constructions such as walls and plates and the reflection from and diffraction around surfaces such as absorbing materials.

Second, the instruments available for the direct measurement of sound intensity have led to new techniques for the determination of the properties of noise reducing elements such as sound transmission loss of structures and impedance characteristics of acoustic materials.

The existing techniques and methods, which are used for standard measurements in acoustic research, were very complicated and required moreover expensive measuring laboratory facilities. The conventionally used sound pressure level measurements did not gave immediately the desired results as the microphone measures the total sound pressure, which can be influenced by the close sound field, multi-direction transmission paths, and directivity sensitiveness or reverberation effects. The sound pressure is a scalar quantity and will give insufficient information about the direction and the size of the sound energy flux of a radiating field. In order to identify sound sources and sound transmission paths, selective enclosures with lead and screens and anechoic rooms were necessary. Measurements of sound transmission loss of building

structures in laboratory facilities require two adjacent perfect diffuse measuring rooms and the measurement of the absorption factor of acoustic materials needs to be done in reverberation rooms and in anechoic chambers.

The advantage of the mesuring technique where the sound intensity vector can be measured is obvious. The sound transmission loss of the most complicated single, multilayered and composed building elements and the ordering transmission ways through building and other structures due to flanking sound transmission, the determination of the sound absorption factor and impedance characteristics of acoustic materials, can be obtained more precisely with the sound intensity technique.

The most self-evident advantage is that a diagnosis can be made of the weak links and its contribution to the total sound transmission loss of complete building constructions by scanning all parts separately. As an incidental advantage can be mentioned that these measurements can be executed in simple measuring rooms.

The purpose is to summarize the progress that has been made in the application of sound intensity techniques to buidling acoustics. The modern development of sound intensity instruments began with the discovery of the fast Fourier transform and with the development of techniques for filtering electrical signals using digital techniques. It was only after these techniques became well established that instruments and procedures for the determination of sound intensity became available for laboratory and field measurements. Applications for these instruments and procedures quickly followed and are still pursued today. In this paper, some of these developments are discussed, with emphasis on those applications directly related to building acoustics. The papers that have appeared in literature are so numerous that it would be impossible to mention them all. Therefore, it has been necessary to be selective in the choice of the presented material. Many of the references are to papers which appeared in International Journals on Acoustics and Noise Control Engineering, in Proceeding of Inter-Noise Congresses, in Proceedings of specialized Symposia on Sound Intensity held at CETIM in Senlis, France [2, 3] and from the book of F. FAHY, titled *Sound intensity* [4].

Widespread use of sound intensity techniques in building acoustics will depend on future standardization. Examples of the importance of standardization include the development of standards for the determination of sound transmission loss properties of building acoustics structures such as walls, floors, ceilings, roofs and facade elements and the determination of sound absorptive properties of acoustical materials, both for normally-incident and oblique and randomly-incident sound waves. It appears that widespread acceptance of methods will only occur after standardization has been done. A first step is the development of instrument standards and standardization techniques for the calibration of instruments. This work is done by IEC-TC 29. Because of widespread interest in the determination of sound absorption and impedance characteristics of acoustic materials, manufacturers of acoustic equipment have already developed the two-micrphone measurement tube equipment, and ISO/TC 43/SC 2 WG 14 is asked to prepare a standard on the two-microphone

method with the tube technique. But up to now no standardization related to the use of a measuring method with the two-microphone technique, at oblique or random sound incidence is under way.

There is also widespread interest in the determination of sound transmission loss of buildings and building elements. At the moment ISO/TC 43/SC 2/WG 18 is revising the different parts of ISO 140. This revision is done in narrow co-operation with CEN/TC 126-"Acoustic properties of building products and buildings". Up to now only in part 5: "Field measurements of airborne sound insulation of facade elements and facades" of ISO/TC 43/SC2/WG 18, the sound intensity measuring technique has been restrained as an informative measuring technique in Annex 2.

Acoustic intensity can be obtained from the sound pressure and particle velocity amplitudes and the phase between the quantities. While sound pressure can be measured directly by small and precise mircophones, there are no suitable transducers to directly measure particle velocity. Because particle velocity is proportional to the pressure gradient, one type of intensity probe approximates the pressure gradient by pressure difference obtained from two closely spaced mircophones (p-p probe). Another probe type (p-u probe) is based on Doppler shift caused by modulating a high frequency ultrasonic wave by the measured acoustic wave. The techniques for the determination of sound intensity are not without errors. A discussion of factors which affect the accuracy of the measurements is beyond the scope of this paper. Some of the papers who discussed problems related to accuracy are listed in references [5 to 12].

The number of papers on sound intensity measurements and applications in the field of building acoustics has grown very rapidly in the last decade, and it is difficult to summarize them all. Therefore, it seems appropriate to select papers on sound transmission loss only and to present a few of the results with emphasis on practical applications. A lot of research has also been done on absorption and impedance characterization of acoustic materials performed by the two-mircophone technique [13]. The results obtained will not be treated in this paper.

3. Sound Transmission Loss Measurements

Sound transmission loss measurements (STL) are based on measurements of the sound power which incidents on the tested partition and which is radiated from the other side. The transmission loss of structures such as walls, panels, facades, floors and ceilings is usually measured between reverberation rooms. By definition the sound transmission loss of a structure is given by:

$$R = 10 \log(P_1/P_2) \quad \text{(dB)}, \tag{3.1}$$

where P_1 and P_2 are the incident and transmitted sound powers. A proportion of the sound power which enters the structure may be transmitted to, and radiated by the adjoining structures, this process is called "flanking transmission". The source room

is supposed to create a diffuse sound field so that the direction of the waves incident on the measured partition would be distributed uniformly. For the determination of the incident sound power, the intensity method is identical to the classic two-room method and P_i is determined by the sound pressure measurement in the diffuse field of the source room. In standard form the incident sound power is based on:

$$P_1=(p_1^2/4\rho_0 c)S \tag{3.2}$$

with p_1 the sound pressure in the source room, ρ_0 the static density of air, c the velocity of sound in air and S the structure surface. The transmitted sound power for the classic two-room method is determined from the sound pressure in the diffuse receiving room based on the relationship:

$$P_2=(p_2^2/4\rho_0 c)A_2, \tag{3.3}$$

where A_2 is the equivalent sound absorption in the receiving room and p_2 the sound pressure in the receiving room. Substitution of equations (3.2) and (3.3) into equation (3.1) and conversion to the decibel scale yields the standardized formulation for the two-room method (ISO 140-3):

$$R=L_{p1}-\mathrm{L}_{p2}+10\log(S/A_2) \qquad \text{(dB)} \tag{3.4}$$

where L_{p1} and L_{p2} are the time and space-averaged sound pressure levels in the source and receiving room.

For the intensity method the transmitted power is determined from the surface averaged sound intensity I_2 as:

$$P_2=I_2 S \tag{3.5}$$

Substituting equations (3.2) and (3.5) into equation (3.1) yields the formulation for the intensity method:

$$R_1=L_{p1}-L_{I2}-6 \qquad \text{(dB)} \tag{3.6}$$

where L_{p1} is the spacial average of the sound pressure level in the source room, and L_{I2} is the averaged normal intensity level measurement on the enveloping surface. The standard formula albeit adequate for general-purpose applications, does not give full account of all the factors which may affect the test results, such as the influence of boundary interference fields near the radiating structure, the composition of the structure, and calibration and absorption errors. The calibration and absorption errros are treated more elaborate elesewhere [14, 15, 16, 17, 18].

The standard procedure for estimating energy density in reverberation rooms involves spatial averaging of the sound pressure level in the central part of the room. WATERHOUSE [19] pointed out that in reverberation rooms there is an increase in energy density at the boundaries. Thus estimates of the total room sound energy based on measurements of the sound pressure level in the central portion of

reverberant rooms will be too low with the result that the sound reduction indices obtained by the intensity method will be underestimated. This phenomenon which is particularly significant at low frequencies is believed to be at least partly responsible for the small, though consistent, discrepancies between intensity and conventional two-room method results which have been published [15, 20, 21, 22, 23, 24, 25].

Taking into account the Waterhouse correction, the extended formulation of the STL is:

$$R_1 = L_{p1} - L_{I2} - 6 + 10 \log (1 + \lambda S_1 / 8 V_1) \qquad \text{(dB)} \tag{3.7}$$

where λ is the wavelength, and S_1 and V_1 are the internal surface area and the volume of the source room, respectively. The Waterhouse correction is only applicable at low frequencies. For a room with volume 100 m³ the correction is 0.5 dB at 500 Hz, 1.0 dB at 200 Hz, 2 dB at 100 Hz and 3 dB at 50 Hz.

In practice, the assumption of equal measurement and test object surface area is justified only in the case of short distance measurements with the intensity probe in relation to the radiating structure, as is shown in Fig. 3, where is presented a vertical section of the sound tranmission rooms together with the used measuring equipment. The transmitted sound intensity distribution is normally measured on a surface parallel to the partition. Measurements on the peripherical faces of the enclosing surface must not be neglected: a significant proportion of the transmitted power may be transported through these faces, especially at frequencies in the neighbourhood of the critical frequency of the panel structure. Some systematic investigations have been made on the influence of measuring distance and sample point density on the accuracy of estimated loss, for example by MINTEN, COPS and WIJNANTS [16] and GUY and DE MEY [26]. In the case the measurement surface S_m, completely enveloping the test object is larger than the object surface S, the sound transmission loss can be inferred by the formulation:

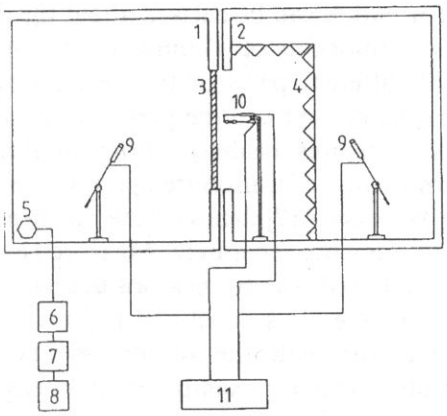

Fig. 3. Laboratory facility to measure the STL of test structures. *1.* Transmitting room, *2.* Receiving room, *3.* Structure, *4.* Absorbing material, *5.* Loudspeaker system, *6.* Amplifier, *7.* Filter, *8.* White noise geneator, *9.* Microphones, *10.* Sound intensity probe, *11.* Sound intensity analyser [23, 30].

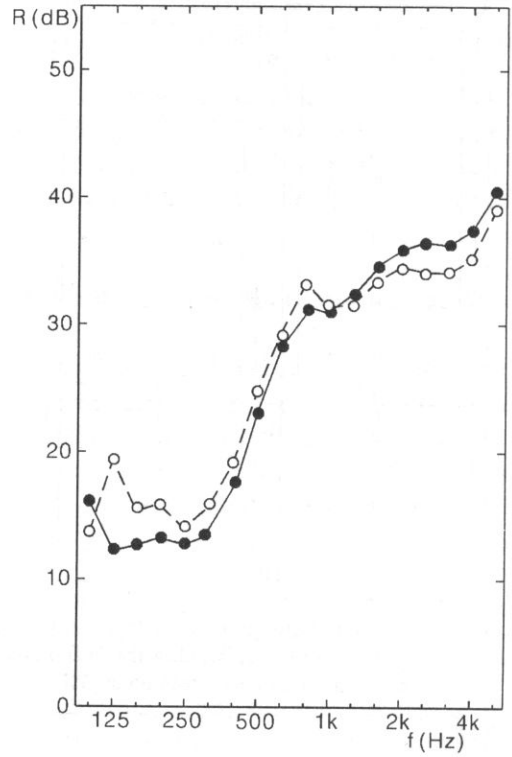

Fig. 6. STL of the complete facade element determined following both measuring techniques. ●——● Intensity method; ○ – – – ○ Conventional method.

together with the results of the overall facade element, are given in Fig. 5. The weakest point in the facade, namely the ventilation clearly shows the lowest results. Figure 6 shows a comparison of the measuring results of the STL of the complete facade element according to the conventional method and the intensity method. The agreement is very satisfying over the whole frequency range.

4.2. Visualization of sound intensity and design

An example of the distribution of sound intensity over a window at 250 Hz and 2 KHz and published by TACHIBANA [31] is given in Fig. 7. In this measurement, the sound was located inside the room and the sound intensity normal to the window was measured outside, at a lot of discrete points. The sound power uniformly transmits through the window at low frequencies, as shown in (a): 250 Hz, whereas sound power transmits dominantly through the edge parts of the window in the case of high frequencies as shown in (b): 2 kHz. GERRETSEN [32] investigated the influence of window frames, the dimensions of window panes and the position of ventilation openings on the STL.

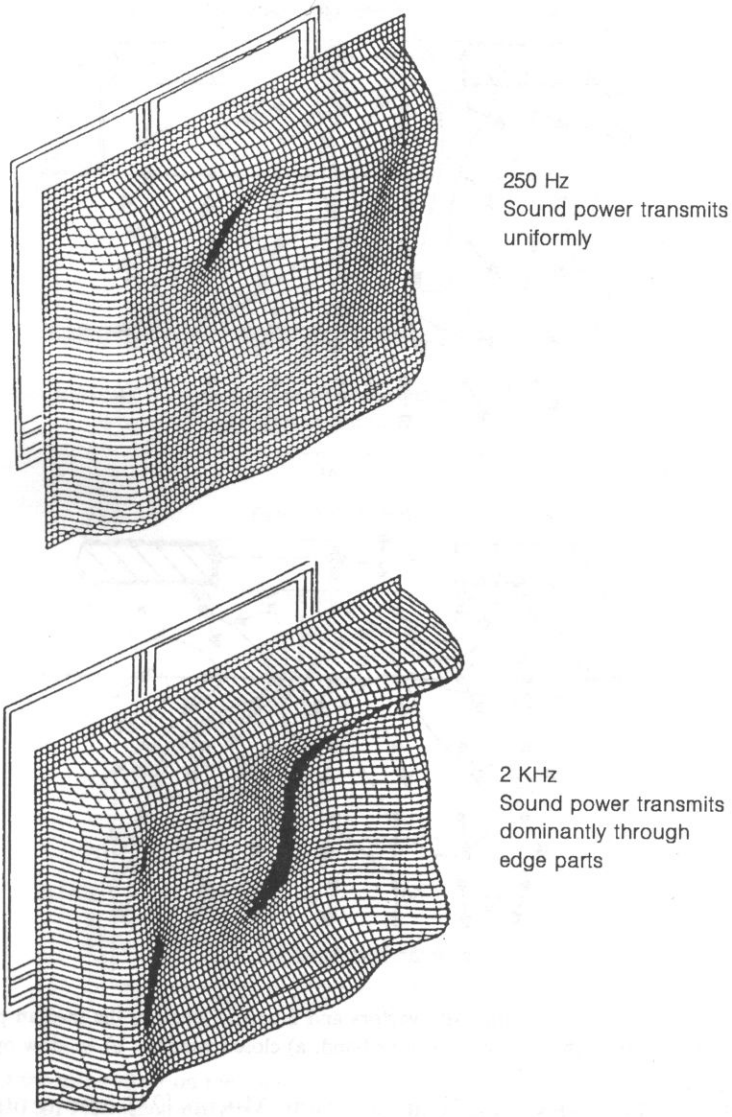

Fig. 7. Sound intensity transmission through a window: a) 250 Hz octave band; b) 2 kHz octave band [31].

Among the many applications of sound intensity measurements to determine the sound properties of building structures are a number which address specific aspects of design, operation and installation. The effects of window opening were investigated by MIGNERON and ASSELINEAU [28] and examples of the sound intensity field are shown in Fig. 8. GUY and DE MEY [26] investigated the effect of absorbent aperture surfaces in the measuring opening on the STL of glazing. They observed significant increases in STL, and concluded the mechanism was not the reduction of sound power radiated by the partition but the subsequent absorption by the reveal.

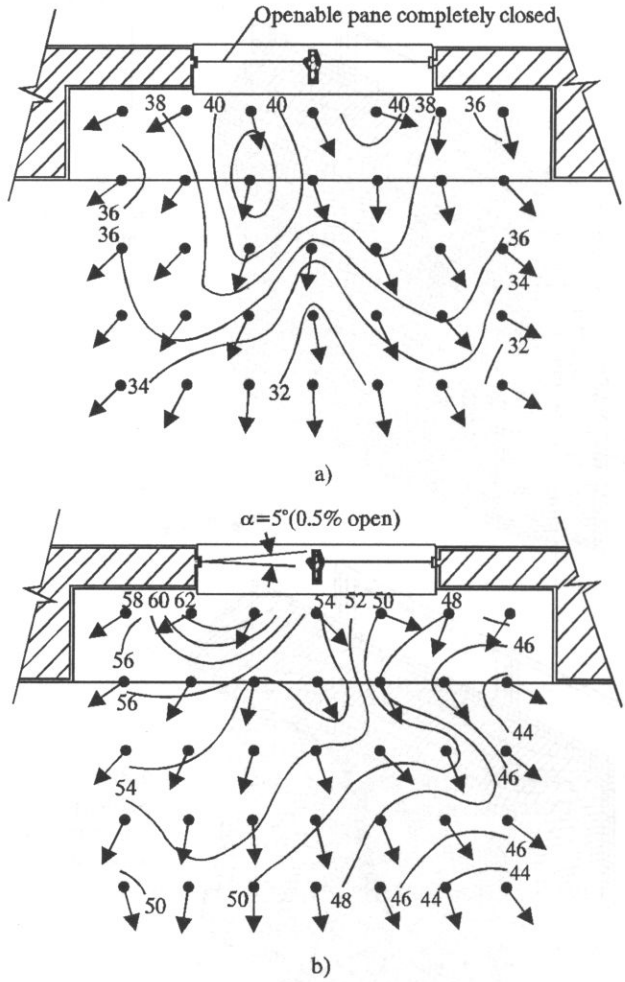

Fig. 8. Distribution of the mean intensity vectors and intensity levels in the median plane of a window transmitting noise in the 1 kHz 1/3 octave band: a) closed window; b) window opened 5° [27].

HALLIWELL and WARNOCK [24] and COPS and MINTEN [23], among others, have used the intensity method to investigate the influence on the STL of the placement of partitions within the thickness of an aperture between two reverberation rooms — the so called "niche effect". Figure 9 shows a vertical section of a two-room measurement facility with an extremely (I) and a centrally placed partition within the niche opening. Figure 10 shows the influence of the niche effect on the STL measurement results obtained with the sound intensity method for a laminated glass panel, together with the standard deviation on the measurement results. COPS, MINTEN and MYNCKE [30] investigated other design parameters such as the influence on the STL of the room volumes, the dimensions and the depth of the opening, the influence of diffusors, loudspeakers and microphones.

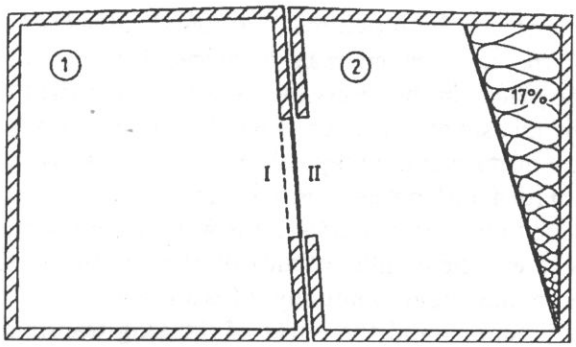

Fig. 9. Horizontal cross section of a two-room measurement facility in order to measure the influence of the niche effect on the sound transmission loss [23].

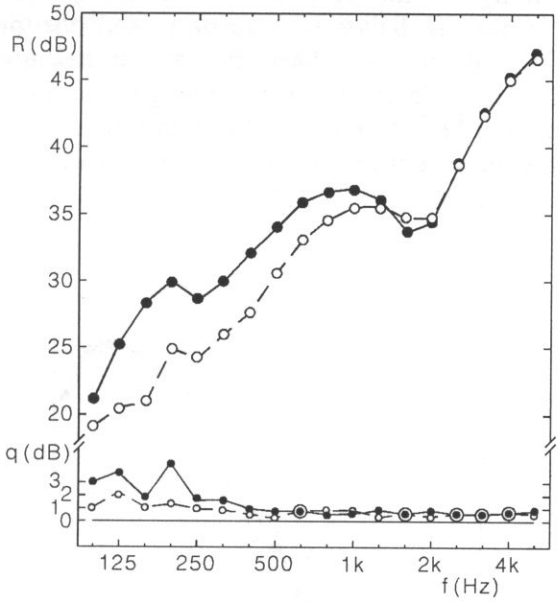

Fig. 10. Influence of the niche effect on the sound transmission loss measurement results for a laminated glass panel [23]. Placement: extremely (●——●); Placement: centrally (○ – – – ○).

4.3. Flanking transmission

Many investigations have been performed on the influence on the STL of flanking effects as well in laboratory facilities as in practice [14, 30, 33, 34, 35, 36, 37]. While carrying out these investigations it was found that problems could arise when attempting to measure the mean intensity from the weakly radiating surface. The instrumentation is not suitable for the use in sound fields where the pressure-intensity index is greater than 13 dB. In practice this may mean that sound intensity from

a separating wall/floor can be measured but sound intensity measurements from a flanking wall in the same room may be unreliable. For this reason acoustic absorbent should be placed in the receiving room to reduce the P-I index as much as possible. Even if the measured P-I index is within the limitations of the instrument, calculated mean intensity values may be misleading if the individual intensity measurements fluctuate a lot between positive and negative values which can happen at low frequencies due to vibration modes in the wall. If there is much variation in the individual intensity levels, the number of measurement positions should be increased to avoid errors due to inadequate sampling. Measurements have been performed on different wall/floor junctions and the effect of flanking transmission on the sound insulation of a timber floor as well as the flanking sound transmission within facade structures. In all these investigations the technique identified the most important sound paths. Disadvantages of the technique are that it requires large quantities of acoustic absorbent, which is bulky to transport, and the procedure is fairly time-consuming which can be a problem in field investigations when time is frequently very limited. At least this technique gives a lot of supplementary information which can not be obtained with the conventional standardized method. In order to prove this, measurements performed on a plastered heavy stone wall,

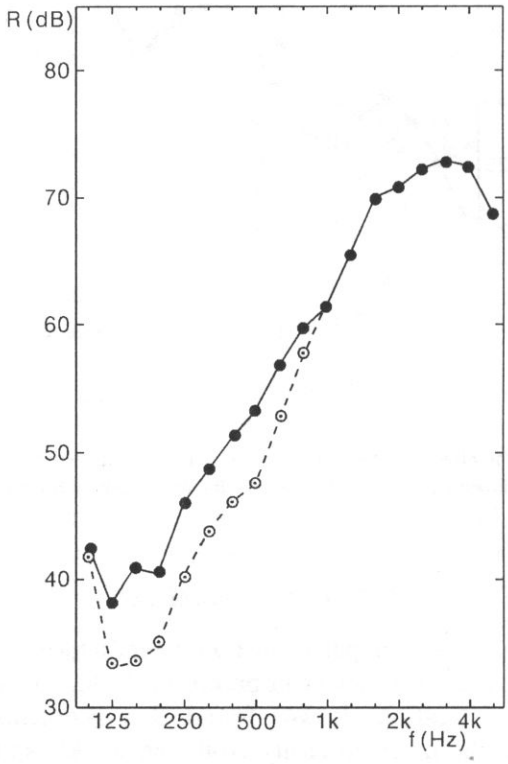

Fig. 11. STL of the plastered heavy stone wall measured with the sound intensity technique. ●——● room 2 to 1 (without correction); ○ – – – ○ room 2 to 1 (with correction).

nearly of the same thickness as the surrounding room walls, and measured in the laboratory facility (Fig. 9) are discussed [30]. The plastered heavy wall, with high sound insulation was fixed in room 1, and measurements with the sound intensity technique where performed in both direction from room 1 to 2 and vice versa in order to observe eventual flanking effects. During the measurements of the STL from room 1 to 2 the radiated sound intensity was determined by scanning the wall in the receiving room. During the measurements of the sound transmission loss in the opposite direction from room 2 to 1, the wall in the receiving room was scanned as well as the flanking walls.

In Fig. 11 the STL results as a function of frequency are shown according to the measurement direction 2 to 1. The full curve shows the results of the STL calculated from the direct radiation of the sound from the wall without any correction for flanking. The dashed curve shows the results taking into account the correction for flanking radiation through the connecting walls. An important flanking transmission occurs at low and medium frequencies. In Fig. 12 the corrected STL according to the measurement direction 2 to 1 is compared with the results in the opposite direction. There is a remarkable good agreement between the STL results.

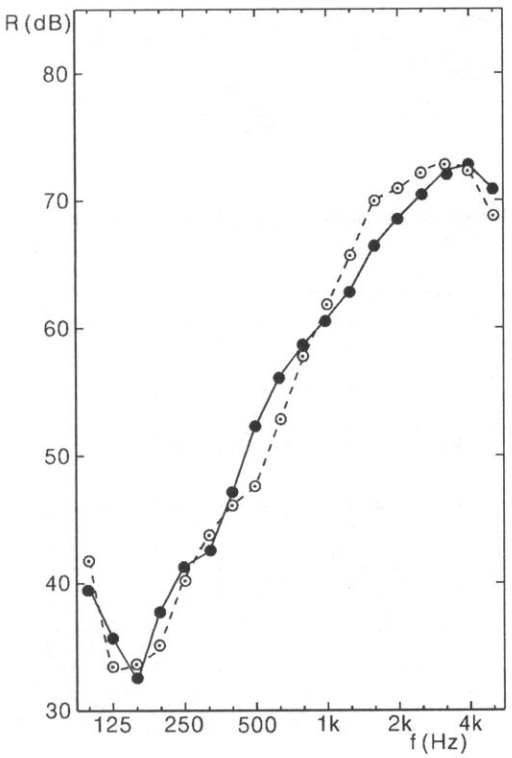

Fig. 12. STL of the plastered heavy stone wall measured with te sound intensity technique in both directions. ●——●: room 1 to 2; ○ – – – ○ room 2 to 1 (with correction for flanking).

4.4. Saddle roof construction

The intensity-based technique has also been successfully applied to the field investigation of the in-situ transmission loss of saddle constructions in Fig. 13 [38]. Measurements are performed on the roof surface and the side facade before and after additional sound insulation elements have been placed, in order to increase the sound insulation against aircarft noise. The different parts were separately scanned and out of this measurements the weak points could be fixed, and improvement of the sound transmission loss could be suggested. Figure 14 shows the STL values obtained with the sound intensity technique for the side facade of the roof construction and clearly presents the weaker points.

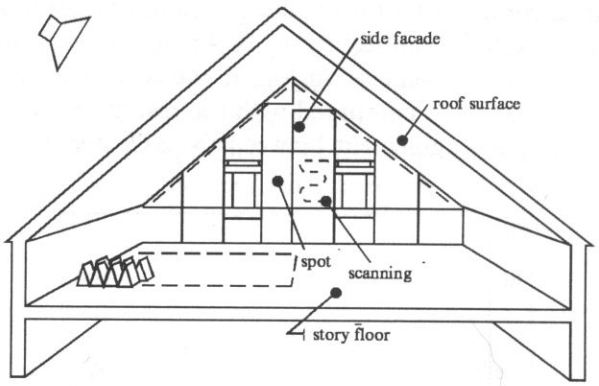

Fig. 13. Detailed drawing of the saddle roof construction [38].

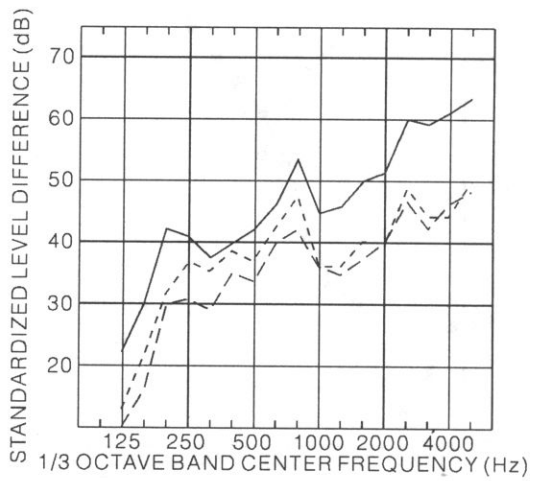

Fig. 14. STL results obtained with the sound intensity technique of the side facade of the saddle roof construction [38]. ——— brickwork; ..... glazing; – – – – – silence box.

4.5. Other applications

The effect of reverberation time in the receiving room, in a laboratory facility, on the STL using sound intensity has been investigated for different reverberant conditions by J. LAI and D. QI [39]. Results indicate that the sound intensity measurements are virtually independent of the reverberant conditons, provided that the pressure-intensity index of the measurements does not exceed the dynamic capability of the measuring system.

J. LAI and M. BURGERS [40] investigated the STL for different field conditions of composite partitions and discussed the importance of the experimental procedure. M. LIM [41] investigated the structural damping of panels by using a sound intensity technique. The panel was mounted at the opening of a box structure or onto a window separating two rooms and was subjected at the opening of a box structure or onto a window separating two rooms and was subjected to an excitation by broad-band white noise. The sound pressure behind the panel, the vibratory velocity of the panel and the radiated sound intensity in front of the panel are used to calculate the panel's structural loss factor.

4.6. Round Robin Test measurements

During a Round Robin Test performed in different Scandinavian laboratories [25, 42] about 30 different measurements have been carried out to estimate the precision of

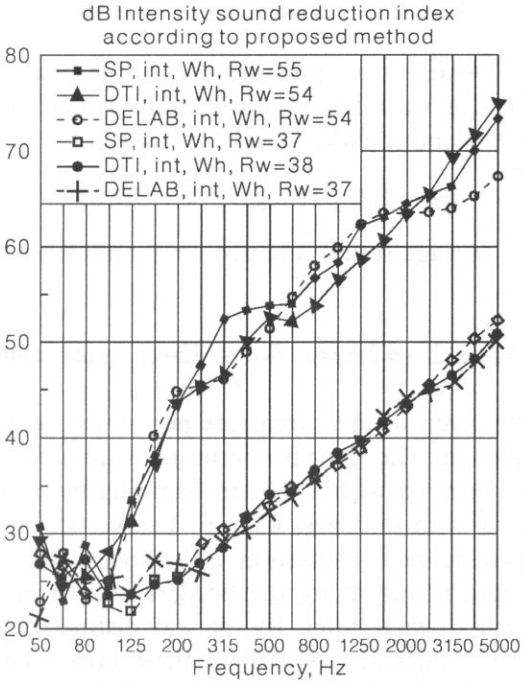

Fig. 15. Intensity sound reduction index of a Scandinavian Round Robin Test for a single metal leaf window (lower curve) and a double metal leaf window (upper curve) [25, 42].

the intensity mehtod when compared with the conventional standardized method. Figure 15 shows the results of intensity sound reduction index for the interlaboratory comparison for a single metal leaf window (lower curve) and a double metal leaf window (upper curve) obtained during the Scandinavian RRT. The results show an excellent agreement. The small differences between the laboratories seem to be the same for the intensity and conventional method.

General conclusions from all the measurements discussed are: the direct measurements of the transmitted sound intensity offers a number of substantial advantages compared to the conventional method: 1. The receiving room does not have to be calibrated for its acoustic absorption, nor is such room actually necessary, 2. The sound power radiated by composite partitions, such as dividing walls between rooms and facades in buildings, may be separately determined, thereby allowing detection and precise quantification of flanking sound transmission; 3. The distribution of transmitted intensity over the surface of the partition may be determined, thereby revealing the presence of weak areas, or leaks.

5. Normalized Impact Sound Level Measurements

The normalized impact sound pressure level L_{pn} is given by:

$$L_{pn} = L_{pm} - 10 \log (A_0/A) \qquad \text{(dB)} \tag{5.1}$$

with L_{pm} the measured average sound pressure level, A the measured absorption in m^2 in the receiving room and A_0 the reference absorption. By agreement A_0 equals 10 m^2. The normalized impact sound intensity level L_{In} is given by:

$$L_{In} = L_{Im} - 10 \log S - 4 \qquad \text{(dB)} \tag{5.2}$$

with L_{lm} the measured average sound intensity level and S the surface of the floor.

6. Normalized Impact Sound Level Applications

An example will be given of measurements performed on a floating floor with dimensions 2.80 m × 2.80 m. The floor is composed of reinforced concrete elements with thickness 0.12 m, covered with a 0.02 m damping material "antison" and an upper floating slab layer with thickness 0.05 m. The vertical section of the floor is presented in Fig. 16. During the construction of the floor a lack of attention has been given to the correct tight fitting along the borders and to the tight fitting of the reinforced concrete parts to each other. By the way distinct leaks of noise could be measured with the sound intensity method at these areas. This was most clearly perceptible from the measurements of the air-borne sound transmission loss measurement but also from the impact sound level measurements.

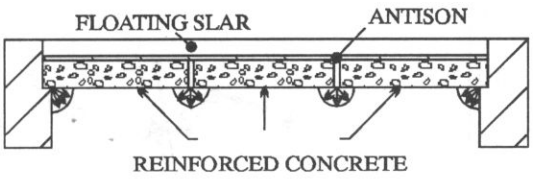

Fig. 16. Vertical section of the floating floor. Dimensions: 2.80 m × 2.80 m
Thickness: Floating slab: 0.05 m; Damping layer antison: 0.02 m; Reinforced concrete: 0.12 m.

Measurements of the sound transmission loss, carried out with the sound intensity method are represented in Fig. 17. Successively the sound transmission loss of the concrete elements of the floor, the leaks at the borders and the leaks between the concrete elements have been scanned and measured. From these measurement data the total sound transmission loss of the floating floor is calculated. The unfavourable influence of the leaks on the total sound transmission of the floor is remarkable. This is clearly shown in Fig. 18, where the sound transmission loss results of the floor were scanned in the same way as before. Almost no difference is observed between the measurement results, as shown in the figure. The total sound transmission loss,

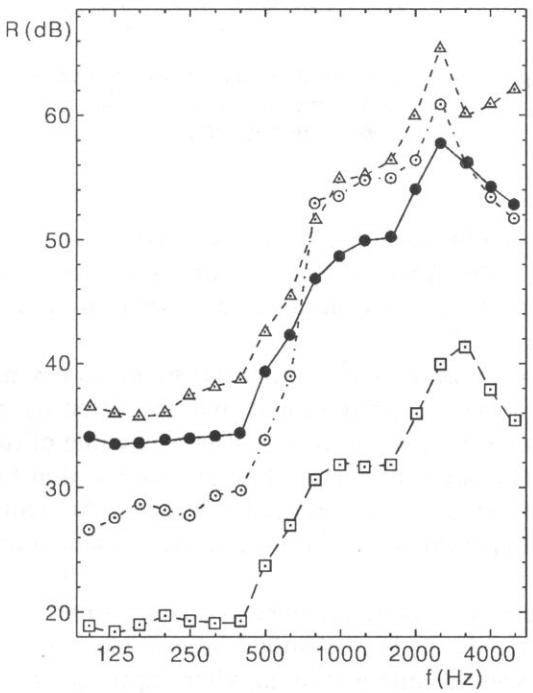

Fig. 17. STL of the floating floor measured with the sound intensity technique. Inaccurate fitting of leaks. □ – – – □: Border leaks; ○ – – – ○ Leaks between concrete elements; △ – – – △ Concrete elements; ●——● Total STL.

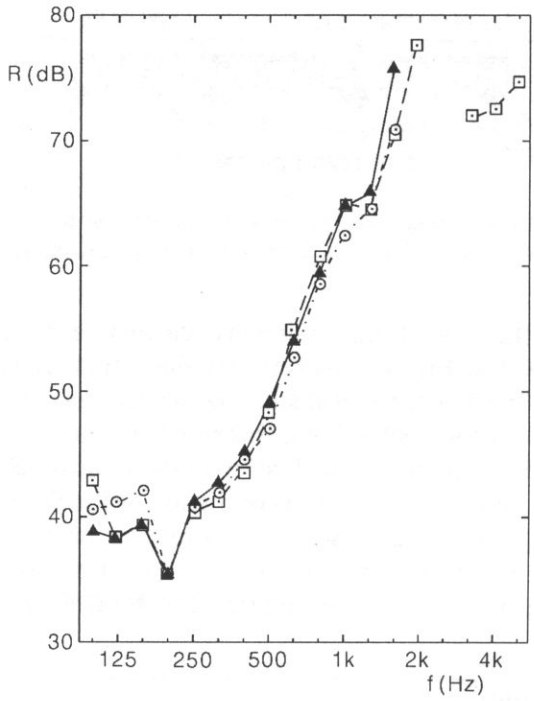

Fig. 18. STL of the floating floor measured with the sound intensity technique, after tight fitting of leaks. □ – – – □: Border leaks; ○ – – – ○ Leaks between concrete elements; △ – – – △ Concrete elements; ●——● Total STL.

compared to the result obtained in Fig. 17, increases strongly over the frequency region of interest. With the tightened floor, at the higher frequencies, due to the high sound insulation of the floor, it was impossible to perform exact measurements with the sound intensity method.

Parallel to the measurements of the sound transmission loss, measurements of the impact sound level with the conventional and the intensity method have been performed. Measurement results before and after tightening of the leaks of the floor and determined with the conventional method are presented in Fig. 19. At the lower frequencies no improvement of the results is obtained. At frequencies higher than 1000 Hz a distinct improvement of the normalized impact sound pressure level is obtained.

In Fig. 20 measurement data, obtained with the sound intensity method, are presented. In this case only the impact sound intensity level of the different parts of the floating floor are scanned and measured, after improvement of the quality of the floor by tightening. From these results the total value of the impact sound intensity level is determined. A comparison of the results, obtained with the conventional and sound intensity technique, is shown in Fig. 21. The agreement is very convincing.

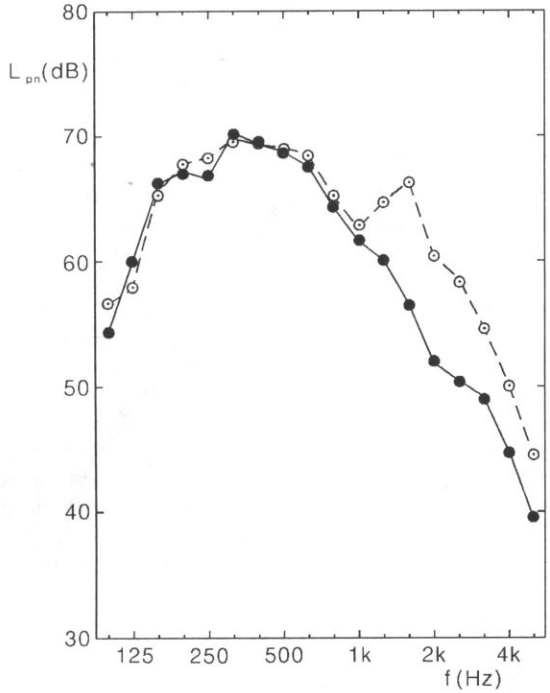

Fig. 19. Normalized impact spind pressure level of the floating floor. ○ – – – – – ○ before tight fitting of leaks; ●———● after tight fitting of leaks.

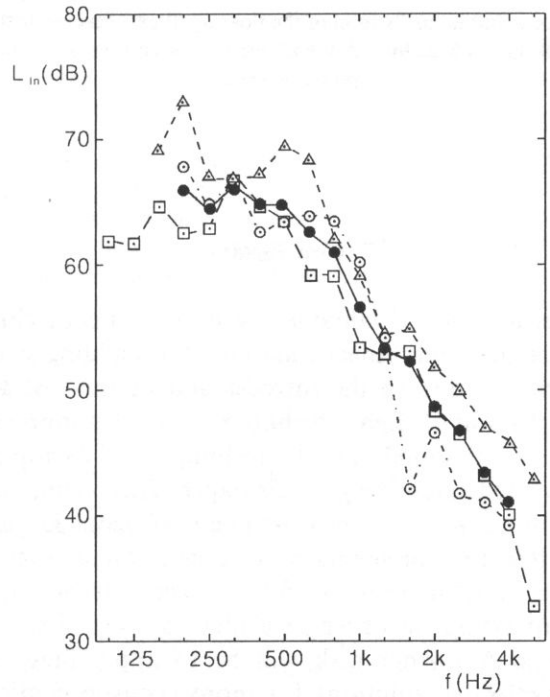

Fig. 20. Normalized impact sound intensity level of the floating floor after tight fitting of the leaks. △ – – – △: center central concrete element; ○ – – – ○ sides central concrete element; □ – – – □ side concrete elements; ●——● Total impact sound intensity level.

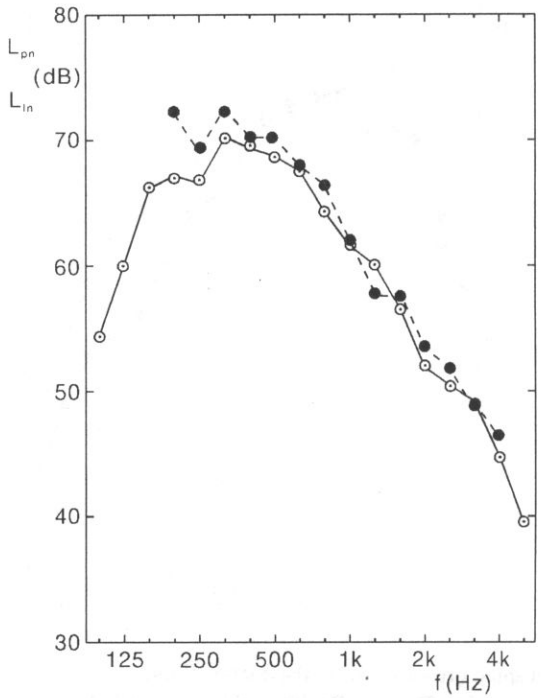

Fig. 21. Normalized impact sound intensity level of the floating floor measured with the conventional and intensity method. ● – – ●: normalized impact sound intensity level; ○——○: normalized impact sound pressure level.

7. Conclusions

During the last decade a lot of valuable new measurement techniques, to perform the sound transmission loss and impact sound level of building structures, have been developed. This is mainly due to the introduction of the fast Fourier transform analyzers and the perfection of digital technology and the improvement of acoustic transducers. One of this, the sound intensity technique and its application to building acoustics, has been treated extensively in this paper. This technique has contributed, in a large sense, to more accurate measurements of acoustic parameters, such as sound transmission loss measurements and impact sound level measurements of complicated building constructions. A future task will be the development of international standardization, in order to achieve a widespread acceptance of the measurement methods. A further task will be to apply these technique for the development of cost-effective solutions for more acoustic comfort in the field of building acoustics.

References

[1] H. TACHIBANA, *Visualization of sound fields by the sound intensity technique* (in Japanese). Proceedings of the Second Symposium on Acoustics Intensity, Tokyo, 117–126, 1987.

[2] CETIM, Proceedings First International Congress on Acoustic Intensity, CETIM, Senlis, France, 1981.

[3] CETIM, Proceedings Second International Congress on Acoustic Intensity, CETIM, Senlis, France, 1985.

[4] F. FAHY, *Sound intensity*, Elsevier Applied Science Publishers, London and New York, 1990.

[5] J.K. THOMPSON and D.R. TREE, *Finite difference approximation errors in acoustic intensity*. J. Sound and Vibr. **75**, 229–238 (1981).

[6] A.F. SEYBERT, *Statistical errors in acoustic intensity measurements*, J. Sound and Vibr., **75**, 519–526 (1981).

[7] S.J. ELLIOTT, *Errors in acoustic intensity measurement*, J. Sound and Vibr., **78**, 439–445 (1981).

[8] G. KRISHNAPPA, Cross-spectral method of measuring acoustic intensity by correcting phase and gain mismatch errors by microphone calibration, J. Acoust. Soc. Am., **69**, 307–310 (1981).

[9] J. TICHY, *Some effect of microphone environment on intensity measurements*, Proc. 1st Int. Con. Acoustic Intensity, 25–30, CETIM, Senlis, France (1981).

[10] J.C. PASCAL and C. CARLES, *Systematic measurement errors with the two-mircophone sound intensity meters*, J. Sound and Vibr., **83**, 53–65 (1982).

[11] M.P. WASER and M.J. CROCKER, *Introduction to the two-microphone method of determining sound intensity*, Noise Con. Eng., J., **22** (3), 76–85 (1984).

[12] F. JACOBSEN, *A simple and effective correction for phase mismatch in intensity probes*, Appl. Acoustics, 33, 165–180 (1991).

[13] A. COPS and W. LAURIKS, *Characterization of sound absorbing materials and in noise control engineering*, Archives of Acoustics, Polish Academy of Sciences, **18** (2), 209–248 (1993).

[14] J. ROLAND, C. MARTIN and M. VILLOT, *Room-to-room transmission. what is really measured by intensity*, Proc. 2nd Int. Con. Sound Intensity, CETIM, Senlis, France, 539–546 (1985).

[15] B. VAN ZYL, P. EERASMUS and F. ANDERSON, *On the formulation of the intensity method for determining sound reduction indices*, Appl. Acoustics, **22**, 213–228 (1987).

[16] M. MINTEN, A. COPS, and F. WIJNANTS, *The sound transmission loss of a single panel measured with the two microphone and the conventional method — comparison with the statistical energy analysis method*, Appl. Acoustics, **22** (4), 281–295 (1987).

[17] A. COPS and F. WIJNANTS, *Laboratory measurements of the sound transmission loss of glass and windows — Sound intensity versus conventional method*, Acoustics Australia, **16** (2), 37–42 (1988).

[18] M. VERCAMMEN, H. MARTIN and W. CORNELISSEN, *Application of the intensity measurement technique to building acoustics and the influence of an absorbing partition wall on the measured intensity*, Appl. Acoustics, 46–62 (1988).

[19] R. WATERHOUSE, *Inteference patterns on reverberant sound field*, J. Ac. Soc. Am., **27**, 247–258 (1955).

[20] J. ROLAND and M. VILLENEUVE, *Intensimetric acoustique, application a la recherche des chemins de transmission du son*, Cahier 1931 du C.S.T.B., Paris, France (1984).

[21] M.J. CROCKER, P. RAJU and B. FORSSEN, *Measurement of transmission loss of panels by the direct determination of the transmitted acoustic intensity*, Noise Con. Eng. J. **17**, 6–11 (1981).

[22] A. COPS, *Acoustic intensity measurements and their application to the sound transmission loss of panels and walls*, Proc. Inter-Noise 83, 567–670 (1983).

[23] A. COPS and M. MINTEN, *Comparative study between the sound intensity measurement and the conventional two-room measurement*, Noise Con. Eng. J. **22**, 104–111 (1984).

[24] R. HALLIWELL and A. WARNOCK, *Sound transmission loss: Comparison of conventional techniques with sound intensity techniques*, J. Ac. Soc. Am., 77, 2094–2103 (1985).

[25] H. JONASSON, *Sound intensity and sound reduction index*, Appl. Acoustics, **40**, 281–293 (1993).

[26] R. GUY and A. DE MEY, *Exploiting the laboratory measurement of sound transmission loss by the sound intensity technique*, Canadian Acoustics, **20**, 219–236 (1985).

[27] H. TACHIBANA, H. YANO and Y. HIDAKA, *The scanning method in sound power and sound insulation measurements by intenstiy technique*, Proc. Inter-Noise 91, Sydney, Australia, 1041–1044 (1991).

[28] J. MIGNERON and M. ASSELINEAU, *Utilisation de l'intensimerie pour l'analyse du comportement d'une façade soumise a l'impact du bruit de la circulation*, Proc. 2nd Int. Con. Acoustic. Intensity, Senlis, France, 477–484 (1985).

[29] M. CROCKER, Z. VALC, *New techniques to measure the transmission loss of partitions using sound intensity and single microphone sound pressure measurements*, Proc. Inter-Noise 90, Gothenburg, Sweden, 103–108 (1990).

[30] A. COPS, M. MINTEN and H. MYNCKE, *The use of intensity techniques in building and room acoustics and noise control*, Proc. FASE Con., Thessaloniki, Greece, 67–84 (1985).

[31] H. TCACHIBANA, H. YANO and Y. HIDAKA, *Vizualization of sound radiation and sound propagation by the sound intensity method.* To be published in Vizualization Soc. of Japan, 1994.

[32] E. GERRETSEN, *Some practical applications of intensity measurements in building acoustics*, Proc. inter-Noise 90, Con., Gothenburg, Sweden, 113–116 (1990).

[33] T. CARMAN, and L. FOTHERGILL, *Application of the sound intensity technique to the measurement of sound transmission loss in buildings*, Proc. Inter-Noise 90, Gothenburg, Sweden, 95–98 (1990).

[34] X. BOHINEUST, P. WAGSTAFF and J. HENRIO, *Investigation to the flanking transmission characteristics of timber frame construction using acoustic intensity measurements*, Proc. 2nd Int. Con. Acoustic Intensity, Senlis, France, 491–494 (1985).

[35] B. VAN ZYL and P. ERASMUS, *Application of sound intensimetry to the determination of sound reduction indices in the presence of flanking transmission*, Proc. 2nd Int. Con. on Acoustic Intensity, Senlis, France, 555–560 (1985).

[36] X. BOHINEUST and P. WAGSTAFF, *Measurement of the effect of different connections on the sound transmission loss of timber frame walls using acoustic intensity*, Proc. Inter-Noise 88 Con., Avignon, France, 139–142 (1988).

[37] Y. HUANG and B. GIBBS, *The measurement of structure-borne sound transmission at plate junctions by an energy intensity method*, Appl. Acoustics, **35**, 47–61 (1992).

[38] B. PUTS and H. CAUBERG, *Determination in situ of the transmission loss of various components of a building facade with the aid of sound intensity measurements*, Proc. 2nd Int. Con. on Acoustic Intensity, Senlis, France, 503–510 (1985).

[39] J. LAI and D. QI, *Sound transmission loss measurements using the sound intensity technique; Part I: The effect of reverberation time*, Appl. Acoustics, **40**, 311–324 (1993).

[40] J. LAI and M. BURGESS, *Application of the sound intensity technique to measurements of field sound transmission loss*, Appl. Acoustics, **34**, 77–82 (1991).

[41] M. LIM, *A sound intensity technique for determining structural damping of a panel exposed to noise*, Appl. Acoustics, **32**, 311–319 (1991).

[42] H. JONASSON, *Measurement of sound reduction index with intensity technique*, Nordtest Project 746-88, Swed. Nat. Testing and Res. Inst., SP Report 23, 1991.

ARCHIVES OF ACOUSTICS
21, 3, 255–266 (1996)

ACTIVE CONTROL OR PASSIVE CONTROL? (OUTLINE OF ACTIVE NOISE CONTROL AND IT'S APPLICATION TO PRACTICAL PROBLEMS)

KEN'ITI KIDO

Chiba Institute of Technology
(Tudanuma 2-17-1, Narashino 275, JAPAN)

This paper overviews the history, the principle and some key technologies of the active noise control and points out that the passive control should be incorporated with the active control to improve the annoyance of noise. That is, the suppression of higher frequency noise by the passive method should be jointly used with the active control. There are feed forward method and feed back method in the active control system, but this paper concerns with the feed forward method only as the stability is important. This paper concentrates the technology using FIR filter, and the renewal algorithm of the coefficients of FIR adaptive filter is shown in unified form. Next, the relation between the arrangement of additional sound source and the reduction of noise radiation is given according to the numerical computation and the control of power transformer noise is briefly explained as a practical example carried out by the author. Finally, the change in A-weighted noise level and the sound quality in hearing by the ANC is discussed.

1. Introduction

The active control of sound and vibration has much progressed in recent years by the progress in digital signal processing technology. Even now, the researches on the active noise and vibration control are very active. Since the first international symposium on the active control of sound and vibration held in Tokyo [1] in 1991, there have been many conferences on the active control. Another symposium "ACTIVE 95" will be held in the beginning of July 1995 in Newport Beach, California, U.S.A. And there are various publications on the active control [2, 3, 4, 5]. There are some industrial products using the active control technology [6, 7]. And someone expects that the active control will grow up to the main technology in the noise control and the conventional passive technology will go out of use.

This paper overviews the short history of the progress of active control and the principal technology of active noise control and discusses the role of active control in the noise control engineering.

2. The outset of active control

The first ideas of active control of sound and vibration concern with the rolling of ships. Thonycroft proposed to move a weight on the deck [8] in 1891 and Motora proposed to steer the side fins [9] for the same purpose. The Motora's method was practically used for a 3.600 ton class big ship in 1922 and this method is now widely used after some improvements [10]. The methods using weight or water in tank are now used not only for the control of ship but also for the supression of the quake of highrise buildings [11, 12, 13]. Some different methods are developed and practically used in which the cabin is supported by the oil pressurized pistons which are controlled to keep the cabin at rest [14]. The similar technologies are used in the vehicles on land [15].

While the proposal of the first idea of the active control of acoustic noise [16] was in 1930's and the first trial [17] of the active noise control was carried out in 1940's. And it was 1960's that the active noise control had become a practical research object of a number of researchers [18, 19, 20].

3. Principle of the active noise control

As described in the previous chapter, the active control of vibration has already been practically used in various field. But the active control of noise is not yet so widely used. One of the most crucial reason is considered to be the frequency range to be controlled. In case of ship rolling or building vibration, the frequency range is usually lower than a few Hz, while the audible frequency range is higher than 20 Hz. Usually, the frequency range of noise to be controlled is between 20 or 100 Hz and 10.000 Hz.

Figure 1 illustrates the principle of active noise control. The noise can be diminished by the superposition of the sound wave having the same wave form. How to make the sound of such the wave form and how to extend the controlled space are the main problems in the active noise control.

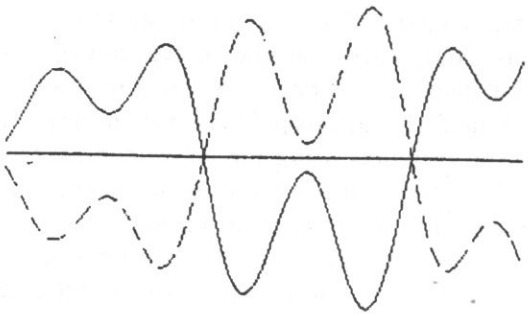

Fig. 1. Conceptual illustration of active noise control by superposing sound of opposite phase on the noise.

In the view point of controlled space, the active noise control is roughly divided into three categories. One of them is to reduce the total noise radiation, anohter one is to reduce noise level of a specified direction and the remaining one is to reduce noise level at a specified space.

The first one can be achieved by setting the additional source very close to the primary noise source if the dimension of the noise source is much smaller than the wave length of the objective noise. The ANC of duct noise belongs to the first category as the cross sectional size of the duct should be smaller than the wave length of the controlled noise. The second one can be achieved even if the size of the noise source is not so small. The author succeeded in the active control of power transformer noise by the directivity synthesis [19]. The third one can be used to reduce the noise level at the ears of a specified person.

In the other view point, the ANC technology can be divided into two categories. The first one is the feed forward method and another one is the feed back method. The signal to drive the additional source, that is called here the control signal, is synthesized using the wave form of primary noise source in the feed forward method as shown in Fig. 2 (a) and is synthesized using the resultant sound in the feed back method as shown in Fig. 2 (b).

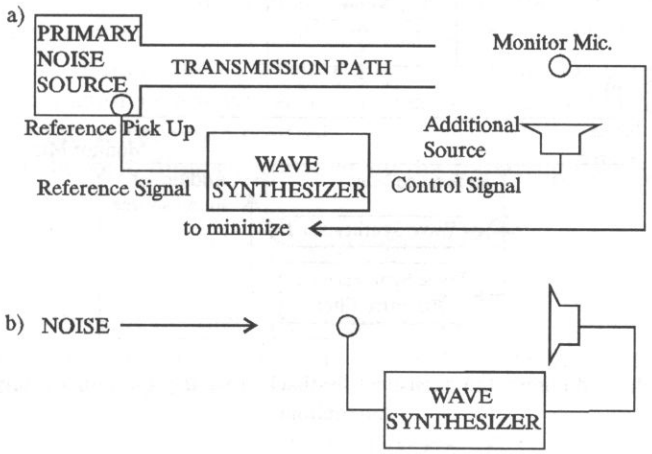

Fig. 2. Block diagram of active noise control system (a) feed forward system (b) feed back system.

It is anticipated that the feed back system can be unstable as there is a closed loop and the feed forward system is stable. But, there can be a closed loop which causes instability of the system even in the feed forward system as long as the sound radiated by the additional source propagates to the reference microphone whose output signal is used to synthesize the control signal.

The wave form coherent to the primary noise source is necessary for the synthesis of the control signal. When the source signal is picked up by the reference microphone set close to the primary noise source to synthesize the control signal, the sound radiated by the additional source propagates to the reference microphone through the

noise transmission path. The acoustic feed back through the additional sound source to the reference microphone is inevitable in such the system.

Some method to diminish the acoustic feed back is proposed. Figure 3 shows two typical methods. The first method uses the difference of the outputs of two microphones set at symmetrical points to the additional sound source to synthesize the control signal and the microphone at the downstream is used as the monitor microphone (error microphone) as shown in Fig. 3 (a). The second method uses an electric circuit (Wave synthesizer 1 in Fig.) which is equivalent to the transfer function from the driving point of the additional sound source to the output terminal of the reference microphone as shown in Fig. 3 (b). The stability of the system is achieved by such the methods.

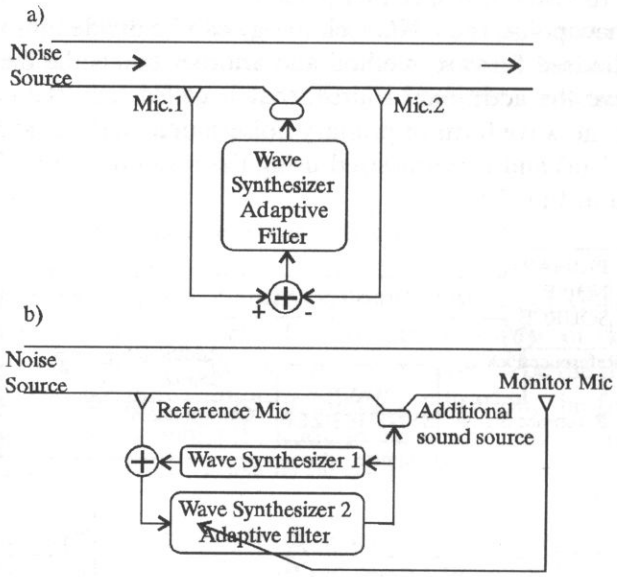

Fig. 3. Two methods to diminish the acoustical feedback from the additional source to the reference microphone.

4. Adaptive control of filter coefficients

An FIR filter is usually used to synthesize the control signal. The schematic diagram of FIR filter is shown in Fig. 4, where the triangles indicate the multiplication with the filter coefficient $w(i)$ and the direction of signal flow. The filter coefficients are adaptively controlled so as to minimize the output of the monitor microphone.

The original noise output transmitted through the noise transmission path is expressed as follows:

$$y(n)=\sum_{i=0}^{N-1} h(i)\cdot x(n-i) \tag{4.1}$$

where $y(n)$ — the output noise at n, $x(n)$ — the source signal at n, $h(n)$ — the impulse response of noise transmission path.

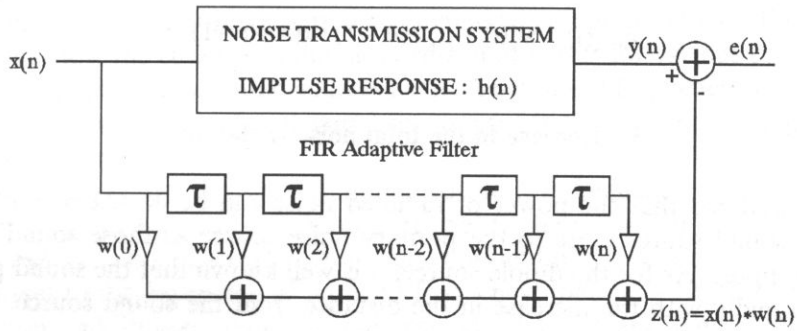

Fig. 4. Active noise control system with FIR filter.

The noise output can be made zero subtracting the output signal $z(n)$ from the output noise $y(n)$, if the coefficients of the filter $w(i)$ are made the same as $h(i)$.

The filter coefficients to synthesize $z(n)$ should be adaptively controlled to minimize $y(n)-z(n)$, because the environment of sound field, the temperature, doors or moving man etc. changes always. And the theory of the system identification is effectively used in the active noise control.

The output of the FIR filter is expressed by the following equation:

$$z(n)=\sum_{i=0}^{N-1} w_n(i)\cdot x(n-i), \tag{4.2}$$

where $w_n(i)$: i-th coefficient of filter after n-th renewal.

The well known renewal algorithm [21, 22] of the filter coefficients is the LMS algorithm shown in the following:

$$w_{n+1}(i)=w_n(i)+\mu\cdot e(n)\cdot x(n-i), \tag{4.3}$$

where, $e(n)=y(n)-z(n)$ — the error signal, μ — the step size parameter.

Some alternatives of the LMS algorithm have been proposed which are expressed by the following equations:

$$w_{n+1}(i)=w_n(i)+\mu\cdot e(n)\cdot \operatorname{sign}[x(n-i)], \tag{4.4}$$

$$w_{n+1}(i)=w_n(i)+v\cdot\mu\cdot e(n)\cdot \operatorname{sign}[x(n-i)], \tag{4.5}$$

$$w_{n+1}(i)=w_n(i)+v\cdot\mu\cdot e(n)\cdot x(n-i)^m\cdot \operatorname{sign}[x(n-i)], \tag{4.6}$$

where,

$v=1$ for $x(n-i)\geqslant$ thershold, $v=0$ for $x(n-i)<$ threshold.

Eq. (4.6) involve Eqs. (4.4) and (4.5) as the special cases.

Using the following delayed LMS algorithms, the computation time can be shortened to 2/3 of the normal LMS algorithm [23].

$$w_{n+1}(i)=w_n(i)+\mu\cdot e(n-1)\cdot x(n-i-1). \tag{4.7}$$

5. Decrease in the total noise radiation

It is considered that the power of radiated noise can be decreased putting the additional sound source close to the primary noise source as those sound sources compose a dipole. As for the dipole source, it is well known that the sound pressure decreases rapidly with the increase in the distance from the sound source. But the

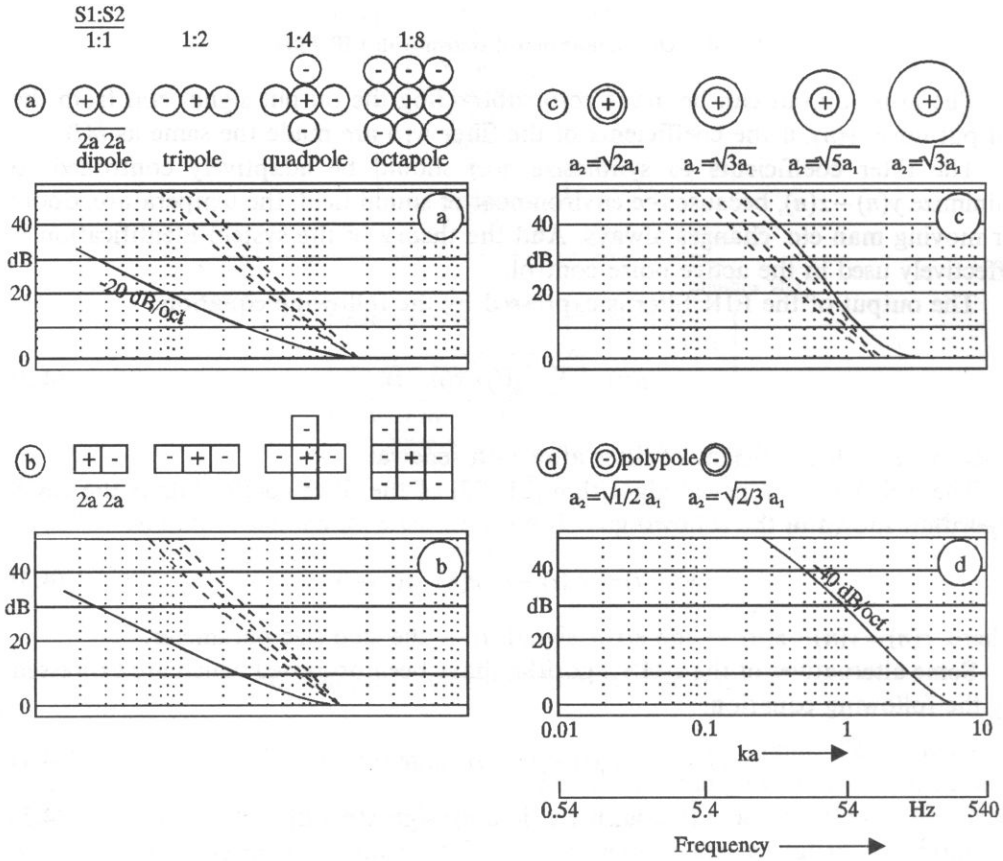

Fig. 5. The attenuation of radiated power by setting additional sound sources for the arrangements shown in the top of each figure, where the volume velocity of the additional sound source (a) is the same as that of the primary source except for the sign.

noise source and the additional sound source can not compose a perfect dipole as the dimension of noise source is not always much smaller than the wave length. The shapes and the arrangement of the primary and additional sources have a big effect on the total noise radiation.

We investigated the effect of the arrangement of primary and additional sound sources on the sound power radiation by numerical computation [24]. Figures 5 (a) through (c) show the changes in the radiated sound power for various combinations of primary and additional sound sources as the functions of frequency. The geometry of the primary and the additional sound source used in the numerical computation is illustrated in each figure.

In all the cases, the decrease is limited to the low frequency range. In the low frequency range, the attenuation is proportional to the reciprocal of frequency, that is, the slope is -6 dB/octave, when only one additional source is used, and is proportional to the reciprocal of squared frequency, that is, -12 dB/octave, when two or more additional sound sources encircle the primary source. The biggest attenuation is achieved when the additional sound source is at the center of the primary source.

An arrangement of additional source shown in Fig. 6 is consisted from those results for duct noise suppression system. Using such the arrangement, the closed loop gain through the additional source to the reference microphone can be neglected.

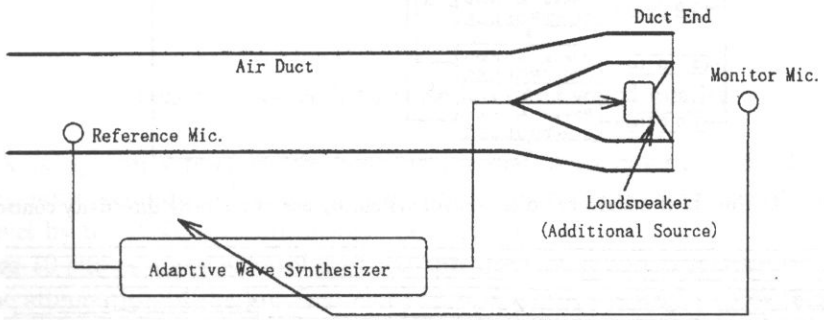

Fig. 6. Schematic diagram of active noise suppression system for duct noise where the additional sound source is set at the center of duct end.

6. Noise reduction by directivity synthesis

We have succeeded the noise control of transformer noise [19, 25] by use of the directivity synthesis. The transformer noise is composed of discrete frequency component and the random component. The former component is caused by the magneto-strictive vibration of iron core and the latter by the cooling fan. The former one is composed of even numbered harmonics of power frequency and stable both in frequency and amplitude. This type of steady sound can be frequently an object of

complaint as it has a special sound quality. The control of directivity pattern by the analogue computers was planned as the sound is very stable.

Figure 7 shows the outline of the system. The directivity pattern is controlled by use of the additional loudspeakers surrounding the power transformer. The loudspeakers are driven by the signals which is synthesized from the wave form of the power line. Therefore, there is no feedback loop in the system and the system is completely stable.

The amplitude and the phase of each frequency component are controlled so as to make the power sum of the output of monitor microphones set on the field minimum by an adaptive controller. The experimental system is composed of three controllers, three microphones and three loudspeakers. The amplitudes and the phases of the frequency components up to 300 Hz are effectively controlled.

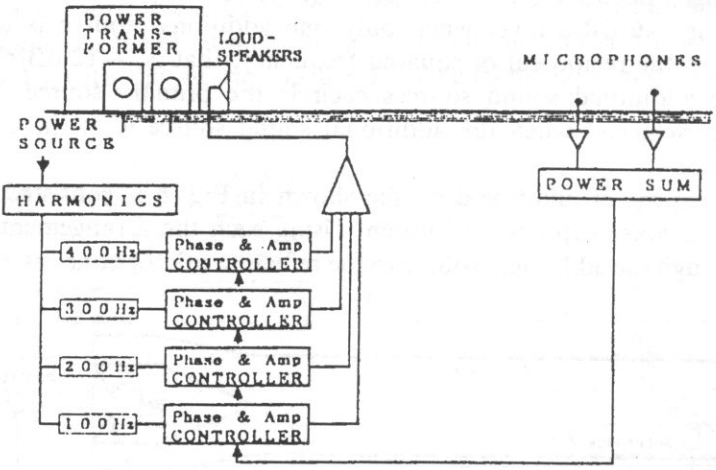

Fig. 7. Outline of transformer noise control system by use of adaptive directivity control.

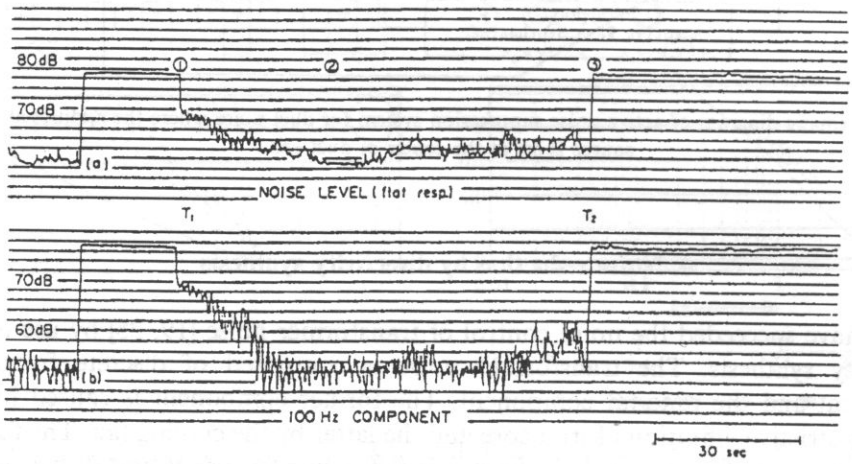

Fig. 8. Transient change in the noise level of the transformer.

Figure 8 shows the transient characteristics of the system. The system reaches the final state in 20 seconds after switch is turned on. The largest attenuation in sound pressure level is observed in 100 Hz component. Figure 9 shows the directive distribution of the sound pressure in 100 Hz component. Figure 9 shows the directive distribution of the sound pressure level on a semicircle of 10 meter radius. Using three monitor microphones, the sound pressure level within 30 degrees decreases more than 10 dB. But the sound pressure increases in some direction. More loudspeakers and monitor microphones will be necessary to decrease sound pressure level in a wider angle. The loudspeaker interval should be less than a quarter wavelength. It may give a practical limitation of the use of this system for the higher frequency range.

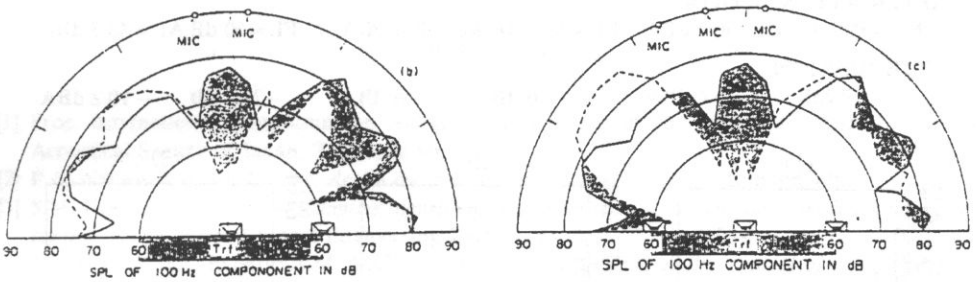

Fig. 9. Changes in the directivity pattern of the transformer by active control.

7. Changes in A-weighted noise level and sound quality

The ANC system suppresses the noise in the low frequency range but the higher frequency noise remains unchanged. Therefore, much decrease in the A-weighted sound level by the ANC can not always be expected.

Figure 10 shows some examples of the spectrum of power transformer noise in which the attenuation of the low frequency components is assumed according to our former experiments. The attenuation assumed here in 100 Hz component is 26 dB, that in 200 Hz component is 16 dB and that in 300 Hz component is 6 dB. Those values are considered to be practically maximum attenuation only by the active control method in the field.

The attenuation of sound pressure level in the flat weighting is remarkable for all the noise, but the attenuation in A-weighted level is not so. In the case of the transformer (2), the attenuation is only 2.4 dB because the transformer noise has much higher frequency components. The attenuation in the transformer (3) is more than 10 dB in A-weighted level, because the transformer is well furnished to suppress higher frequency noise.

We have carried out simple hearing test using those noise. According to the results, this type of noise suppression will get good evaluation in the noise (3), that is, the hearing evaluation was better after the attenuation than before the attenuation.

But, in the noise (2), the result was opposite. In the noise (1), we could not get clear result.

More close investigation will be necessary to make clear the relation between the change in the spectrum and the hearing evaluation. There can be another factor in the annoyance of noise than the loudness. But, it may be sure that the attenuation in the higher frequency components is important.

ATTENUATION FOR EACH FREQUENCY COMPONENT:
10 Hz: 26 dB 200 Hz: 16 dB 300 Hz: 6 dB 400 Hz: 0 dB

BEFORE ATTENUATION:
FL = 75.1 dB AL = 57.3 dBA FL = 63.1 dB AL = 51.5 dBA FL = 72.2 dB AL = 54 dBA

AFTER ATTENUATION:
FL = 55.9 dB AL = 50.9 dBA FL = 53.5 dB AL = 49.1 dBA FL = 50 dB AL = 43.3 dBA

ATTENUATION:
−19.2dB −6.4 dBA −9.6 dB −2.4 dBA −22.2 dB −10.2 dBA

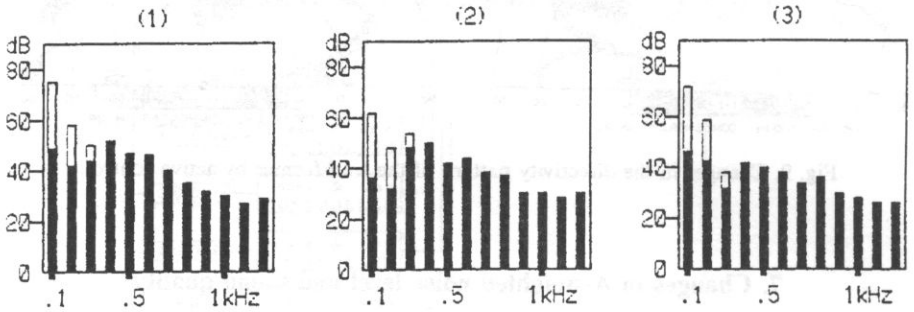

Fig. 10. Examples of the transformer noise with the decrease of low frequency components.

8. Conclusion

By surveying the history of the active control of sound and vibration, we can see the active control technology has quite a long history and is well applied to suppress the rolling of ships and the quake of high-rise buildings. But the active control is not yet so popular in audible noise control. The main reason is in the frequency range to be controlled. We have to process complicated wave form of higher frequency in the noise control engineering. Those problems are solved by the use of FIR adaptive digital filters, where a number of computation is necessary. The difficulty in the computation speed is now become out of problem by the progress of the digital signal processors, but there remains some other difficulties in the practical applications. How to diminish the feed back from the additional sound source to the reference microphone is one of the key points. This paper introduces typical two methods for reducing the feed back. Then, the algorithms of the adaptive control of the filter coefficients are shown in a unified form. As the another key problem, the relation

between the arrangement of additional sound source and the reduction of noise radiation is given according to the numerical computation. Next, the control of power transformer noise by the adaptive synthesis of directivity is briefly explained as a practical example carried out by the author. Finally, the change in A-weighted noise level and the sound quality in hearing by the ANC is discussed. As the ANC is effective only in the low frequency range, much decrease in A-weighted sound level can not be expected only by the ANC. And in some case, the annoyance of the noise can increase by the decrease in the very low frequency noise. It is important to decrease the noise of higher frequency range by the passive noise control method in the application of the ANC.

References

[1] Proc. International Symposium on Active Control of Sound and Vibration, April 9–11, 1991, Acoustical Society of Japan, Tokyo, Japan.

[2] P.A. NELSON and S.J. ELLIOT, *Active control of sound*, Academic Press, London 1991.

[3] S.M. KUO and D. VIJAYAN, *Adaptive algorithms and experimental verification of feedback active noise control system*, Noise Control Engineering Journal, **42**, 2, p. 37–46 (1994).

[4] T.J. SUTTON, S.J. ELLIOT, A.M. MCDONALD and J. SAUNDERS, *Active control of road noise inside vehicles*, Noise Control Engineering Journal, **42**, 4, p. 137–147 (1994).

[5] M. NISHIMURA and T. ARAI, *Active control of noise radiated from duct end*, J. Acoust. Soc. Jpn. (J), **45**, p. 672–680 (1989).

[6] S. SUZUKI, K. Nagayama, T. Hayashi, S. Saruta, H. Tamura, Y. Sekiguchi and K. Nakanishi, *A basic study on an active noise control system for compressor noise in a refrigerator*, Proc. International Symposium on Active Control of Sound and Vibration, Acoustical Society of Japan, Tokyo, Japan, p. 255–260 (1991).

[7] S. HASEGAWA, T. Tabata, A. Kinoshita and H. Hyodo, *The development of an active noise control system for automobiles, SAE Technical Paper 922086*, ISSN 0148-7191, p. 1–9 (1992).

[8] J.I. THORNYCROFT, *Studying vessel at sea*, TINA, **33**, (1892).

[9] S. MOTORA, On motora's ship rolling suppression system, Bull. Ship Build. Assoc., 32, (1923).

[10] S. WATANABE, *Method for the reduction of ship rolling (2)*, Proc. Symposium Ship Stabilization, Jpn. Soc. Ship Build., 156–179 (1969).

[11] T. KOBORI, *Active vibration control for architectural structure*, Proc. International Symposium on Active Control of Sound and vibration, Tokyo, p. 87–98, 1991.

[12] K. YOSHIDA and T. WATANABE, *Active vibration control of high-rise buildings*. Proc. Internat. Symposium on Active Control of Sound and Vibration, Tokyo, p. 185–194, 1991.

[13] M. IZUMI, *Control of structural vibration — Past, present and future*, Proc. Internat. Symposium of Active Control of Sound and vibration, Tokyo, p. 195–200 (1991).

[14] I. TAKAHASHI, *Development of ship with no pitching nor rolling cabin*, Jour. Ship Build. Society of Japan, 733 (1990).

[15] M. NAGAI, *Vibration control of vehicle by active suspension*, Jour. INCE/J, **12**, 3, p. 197–201 (1988).

[16] P. LUEG, *Verfahren zur Daempfung von Shallschwingungen*, Germ. Pat. No. 655508, Field: Jan. 27, 1933, Patented: Dec. '37. US Equivalent Process of Silencing Sound Oscilations, US Patent No. 2,043,416. Field: Mar. 8, '34, Patented June 9, '36.

[17] H.F. OLSON and E.G. MAY, *Electronic sound absorber*, J. Acoust. Soc. Am., **25**, p. 1130–1136 (1953).

[18] J. OKDA, T. NIMURA and K. KIDO, *Internal impedance of a system of electroacoustic transducers*. J. IECE Jpn., 44, p. 330–334 (1961).

[19] S. ONODA and K. KIDO, *Automatic control of stationary noise by means of directivity synthesis*, Proc. 6th ICA, F15-3, p. F185–188, 1968.

[20] M.J.M. JESSEL and G.A. MANGIANTE, *Active sound absorbers in an air duct*, J. Sound and Vibration, 23, 283–390 (1991).

[21] C.F.N. COWAN and P.M. GRANT, *Adaptive filters*, Prentice-Hall; Englewood Cliff, New Jersey 1985.

[22] B. WIDROW and S.D. STEARNS, *Adaptive signal processing*, Prentice-Hall; Englewood Cliff, New Jersey 1985.

[23] S. ISE, *Hardware and software techniques for adaptive filter*, J. Acoust. Soc. Jpn., 48–7, p. 501–505 (1992).

[24] H. KANAI, M. ABE and K. KIDO, *A new method to arrange an additional sound source in active noise control*, Acustica, **70**, p. 258–264 (1990).

[25] K. KIDO and S. ONODA, *Automatic control of acoustic noise emitted from power transformer by synthesizing direcivity*, Sci. Rep. Res. Inst. Tohoku Univ. (RITU), Ser. B, Part I, Rep. Res. Inst. Electr. Commun., **23**, p. 97–110 (1972).

ARCHIVES OF ACOUSTICS
21, 3, 267–274 (1996)

NOISE AS MUSIC

A. RAKOWSKI

Fryderyk Chopin Academy of Music
(Okólnik 2, Warsaw, Poland)

It cannot be denied that music and noise have some common features. Since sounds of nature and sounds of acoustic environment are sometimes perceived in an aesthetic mode like music, the fundamental questions arise: *What is music?* and: *Can noise become music?* To answer these questions several problems are briefly discussed. First, music is presented as a communication process where information about the sound structure is transmitted from Sender to Receiver basing on a communication code known to both participants. Recognition of the structure is a source of aesthetic pleasure and involves rich (mostly emotional) connotations. Next, examples are given of contemporary music in which sounds, previously considered as "non musical" play an essential part. Music of Italian Futurists and French "Musique Concrète" are described in more details.

1. Introduction

Music and noise appear as totally contradictory notions, though both concerning sound and its perception by human listeners. Music brings joy and amusement, it gives aesthetic pleasure to listeners, sometimes causes irritation, but in general means something positive, existing to make our life happier. Noise is a word that has two meanings. Its physical meaning concerns vibrations of a random character. Its psychological meaning concerns unwanted, annoying sound. In both meanings, and especially in the second one noise seems to be a contradiction of what we are traditionally inclined to think of as music. A closer look into the problem may change our opinion in that matter.

2. Can noise be music?

The famous American composer of modern music John Cage said in one of his writings: "Music is sounds, sounds around us whether we're in or out of concert halls" [2]. This is a very interesting statement. Certainly very unusual and unacceptab-

le for traditional music lovers, and at the same time most challenging for contemporary composers. Certainly according to such ideas Italian Futurists and French composers of Musique Concrete formulated their artistic programs. However it should be clearly stated that in its general form Cage's statement presented above is not true. There is an intuitive difference between the notions of music and noise. The question arises: *is it at all possible and under what conditions that noise becomes music?* To answer this we must first answer a much more fundamental question. The question that today seems very controversial: *What does the word "music" mean?*

There is generally no doubt that speaking about music we think of art using sound as its material. An indispensable feature of every art is the element of creativity — the creative organization of matter. Another important element is its communicative function. Art is a means of transmission of some kind of information from Sender (a painter, a sculptor, a composer etc.) to Receiver (listeners, viewers, a public). In the domain of music part of the transmission line is usually a performing musician, though his presence is not an obligatory condition for the communication process to exist. For musical communication two elements are absolutely necessary: a creative organization of sound and a communication code known both to the sender and to receiver.

Let us now look at various types of music being produced and to the accompanying perceptual processes. Most typical situation occurs when music composed by a composer is presented to the public at a concert or when it is individually perceived by listeners in front of their home radio or sound reproducing sets. Less typical, though more and more popular form of music communication is listening to experimental music produced by a composer directly on a magnetic tape or on a computer. It should be stressed, however, that even in most typical, "traditional" presentations of music the musical communication process may not even be initiated if the communication code used by the composer is not sufficiently familiar to the listeners. It may be assumed with sufficient degree of probability that to some inhabitants of equatorial jungle who have never had any contact with white man music and were suddenly transferred to the philharmonic hall, the Beethoven's symphony would sound almost exclusively as a terrifying, sensless sequence of noises.

But there are still more difficult problems to explain. Henryk Górecki, the excellent Polish composer, recently particularly well known to the world due to the international success of his Third Symphony, said in one of the interviews that for him the most valuable music is singing of birds. How could we interpret such a statement from a person whose competence in music cannot be denied? What is music in that case? Where is the communication process? Are birds performers of music composed by themselves? And also, who is the sender of "music" perceived by people listening to a melody played by the wind on telephone wires (the ancients thought that it was Eol, god of the wind, who played on the strings of the Eol's harp). And what about the melody of water dripping to a resonating tank? And finally how should we interpret the exaggerated, though fully serious statement of John Cage that noise is music?

It seems that there may be only one answer to all these questions. In every case when listening to sounds of nature people begin to experience the aesthetic pleasure they themselves are both senders and receivers of a musical message. Musical hearing and musical imagination helps them in imposing internal organization upon a flow of incoming acoustic events and recognizing resulting structure in terms of a previously established musical code. Such a creative endeavor may result in a purely aesthetic feeling and bring with it emotional connotations which normally accompany the reception of music. And this is music! The more sonorous, pleasant, not too loud and "friendly" are sounds of the acoustic environment the more likely is their positive musical reception by man's hearing. Therefore the efforts of sound designers and engineers to decrease the negative aspects of noise not only in a sense of its loudness are highly appreciated.

3. "Pleasant" and "unpleasant" sounds of the environment

Within the past decades of engineers' endeavor concerning noise abatement most effort has been put in eliminating sounds too loud and therefore dangerous to hearing. However, for some time there has been a growing interest in some features of auditory sensation other than loudness. Their investigation was carried on with both acoustical and psychological methods.

One of the elements of hearing sensation that clearly influences its pleasant or unpleasant character is the so-called sensory dissonance. Sensory dissonance mean a specific kind of timbre of sound caused by amplitude modulation [10]. In the frequency range of modulation below 20 Hz sensory dissonance appears as separately perceived fluctuations [3]. Between about 20 and 200 Hz it is perceived as roughness and plays an important part in the characteristic of dissonant music chords [1, 4, 13].

It is well known that the phenomenon of consonance and dissonance belongs to the most fundamental features of music. The dissonating sound structures are being used particularly often in modern music. It would be difficult to convince a contemporary composer that "dissonance" means "unpleasantness of timbre", however there is a psychological evidence showing the correlation of this phenomenon with a negative estimation of sound. For some, not fully recognized reasons the transmission of neural pulses from the peripheral hearing organ to the brain exhibits some anomaly resulting as a sort of fatigue effect selectively dependent on the frequency of modulation of the input signal. The modulatin (in most cases due to the acoustic beats) shows the effect of "maximum unpleasantness" at a specific frequency. That specific frequency of modulation for maximum unpleasantness is dependent on frequency of the signal and changes from about ten to about two hundreds [11].

As it was told, sensory dissonance is a phenomenon most important in music. However, its effect in non-musical phenomena may be still more striking. It is also directly related to the negative reception of noise. One can easily imagine scratching

glass surface with a knife, rubbing the blackboard with a piece of chalk, howling of improperly regulated brakes and many other sounds from the acoustic environment. Our reaction ot the above-mentioned startling sounds may be a sign that there are some other factors, besides loudness, which contribute to particularly negative assessment of noise.

A specific factor that plays a part in human reactions to noise, and which can strengthen them, is the spatial distribution of sound stimuli. Some investigations of this effect were reported recently be German authors [8]. The industrial noises recorded with the artificial head were reproduced equally loud in a monophonic and stereophonic sound system. The physiological reaction of listeners was tested with the method of finger-pulse amplitude. The results imply that the listeners experienced a multi-directional incidence of sound as being more of a strain. Still stronger effect was found when the virtual source of sound was moving in space.

There is an interesting, though not fully confirmed hypothesis concerning susceptibility of musicians to damaging effect of loud musical sounds on hearing. Some researchers find that many orchestral musicians being exposed to very high level of sound for decades nevertheless do not exhibit hearing loss to such a degree as people exposed to similarly strong industrial noises. The hypothesis claims that the negative effect of exposition may be to some degree diminished by active involvement of listeners in the perception of incoming signals. The informative content of a signal may contribute to more efficient adaptation of the hearing organ to loud sounds. Unfortunately, this effect, even if really existing is limited in range and not capable of protecting many young people against serious damage of hearing due to listening with excessive level to pop music in concerts and with portable sound-reproducing devices [7].

Interesting investigations of physiological reactions accompanying listening to music and to noise were conducted in early sixties by JANSEN and KLENCH [6]. It was demonstrated that the cardiac output of most subjects was reduced when they were exposed to noise for some minutes. To compare these responses with the effects of exposition to classical music, Allegro and Adagio from 3rd Brandenburg Concerto No 3 in G by J.S. Bach was chosen. This piece of music covers a wide range of frequencies and keeps a relatively constant sound level. Both stimuli were presented with loudness level of 90 phon for a duration of 7 min. There was a clear distinction in the mean change of cardiac output between application of the music and the noise sitmulus. The broadband noise had a stronger influence on blood circulation as compared with Bach concerto. Unfortunately these researches were not continued.

4. Revolution in the way of thinking about sounds that may create music

Among the first artists who openly acknowledged the beauty of the common sounds of a big city was the famous architect of "Art Nouveau" August Endell. He wrote "It is so strange: the croaking of ravens, the winds blowing, the sea foaming

seems poetical, seems grand and noble. But the noises of the town don't even seem to be worthy of attention, and yet they alone form a remarkable world which must make the town appear a richly structured being, even to a blind man. You only have to listen and hear the voices of the town. The lightly rolling hackney carriages, the heavy pounding of the post coaches, the clip-clop of hooves on the asphalt, the swift, sharp staccato of the trotters, the dragging steps of the hackney carriage horses, each has its peculiar character, more finely graded than we are able to express in words... How jolly the rolling wheels sound, how strange when they suddenly die away as the carriage turns into a side road. How penetrating the echoing steps of lonely pedestrians sound. How fleeting, how soft almost dainty the steps of many people in narrow streets sound, wher a carriage rarely appears, as can often be heard in Schloßstraße in Dresden. How passionately muffled is the pushing and shuffling of the waiting crowd. How varied are the voices of the cars, their roar as they approach, the cry of the horn, and then roaring, sounding metallic, now coarsely pounding, now finely with a clear beat... One can roam through the town for hours, listening to its loud and soft voices, feeling its strange, interwinded life in the silence of lonely places and the roar of its busy streets. Words fail me to describe the appeal of all these things." [12]:3.

Similar view, but in a more radical form appeared in a group of young Italian artists, calling themselves Futurists. They were painters, sculptures and musicians. Their approach is well shown in the picture of Umberto Boccioni painted in 1911, entitled "The street enters the house". It presents a woman looking from a balcony window out over the town. Irregular spirals in the picture symbolize noises that rise from streets of the town and penetrate the calm interior of a bourgois house.

In 1913 Carlo Carra published his manifesto "La pittura dei suoni, rumori, odori" (the painting of sound, noises, and smells) explaining how lines, surfaces, and colors may design the architecture of a musical composition. Soon, however, a much more radical declaration appears concerning the modern view on substance of music: Luigi Russolo announces his famous manifesto on the art of noises. The noise, the non-musical sound is announced here as a fundamental material for musical composition. It becomes the essence of the new music which produces completely new world of sound. Rumbles, hisses, booms, crackles and buzzes become musical material substituting the so-far dominating harmonic sounds and tonal harmonies. Traditional orchestra is banned from concert halls and replaced with the world of machines and mechanical sound-producing devices, the world of common-world sounds designed according to musical imagination of the young artists. We read in the Manifesto: "We Futurists have deeply loved and enjoyed the harmonics of the great masters. For many years Beethoven and Wagner shook our nerves and hearts. Now we are satiated and we find far more enjoyment in mentally combining the noise of trams, backfiring motors, carriages and bawling crowds than re-hearing, for example the Eroica or the Pastoral". [12]: 4.

Russolo did not limit himself to theoretical declaration. He designed and constructed many instruments for the new music. These „Russolphones" were divided in 6 groups constituting a futuristic orchestra [5]. There were:

1. Rumbles, Roars, Explosions, Crashes, Thuds, Booms
2. Whistles, Hisses, Snorts
3. Whispers, Murmurs, Mutters, Rumbles, Gurgles
4. Creaks, Rustles, Buzzes, Crackles, Scrapes
5. Percussive noises obtained from metal, wood, skin, stone, etc.
6. Voices of animals and men: Shouts, Screams, Howls, Laughs etc.

Russolo's insturments, mostly made of wood and metal, were a proof of the mental revolution that took place in the artists' minds. It concerned the new way of thinking about the material of music. This revolution developped fully only some years later, when the technology of sound recording was used by the composers of musique concrète.

5. Musique-concrète — the music of noises

In 1923 Artur Honegger composed his famous "Pacific 231", a musical piece that paid tribute to modern technology. The composition represented, with orchestral means, the power and speed of the great intercontinental traction engine. It also revealed the artist's sympathy to the world of machines and his solidarity with the composers who used artistic transformation of the ambient sounds in their musical works. Honegger must have been surprised, when exactly quarter of a century later someone made a similar attempt, this time however, not bothering with making an orchestra sound like a railway engine, but simply going to the railway station, recording all posssible noises of a train, and making a musical composition out of them. The man who did this was head of the Studio d'Essay of the French radio, sound producer, writer, and composer Pierre Schaeffer, and the title of the composition was "Étude aux Chemins de Fer" [9].

Pierre Schaeffer was always fascinated with avant-guarde music. He wanted to explore the expressive possibilities of sound effects used in various radio and TV programs and to compose music using sounds of the acoustic environment. He tried to compose using recorded "l'objects sonores" (sound objects) and called the result "musique concrète" (concrete music). The word "concrete" reminded that unlike in traditional music, the object of musical art was here not only an idea described in notes, but a physically produced, concrete object, recorded and ready to be demonstrated to the public.

On October 5, 1948 Paris Broadcasting Service produced a radio concert called "Concert de bruits", ("Concert of Noises"). It consisted of "Étude aux Tourniquets" made out of recorded percussive sounds, "Étude aux Casseroles" made out of sounds recorded in a kitchen and "Étude aux Chemins de Fer". Sound objects gathered to produce this last Étude were quite numerous. There were starting sounds of the engine, rattling of the wheels, bumps of the buffers, sounds of moving trains and so on. Though having gathered such an unconventional material the composer wanted to organize it according to traditional musical rules. Structural analysis showed there

a strict musical construction with many elements of polyphony. There was an interesting rhythmic counterpoint, accelerando and crescendo, solo of the engine and tutti of the cars. However, to the artist's despair for someone hearing the piece for the first time only one thing was sure: Here is a train in motion.

This was the first experience and first disappointment of the composer of concrete music. Ambient sounds, when easily recognized, carry with them the whole story of their non-musical past which dominates over the musical construction. In spite of the author's intention that his compositions should impress the listener exclusively with abstract auditory elements the public could not free themselves from perceiving the anecdotic level of sound. Thus the important work to be done with the recorded sound material was to transform it into a non-recognizable form. This was not an easy task regarding the early stage of development of sound technology.

One of the most important examples of concrete music was Symphonie pour un Homme Seul (Symphony for man solo). Its main idea was to show the opposition of the human voice and the sounds of the environment. The main instrument here were voices of men, women, and children artificially changed in such a way that the articulatory information was lost, though typical intonation and timbre remained. Human sounds consisted of words, shouts, screams, groans, sighs, laughs, singing, murmuring, breathing etc. Sounds of the environment were knocking at the door, footsteps, ambient noises, and transformed sounds of various musical instruments. The symphony was first prepared as a sort of an avant-guarde radio play. In subsequent versions all the verbal comments were removed and finally "symphonie" was presented as a piece of concrete music. The authors were Pierre Schaeffer and a young composer, former student of Olivier Messiaen's, Pierre Henry.

"Symphonie pour un homme seul" had a strict musical form. It consisted of 10 parts ("sequences") called: Prosepopée I, Partita, Valse, Erotica, Scherzo, Prosepopée II, Eroica, Apostrophe, Cadence, and Strette. However, in spite of the author's declared intentions the anecdotic contents of the material was clearly seen in many parts of the piece. The symphony had many presentations in public concerts and on the radio. It became one of the best known pieces of concrete music and in 1955 was presented in form of a ballet by M. Bejart and J. Laurant. Perhaps its literary content contributed partly to its popularity.

The success of early compositions of concrete music attracted many new composers who after 1950 joined the group and tried the new technique. Among them were Pierre Boulez, Oliver Messiaen, Andre Jolivet and several other leading French artists. At the time technical possibilities of Studio d'Essay were already much more advanced due to the development of magnetic sound recording ("Etude aux Chemins de Fer" and "Symphonic" were produced without any taperecorder, with the use of gramophone-record technique only). Musique concrete strongly influenced the composing style of whole generations of composers in the years to come. It changed their way of thinking about the relations between music and noise.

References

[1] G. BEKESY von, *Über akustische Rauhigkeit*, Z. Techn. Phys., **16**, pp. 276–282, 1935.

[2] J. CAGE, *Silence* (4th ed.), Wesleyan University Press, Midletown, 1979.

[3] H. FASTL, *Fluctuation strength and temporal masking patterns of amplitude-modulated broadband noise*, Hearing Research, **8**, pp. 59–69 (1982).

[4] H. HELMHOLTZ, *Die Lehre von der Tonenpfindungen als physiologische Grundlage für die Theorie der Music*, F. Vieweg u. Sohn, Braunschweig, 1863.

[5] P. HULTON, *Futurismo & Futirismi*, L'edizione Bompiani maggio, Milano, 1986.

[6] G. JANSEN and H. KLENSCH, *Beeinflussung des Ballistrogramms durch Schallreize und durch Musik*, Z. angew. Physiol. einschl. Arbeitsphysiol., **20**, p. 258–270 (1964).

[7] A. JAROSZEWSKI and A. RAKOWSKI, *Loud music induced threshold shifts and damage risk prediction*, Archives of Acoustics, **19**, pp. 311–321 (1994).

[8] G. NOTBOHM, S. SCHWARZE and G. JANSEN, *Noise evaluation based on binarual hearing*, Procedings of 14th International congress on Acoustics (14 ICA), Bejing H2-2, 1992.

[9] A. RAKOWSKI, *Muzyka konkretna we Francji w latach 1949–1953*, (The concrete music in France in the years 1949–1953), Muzyka, **3** (1–2), pp. 134–161 (1958).

[10] A. RAKOWSKI, *Dysonans w świetle badań psychoakustycznych*, (Dissonance in the light of psychoacoustic research). Zeszyty Naukowe PWSM w W-wie, (Research Series of the State College of Music in Warsaw), **6**, 13–36 (1979).

[11] A. RAKOWSKI, *Psychoacoustic dissonance in pure-tone intervals: Disparities and common findings*, In: C. Dahlhaus i M. Krause, (Red.): Tiefenstruktur der Musik, TU Berlin, 1982.

[12] A. SCHICK, *Noise and sounds as objects and means of artistic design*, Proceedings of the International Symposium *Contribution of acoustics to the creation of comfortable sound environment*, Acoustical Society of Japan, Osaka, pp. 1–14, 1992.

[13] E. TERHARDT, *The two-compnent theory of musical consonance*, In.: E.F. Evans i J.P. Wilson [Eds.] Psychophysics and physilogy of Hearing, Academic Press, London, pp. 381–390, 1977.

ARCHIVES OF ACOUSTICS
21, 3, 275–286 (1996)

THE STAND FOR THE INVESTIGATION OF THE AUDITORY DANGER SIGNALS PERCEPTION — PRELIMINARY INVESTIGATION

E. KOTARBIŃSKA, G. MAKAREWICZ, R. OGŁAZA

Central Institute for Labour Protection
(00-701 Warszawa, Czerniakowska 16)

R. PALUCHOWSKI

Warsaw University of Technology
Department of Electroacoustics
(00-665 Warszawa, Nowowiejska 15/19)

P. ROGOWSKI

Chopin Academy of Music
Laboratory of Musical Acoustics
(00-368 Warszaa, Okólnik 2)

This article presents a stand for the investigation of the perception of auditory danger signals which are masked by simulating industrial noise. The test stand enables the generation of signals with specified parameters and the control of the course of an experiment. It also enables the processing of measuring data obtained. In the latter part of the paper, psychoacoustic experiments are described. Some results of preliminary measurements are discussed.

1. Introduction

A number of industrial accidents have been caused by the lack of a danger signal or its wrong interpretation due to its form. Taking into account the importance of this problem, appropriate standardizing [1, 2] and research work [7] has been undertaken. Within the research project No. 7S 10103404 "The method of design and generation of the danger signals used during the operation of machines and devices" which has been realized in the Central Institute for Labour Protection, there have been

undertaken works aimed at the determination of the criteria of selection of auditory danger signals in dependence on the background noise and the psychoacoustic properties of the human being.

The test stand, described in the first part of this paper, consists of an instrument by that the planned goal may be attained by performing experiments connected with the auditory signal perception in the presence of the background noise.

Further in this paper two psychoacoustic experiments on the detection of warming signals in the presence of interfering noise are presented. The results of those preliminary experiments constitute a practical test of the created stand. The experiments have been aimed at selecting temporal and spectral structures of warning signals from the group of elementary signals, e.g. pure tone pulses or frequency- and amplitude-modulated tone pulsees of various temporal patterns.

2. Test stand

The basic foundation of the test stand project was the creation of conditions of the acoustic warning signal perception equal to those we are dealing at real work stands. The only difference between them and the real working conditions was that we could control all the factors influencing the perception's results. On the one hand, it means excluding of the exterior interfering signals (adequate test room) while on the other, it obliges us to generate all the signals which are taking part in the process of detection of the acoustic warning signals.

The basic elements of the stand are: a test room, two independent sonorizing electroacoustic channels, software used for: generation of the testing signals these signals are presented to the subject who has to signal their perception, control of the measurements course and generation of danger signals.

2.1. Instrumentation

During the experiment the subject is positioned inside the test room which fulfils the requirements of the standard [4] concerning the measurement of the acoustical parameters of the hearing protectors by a subtective method.

In order to sonorize the room interior, two independent electroacoustical channels have been used. They consisted of an IBM compatible Personal Computer with a sound card, a power amplifier and a set of loudspeakers. One channel is the generation of the test (danger) signals and the second one for the generation of masking signals (simulating industrial noise) of specified amplitude and frequency parameters. By using two computers as a source of both the test and masking signals. It is also possible to perform the experiments together with a simple computer game which draws and distracts the subject's attention. This allows the experiment conditions to be very similar to the real ones existing at work. The scheme of instrumentation (Fig. 1) shows the architecture of the measurement system and the plan of the test room.

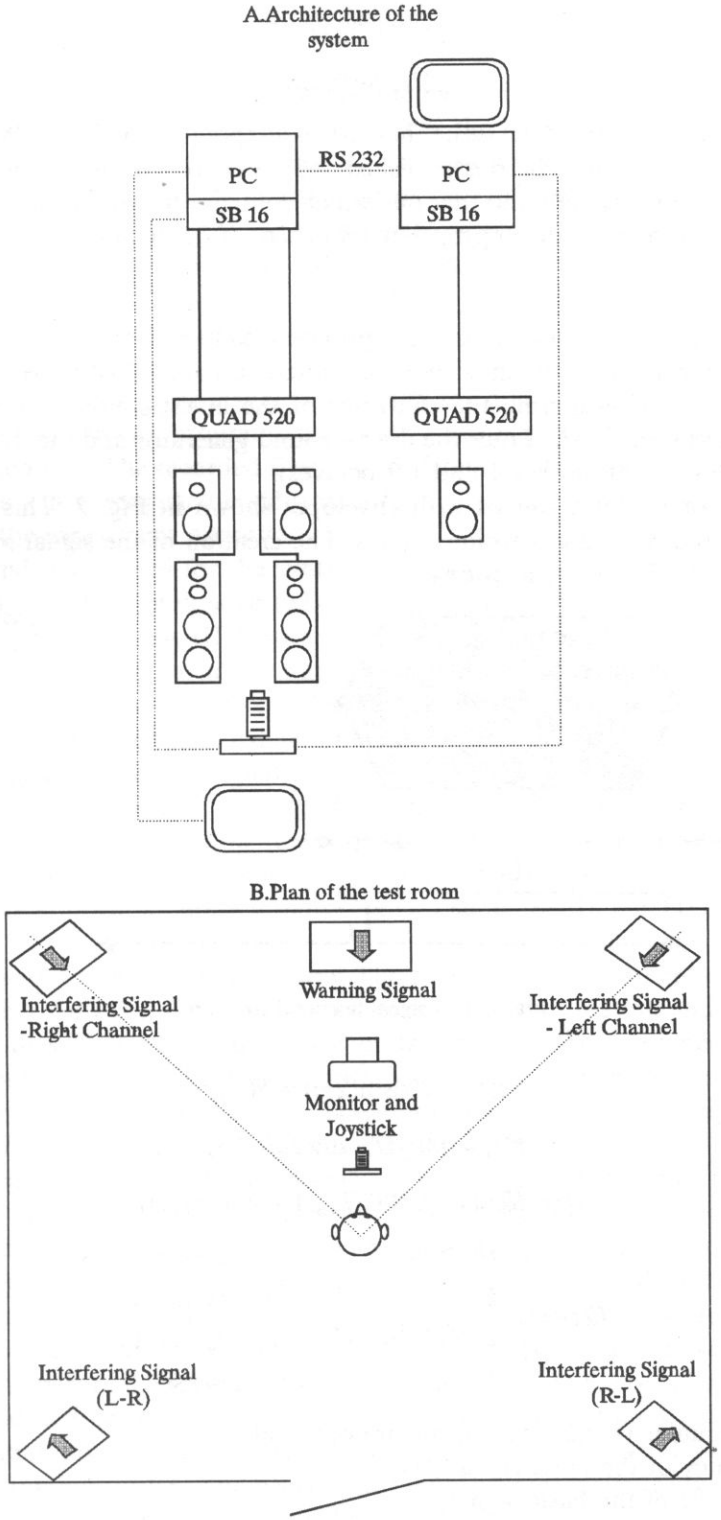

Fig. 1. Hardware part of the stand. Architecture of the measurement system and plan of the test room.

2.2. Software

The software of the test stand has been adapted to work in Windows 3.1. environment. There may be distinguished the software for the generation of the testing and masking signals and that one which controls the experiment course. They act together and prepare the appropriate sequences of files comprising the acoustical signals.

2.2.1. Signal generation programs. The program creates a set of files with sound information recorded by the most popular sound standard (WAV) in the Windows 3.1 environment. Considering the character of the investigation, two independent programs have been worked out: the digital sound generator and the digital filter of the WAV files (filtration in 1/1 and 1/3 octaves).

The first one creates signals with envelopes shown in Fig. 2. This part of the software is used to create warning signals. The creation of the signal $x(t)$ proceeds according to the following relations:

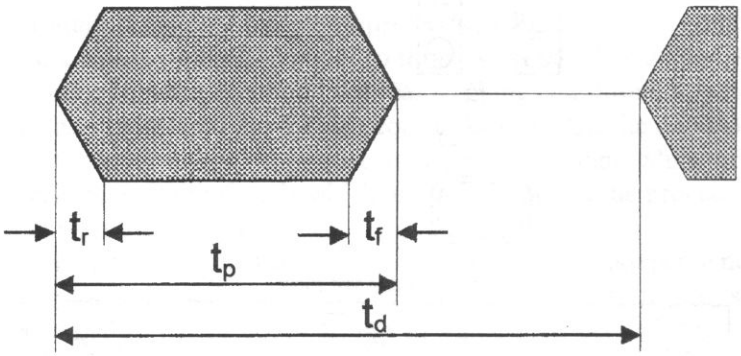

Fig. 2. Test signal temporal structure.

$$x(t)=A(t)\sin(2\pi ft+F(t)), \tag{2.1}$$

$$F(t)=0.01fG_{AF}\sin(2\pi f_F t)/f_F, \tag{2.2}$$

$$A(t)=K(t)(1-0.005G_{AA}(1+\sin(2\pi f_A t))), \tag{2.3}$$

$$K(t)=\begin{cases} Ae^{-\pi k_r(t_r-t)^2} & 0\leqslant t<t_r \\ A & t_r\leqslant t\leqslant t_{s1}-t_d \\ Ae^{-\pi k_d(t-t_{s1}-t_d)^2} & t_{s1}-t_d<t<t_{s1} \\ 0 & t_{s1}\leqslant t\leqslant t_s \end{cases} \tag{2.4}$$

where the parameters indicated below are optional:
f — frequency of the basic signal [Hz],
A — amplitude of the basic signal,

G_{AF} — depth of frequency modulation of the basic signal [%],
f_F — frequency of the signal which modulates the basic signal frequency [Hz],
G_{AA} — depth of amplitude modulation of the basic signal [%],
f_A — frequency of amplitude modulation of the basic signal [Hz],
k_r — factor forming a rise of the basic signal envelope,
k_d — factor forming a fall of the basic signal envelope,
t_r — rise time of the basic signal [s],
t_d — fall time of the basic signal [s],
t_{sl} — basic signal duration [s],
t_s — total duration of the signal recorded in the digital form [s].

A special function in the program can create a sequency of files in which danger signals are recorded. The recorded files have different levels of the samples. They can be reproduced in a sequence conditioned by a selected algorithm applied in the program of the experiment operation.

The second one is used for the synthesis of signals obtained by means of digital filtration of the white or pink noise (33 parallel third-octave band Butteworth's filters of infinite impulse response (IIR) were used). This program filters one WAV file to another one. One of the particular implementation is a situation when these filters synthesize the interfering signals corresponding to the standard spectrum (one of five so called noise classes) which are determined by the Polish Standard [5]. This part of the software creates masking signals.

Due to the psychoacoustic investigations concerning the project, the software has been extended. A new function (described in details in section 2.2.3), which is generating warning signals based on the recorded WAV file (containing real industrial noises) or direct noise monitoring (via sound card), has been added.

2.2.2. Experiment operation programs. The programs of experiment operation act closely together with the above-mentioned programs of generation and filtration of digital signal files. From the point of view of its operation, the experiment consists of two parts both using two different algorithms of the experiment operation.

In the first part the threshold of danger signals hearing is investigated in the presence of the masking signals. In this method (method of tracking [3] — Fig. 3) the subject indicates the presence or absence of the signal by pressing or releasing a button (as in automatic audiometry). By pressing the button the sound pressure level decreases and by releasing it, the direction of the level changes is opposite (i.e. it forces a SPL's increase). It is possible to adjust the rate of the sound level changes and control the accuracy of subject's reaction tracing. During the experiment extreme sound pressure level values causing predetermined subjects reactions are recorded.

The second part of the software enables the realization of the so called algorithms of the method of free response (MFR). It is based on a continuous submission of N presentations divided into 4 periods to the subject (Fig. 4). Test signals are presented in random order. The hearing threshold level is statistically estimated as a level with 75% of observations provided by the subject.

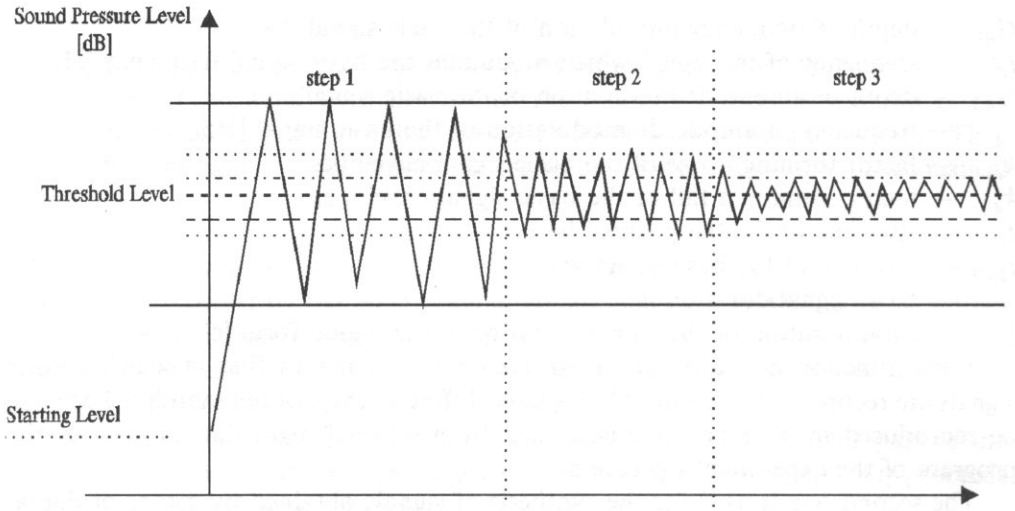

Fig. 3. Tracking of the threshold level according to the algorithm implemented in the presented software.

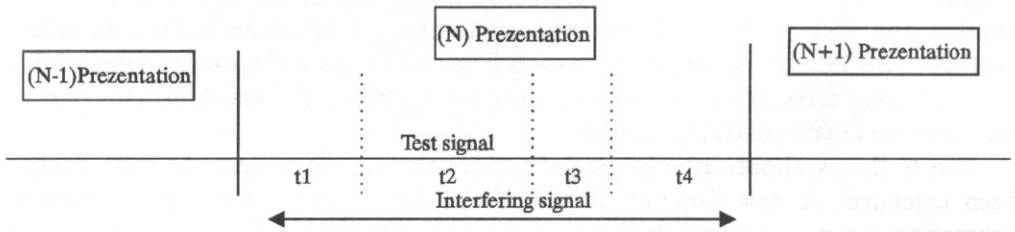

Fig. 4. A description of the MFR algorithm.

A suitable test signal is played only during one of the periods, while the interfering signal occurs during all the time of presentation. In this method, the subject also indicates the presence or absence of the signal by pressing or releasing a button, but his does not change the sequence prepared previously. For each successive presentation a set of 4 numbers is obtained. They show how many times a subject signalled (by means of the button) the test signal perception. A sequence of presentations is selected in a random manner.

In the first part of the experiment the program generates the danger signals according to the subjects reaction, generates the masking signal, controls the results by monitoring the subject's reaction state. It also performs the preliminary statistical processing and sends the collected data in a form which makes the analysis of them possible by means of other programs working in the Window 3.1 environment.

In the second part of the experiment the program generates a sequence of random successive presentations, generates the testing and interfering signals and controls the duration of the appropriate periods. The program enables the monitoring and

recording of the subject's behaviour during the experiment and provides information about the interchange between the signal channels.

Optionally, a function concerning the absorbing of the subject's attention, i.e. the simulation of a situation in which a subject is engaged in the realization of activizies distracting its attention during the perception of the danger signal, can be switched on.

2.2.3. Warning signal generation program. The task of the warning signal generation program is to simulate the work of an adaptable signalling apparatus. Its activity is optimized in order to guarantee the best perception conditions for the subject (worker at a certain work stand). Because the program does not work in a real time, it can be used only at a work stand at which the creation of stationary perception conditions is possible. The simulation of one working cycle (steps' sequence) of the adaptable signalling apparatus is presented in Fig. 5.

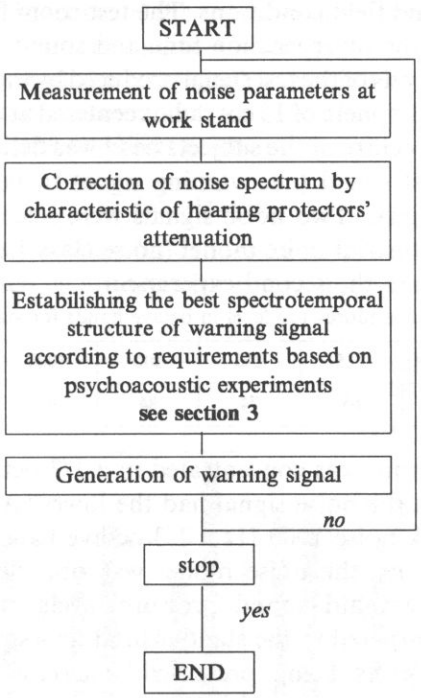

Fig. 5. Algorithm of the adaptable signalling apparatus work.

The temporal structure of the generated signal is presented in Fig. 2. Depending on the noise parameters, the values of the basic frequency (f) and amplitude (A) are subjected to modification. The usage of a signal with determined duty cycle enables the measurements of noise parameters when the warning signal is inaudible.

3. Preliminary investigations

The first two experiments [8] consisted in the establishing the influence of the temporal structure (in the first case) and of the spectral structure (in the second case) on the hearing treshold level of the examined group. A tracking method, used in these experiments, was applied to various signal structures in the presence of noise signals.

3.1. Experimental methods

Subjects. Five subjects (AP, BM, EC, MM, MO) participated in the first experiment and seven subjects (AP, BM, EC, MM, TR, WZ, MO) in the second one. All they had a hearing loss of less than 15 dB in the frequency range 125–8000 Hz and participated voluntarily in the experiments and were paid for their services.

Measurement conditions. Experiments were performed in a test room normally used for measurements of the hearing protectors attenuation. Noise signals were presented in diffuse sound field conditions. The test room fulfills the requirements of ISO 4869 [4] regarding the reverberation time and sound field diffuseness.

The sound pressure levels of the test signal produced by the pair of loudspeakers (JBL 4208) at positions within a sphere of 15 cm radius centered at the reference point differed by less than ± 3 dB. The centre of the subjects head was defined as the reference point.

Test signals. The test signal (i.e. warning signal to be detected) was presented together with a noise signal. Two noise signals were selected : a noise signal based upon a standardized industrial noise model (noise class 1 of the Polish standard [5], Table 1) and pink noise in the second experiment.

Table 1. A-weigthed soundpressure level in octave bands for standardized noise signal

Octave band center frequency, Hz	125	250	500	1000	2000	4000	8000
A-weighted SPL, dB	65	74	84	92	96	97	93

The test signal spectrum was concentrated in a 1/3 octave band (from the range 315–2500 Hz) at which the noise signal had the lowest A-weighted sound pressure level. In the case of pink noise 1000 Hz a 1/3 octave band was selected.

In the first experiment, the noise model was obtained from the octave band filtered pink noise. A-weightd sound pressure levels in the octave bands were proportionally lower compared to the standardized nois signal with relative relations between octave band levels being preserved. Therefore, the A-weighted sound pressure level of the noise signal was 90 dB.

Nine test signals were presented. Each signal consisted of 1000 Hz tone pulses. The repetition frequencies were 0.2, 1 and 5 Hz, and the duty cycles 25, 50 and 75%. The rise/fall time was 5 ms for pulses of a 5 Hz repetition frequency and 25 ms for all other cases.

In the second experiment, pink noise was used as the background noise model. The A-weighted sound pressure level was 72 dB. Five test signals were presented, each having a duration time of 750 ms, repetition frequency 1 Hz, rise/fall time 25 ms. The following signal structure were used:

— 1000 Hz tone pulse (SINE);

— amplitude modulated sine wave, modulation frequency 10 Hz (AM 10), 100% modulation depth;

— amplitude modulated sine wave, modulation frequency 100 Hz (AM 100), 100% modulation depth;

— frequency modulated sine wave, modulation frequency 10 Hz, frequency deviation 90 Hz (FM 10);

— linear sine sweep in the range 900 – 1100 Hz (SWEEP).

All the singals were generated digitally. The signal decrement/increment speed was set at 2.5 dB/s, typical to audiometric measurements [3].

Procedure. Before the test, subjects were familiarized with the test signals. Subjects were instructed to press the button as soon as the test signal is heard and release it immediately once the signal is no longer heard, according to ISO 8253-1 [3]. The test signals were presented at random order in a computer-controlled procedure. Each trial consisted of two phases. The duration time of the first phase depended on the subject's reaction. After a direction of the signal level increment/increment had been switched four times; the second phase allowed during that all levels were recorded. An average sound pressure level of the test signal was taken as the result. Each subject completed five trials for each measurement point. In the first experient subjects were having hearing protectors (Bilsom Viking) on.

3.2. Results

The results of the detection thresholds measurements are shown in Figs. 6 – 10. The thresholds are expressed as averages for each subject and for the group as well.

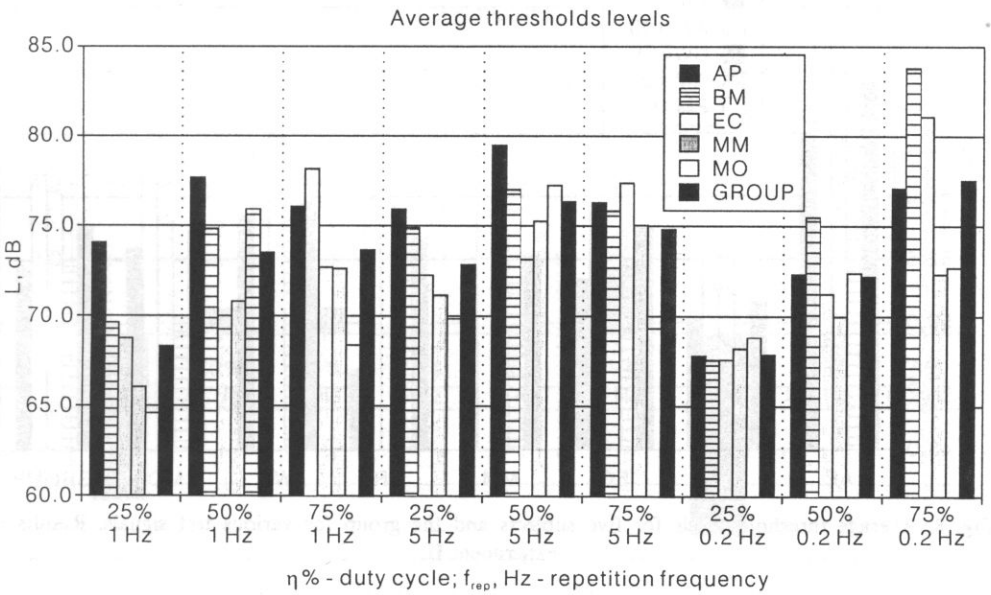

Fig. 6. Average threshold levels for five subjects and the group for various test signals. Results of experiment I.

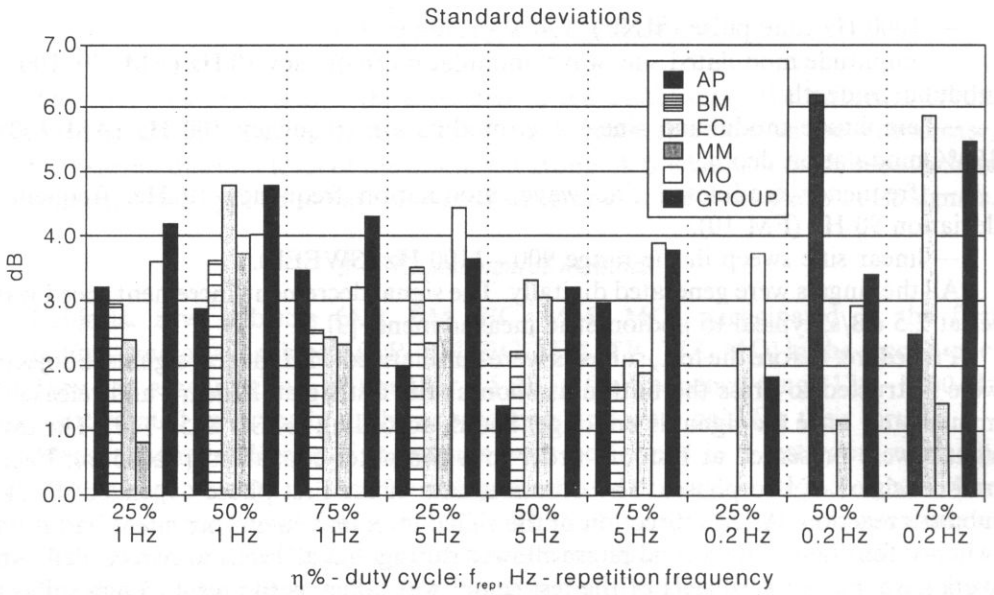

Fig. 7. Standard deviation of thereshold levels of each subject and the group for various test signals. Results of experiment I.

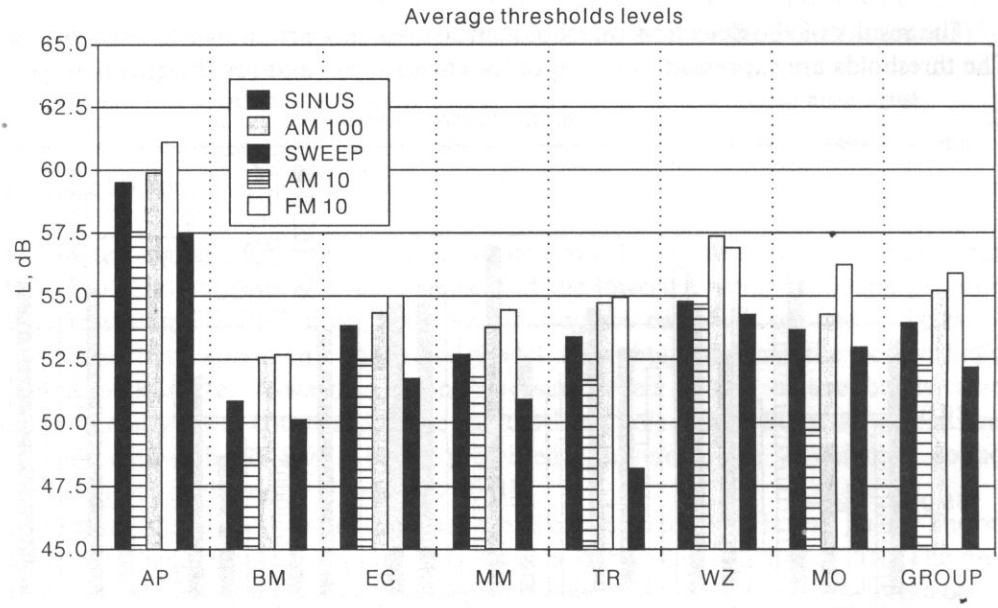

Fig. 8. Average threshold levels for five subjects and the group for various test signals. Results of experiment II.

These results are presented in Figs. 6 and 8. Standard deviation are plotted in Fig. 7 and 9. In order to eliminate the influence of the differences in the detection levels for different subjects, the final results were normalized by subtracting the average of all the data for each subject from partial results. The normalized detection thresholds are shown in Fig. 10.

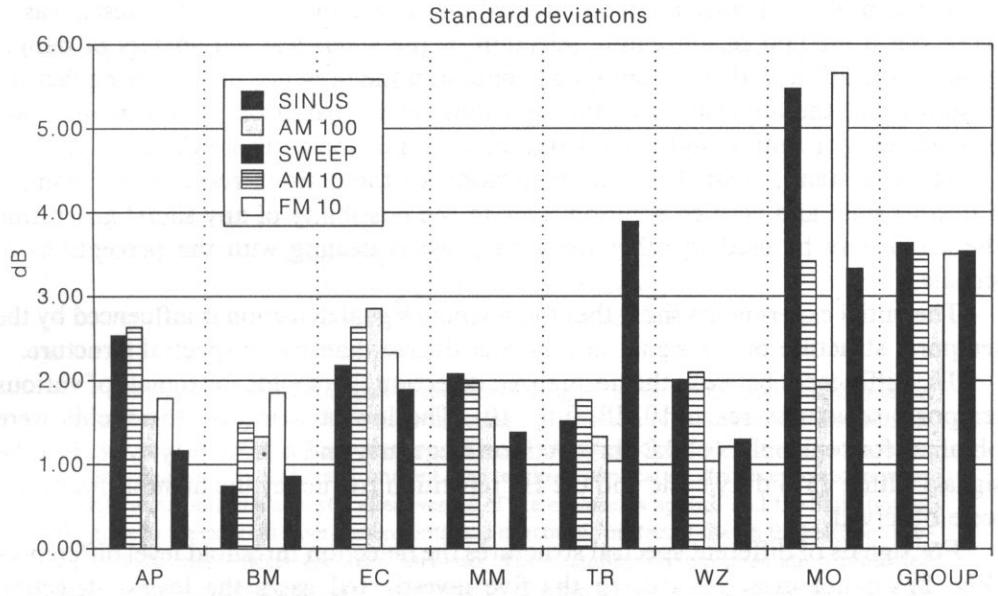

Fig. 9. Standard deviation of thereshold levels of each subject and the group for various test signals. Results of experiment II.

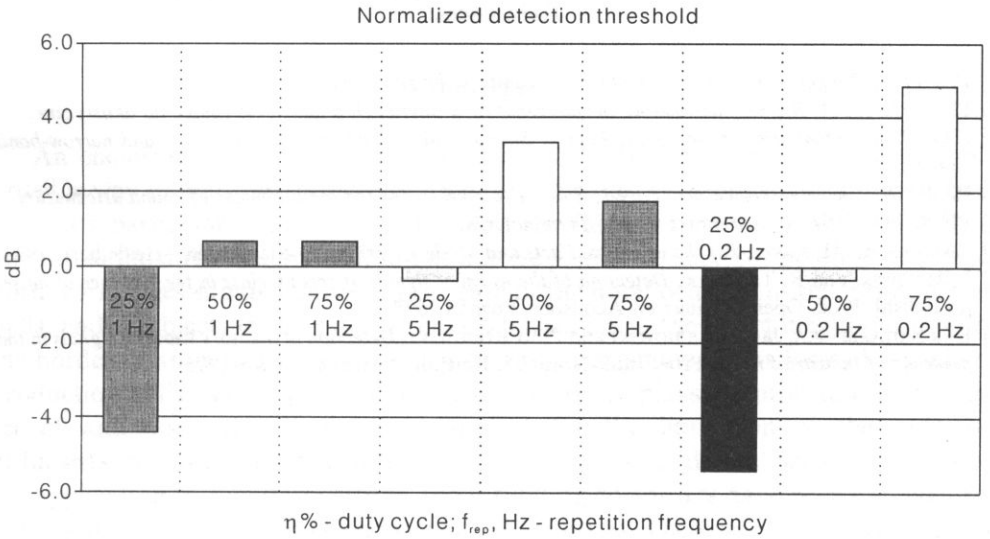

Fig. 10. Normalized detection threshold levels for various test signals. Results of experiment I.

4. Conclusions

The presented test stand enables to investigate the perception of auditory signals (of different time and frequency parameters) which occur in the presence of continuous noise of a freely formed audible spectrum (in the third-octave bands).

The aim of the investigation, conducted on the ground of subjective tests, was to work out a method of automatic selection of the acoustical parameters of danger signals in relation to their optimum perception in the presence of interfering factors. It seems that the application of the signalling device based on such a method will increase the perception and correct interpretation of the auditory danger signals.

The test stand, created for the realization of the definite research program, is a flexible solid and verified solution. Due to the possibility of any signal generation the stand may be used in other research projects dealing with the perceptions of signals.

The initial experiments show that the warning signal detection is influenced by the temporal structure of the signal in a greater degree than by its spectral structure.

The differences between the normalized detection thersholds for signals of various temporal structures reach 10 dB (Fig. 10). The lowest detection thresholds were obtained for tone pulses of 0.2 Hz repetition frequency and a 25% duty cycle. For the signals with a 75% duty cycle and 0.2 Hz repetition frequency the highest thresholds were observed.

For signals of different spectral structures the detection threshold level differences (Fig. 8) do not exceed 4 dB. In the five investigated cases the lowest detection thresholds were obtained for sweep signals.

References

[1] ISO 7731, *Danger signals for work place — Auditory danger signals.*

[2] PN-86/N-08014, *Sygnały dźwiekowe bezpieczeństwa w miejscach pracy — Wymagania akustyczne.*

[3] ISO 8253, *Audometric test methods, Part 2, Sound field audiometry with pure tone and narrow-band signals.*

[4] ISO 4869-1, *hearing protectors, Part 1, Subjective method for the measurement of sound attenuation.*

[5] PN-86/N-01309/02, *Ochronniki słuchu. Terminologia.*

[6] ZWICKER and H. FASTL, *Psychoacoustics. Facts and Models*, Springer-Verlag Berlin – Heidelberg, 1990.

[7] I. RENOWSKI and R. TOMCZYK, *Detection of the warning signals of certain class in the presence of noise.* [in Polish], Proc. Open Seminar on Acoustics, Poznań 1978.

[8] Ewa KOTARBIŃSKA, Jan PALUCHOWSKI and Piotr ROGOWSKI, *Detection of auditory warning signals in the presence of industrial noise*, Proc. Inter-Noise 95, Newport Beach, CA USA 1995.

ARCHIVES OF ACOUSTICS
21, 3, 287–298 (1996)

ENCLOSURES SOLUTIONS, STUDIES OF ACOUSTIC EFFECTIVENESS UNDER REAL CONDITIONS

J. SIKORA

Mechanics and Vibroacoustics Department
Academy of Mining and Metallurgy
(30-059 Cracow, al. Mickiewicza 30)

This reports presents examples of enclosures designed by the author and implemented in the industry. Their purpose is to limit the excessive noisiness of machines and installations that are situated outside of proeduction halls and of technological objects and increase the acoustic degradation of the environment. The results of verification studies executed in order to determine both the acoustic effectiveness of the enclosures applied and the limitation of the noise in the external environment obtained in acoustic protected sites in the neighbourhood of industrial objects are also discussed. The examples of implementation presented confirm the great usefulness and effectiveness of enclosures in anti-noise protection. This report contains also information about experimental studies conducted by the author in order to determine the influence of materials and constructional solutions on the acoustic effectiveness of enclosures. The results of research obtained are useful in designing improved constructional solutions of enclosures.

1. Introduction

An enclosure, which is the passive device of noise limitation, is often the only possible way to limit the sound radiation caused by acoustic active machines or their parts. Its particular importance consists in the fact that the noise level is reduced already in the direct neighbourhood of a noise source. It makes it possible to protect both workplaces situated closely in the case of the noise ocuring inside of production halls, and of objects in the external environment, i.e. in the direct neighbourhood of the border of an industrial plant in which a noisy machine works located outside of production halls. As the practice shows the enclosure plays an important role in the set of antinoise protection means applied for the limitation of the excessive arduosness of industrial noise influencing acoustic protected sites. Scientific works on the application of sound-absorbing and insulating enclosures have been executed for many years in numerous high-industrialized countries. These works or those that can be applied in the design of enclosures have been conducted in three directions:

• a theoretical direction based on the achievements of theoretical acoustics [e.g. 9, 10].

• a scientific direction consisting in the elaboration of computational methods, rules of the selection of sound absorbing and sound insulating materials, technical, functional and architectonic solutions, standards and instructions, as well as in practical applications of new solutions of limitation of the noise caused by a real individual machine or by series of types of machines and installations [e.g. 7, 10, 11, 12];

• a research direction consisting in the study of properties of sound absorbing and insulating materials and in the determination of the influence of material and structural factors on the acoustic effectiveness of enclosures, etc. [e.g. 8, 13];

The investigations executed in the Mechanics and Vibroacoustics Department during the last few years aimed at the elaboration of effective and modern structural solutions of enclosures, comparable to the solutions applied in countries having more experience in this field, such as USA, Great Britain or Germany. The verifying studies executed after application of the designed enclosures in the industry proved that the elaborated solutions were conformable with the international standards of acoustic, as well as exploitation requirements and realization esthetic.

At the Mechanics and Vibroacoustics Department extensive studies were also executed which were aimed at the determination of the influence of the material and structural solutions of enclosure elements on their acoustic characteristics. The studies on the determination of the influence of the following elements on the enclosure acoustic effectiveness deserve special attention: solution of contacts and joints of enclosure components, the kind of seals in the contacts and joints of enclosure walls, the material structure in the constructional solution of the wall and the way of the wall fastening to the frame of the supporting structure. The results of these studies should be treated as an extension of the results of the research works executed in other foreign scientific centers.

2. Solutions of enclosures

In the implementation practice four kinds of enclosures are applied [1, 2]; partial, partly closed, entirely closed and integrated enclosures. The following factors influence the kind of the constructional solution of the enclosure used: the type and principle of operation of the noisy machine, its production or technological process, requirements concerning the necessary acoustic insulation. The basic repartition of the enclosure is presented in Fig. 1.

The classification presented in Fig. 1 can be completed by other repartitions [3] after taking into account more detailed criteria, such as: the kind of the implemented constructional solution, thermic requirements concerning the enclosed machine, the access to the machine during repairs and the course of the production on technological process, the kind of the technological or production process carried out by the

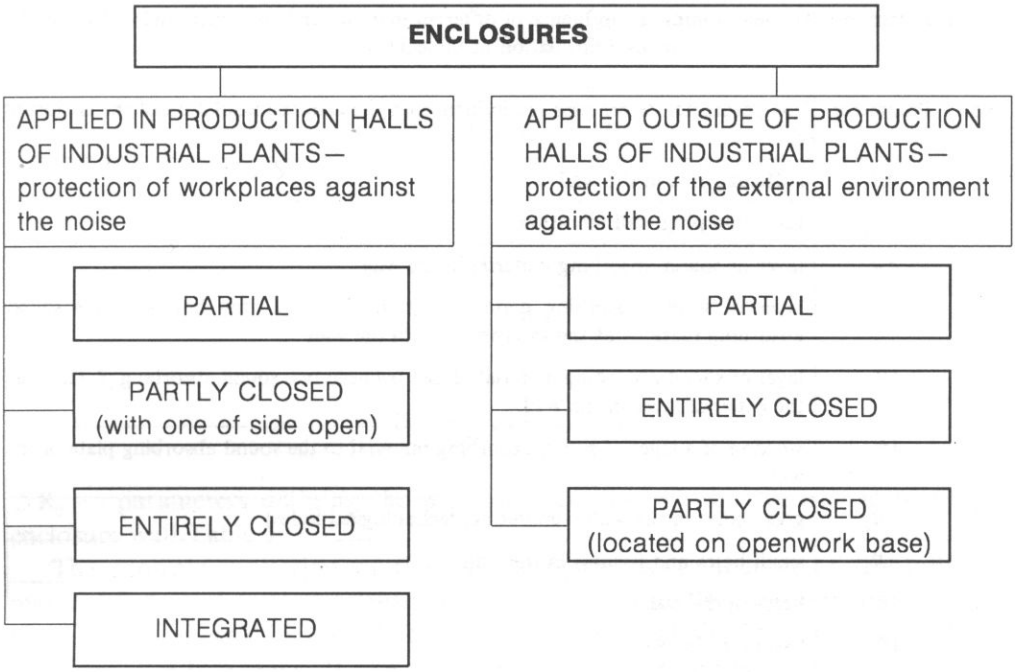

Fig. 1. General classification of enclosures.

enclosed machine, the required acoustic effectiveness of the enclosure, the application of automation elements in the constructional solution of the enclosure, the way of fastening of enclosure walls, the solution of the enclosure shape.

3. Parameters influencing the acoustic effectiveness of enclosures

A measure of the enclosure effectiveness is its acoustic insulation, D_{obud}, which indicates to what extend the enclosure protects against the penetration of the air vibration as well as the material vibration in the outside. The acoustic insulation of an enclosure depends first of all on the specific acoustic insulation R_s of its walls. Next, the value of the acoustic insulation of an enclosure wall depends on the physical properties of the material of which it is made and on its constructional features.

On the basis of the research results obtained up to the present it can be stated that the material and constructional factors occuring in the depending and production phases have an essential influence on the acoustic effectiveness of the enclosures. The following formula describes this relationship:

$$D_{obud} = R_s + \sum_{i=1}^{13} \triangle R_i, \quad \text{dB} \tag{3.1}$$

where R_s — specific acoustic insulation of the thin enclosure wall, dB.

Table 1. Parameters ΔR_i determining the influence of different material and constructional factors on the acoustic insulation of the enclosure

No.	Parameter	This parameter determines the influence on the acoustic insulation of the enclosure of:
1	ΔR_1	stiffening ribs in the wall
2	ΔR_2	layer dumping wall vibration
3	ΔR_3	layer of sound absorbing material in the wall
4	$\Delta R_{3.1}$	layer of sound absorbing material combined with a thin homogeneous sound absorbing plate — as the external layer in the wall
5	$\Delta R_{3.2}$	layer of sound absorbing material placed between two sound absorbing plates — as the external layer in the wall
6	$\Delta R_{3.3}$	sticking of a layer of sound absorbing material to the sound absorbing plate of the wall
7	ΔR_4	great holes in the wall (ventilating, technological holes)
8	ΔR_5	small holes and fissures in the wall
9	$\Delta R_{5.1}$	holes in the wall
10	$\Delta R_{5.2}$	fissurs in the wall
11	$\Delta R_{5.3}$	way of arrangement of holes (perforation) in the wall
12	ΔR_6	way of fastening of the wall to the supporting structure frame
13	ΔR_7	acoustic bridge in constructional solution of layer wall
14	$\Delta R_{7.1}$	linear acoustic bridges
15	$\delta r_{7.2}$	point acoustic bridges
16	ΔR_8	elastic properties of wall material
17	ΔR_9	constructional solution of complex wall — with an element of window or eyehole
18	ΔR_{10}	volume mass of sound absorbing material applied in constructional solution of the wall
19	Δr_{11}	solutions of contacts and joints of components
20	$\Delta R_{11.1}$	kind of joints between the walls
21	$\Delta R_{11.2}$	joints on the contact of doors, windows and flaps and their embrasures
22	$\Delta R_{11.3}$	fissures in joints between walls
23	ΔR_{12}	kind of seals in contacts and joints of the wall
24	$\Delta R_{12.1}$	seals in contacts of wall and enclosure supporting structure
25	$\Delta R_{12.2}$	seals in joints of walls
26	$\Delta R_{12.3}$	irregularity of seal holding down in the joint contact
27	$\Delta R_{12.4}$	sound transmission by the supporting structure
28	ΔR_{13}	material structure in constructional solution of the wall

$$R_3 = \sum_{j=1}^{3} \triangle R_{3j}, \quad \text{dB}$$

$$R_5 = \sum_{j=1}^{3} \triangle R_{5j}, \quad \text{dB}$$

$$R_7 = \sum_{j=1}^{2} \triangle R_{7j}, \quad \text{dB}$$

$$R_{11} = \sum_{j=1}^{3} \triangle R_{11j}, \quad \text{dB}$$

$$R_{12} = \sum_{j=1}^{4} \triangle R_{12j}, \quad \text{dB}$$

$\triangle R_i$ — parameters defining the increase (decrease) of the acoustic insulation of enclosure wall Table 1.

The acoustic insulation of the enclosure wall is a function of the following material factors: the volume density of the wall material, the longitudinal modulus of elasticity, the internal loss coefficient in the wall material, the Poisson's ratio, the wall thickness, the frequency of the incident sound wave, the void ratio of the wall material.

The following constructional factors that influence the acoustic insulation characteristics of the enclosure wall should be mentioned the acoustic homogeneity or heterogeneity of the wall, the acoustic homogeneity or heterogeneity of the wall surface, the type of joints and the way of fastening of the wall to the circuit, the tightness of the wall on the entire surface etc.

4. Study of the material and constructional solutions on the acoustic effectiveness of enclosures

The important acoustic effectiveness, a large range of applications the only possible way to limit the noise in many cases — these are the arguments for the application of enclosures in industrial plants, as well as for further studies of new improved material and constructional solutions. The author has executed many experimental studies [3] in order to determine the influence of the material and constructional factors on the acoustic effectiveness of enclosures. The research work included:

1. Investigations of the influence of the solutions of contacts and joints of enclosure components taking into account:

a) the influence of the kind of joints between the walls,

b) the influence of the joints on the contact of doors, windows and flaps and their embrasures,

12.

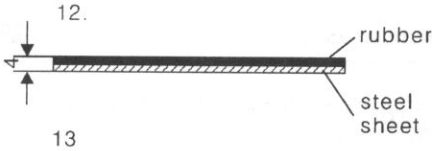

13

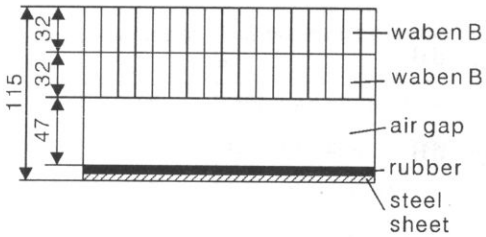

14.

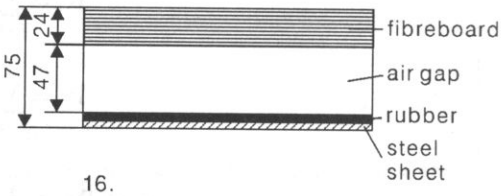

15.

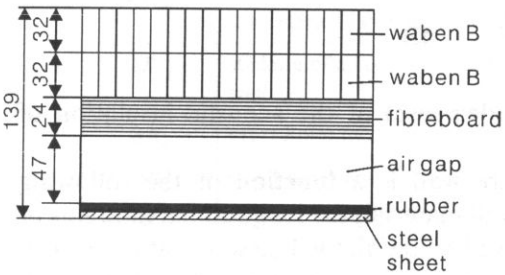

16.

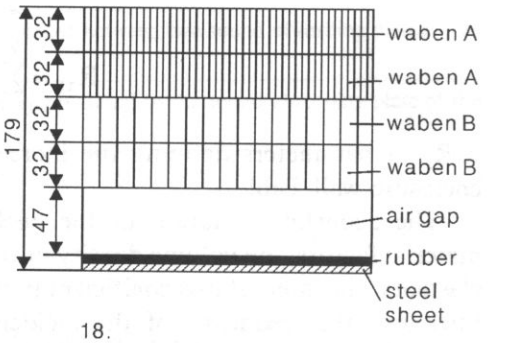

17.

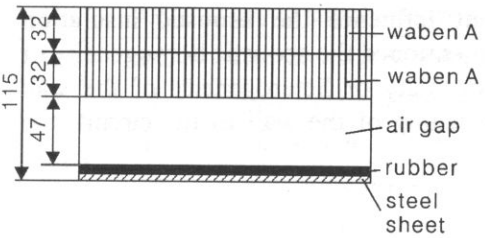

18.

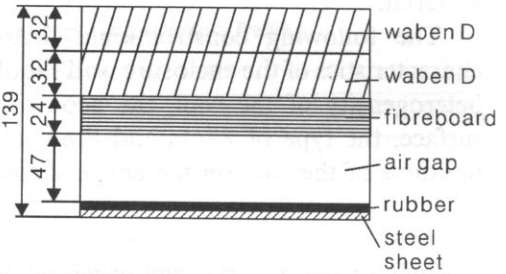

19.

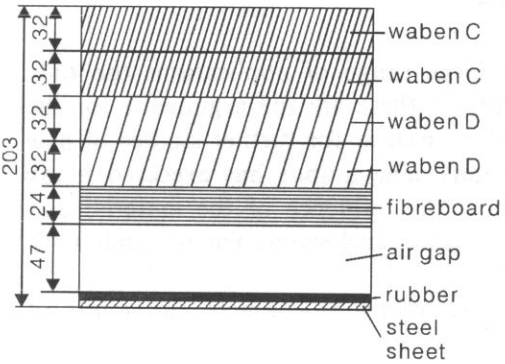

20.

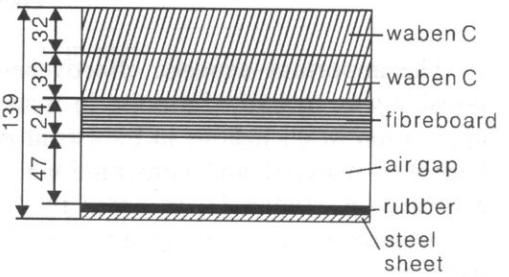

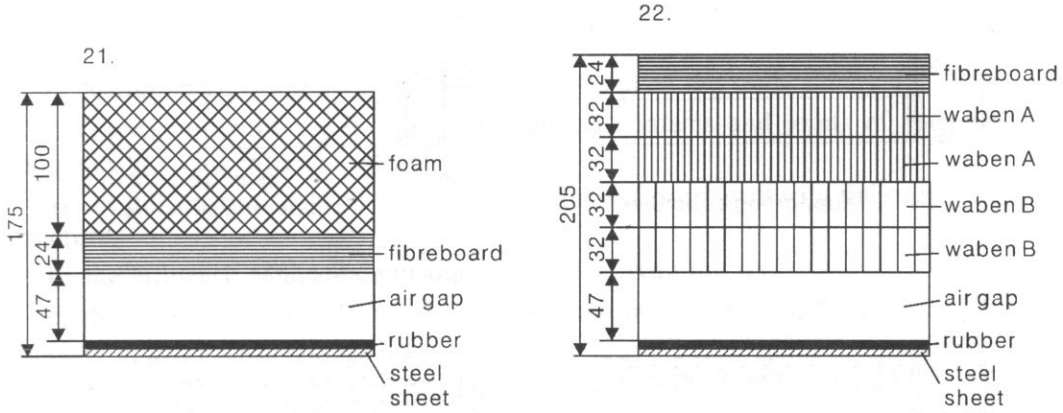

Fig. 2a. Schemes of variants of layer walls used in the experimental research of the influence of the wall material structure on the acoustic insulation of an enclosure.

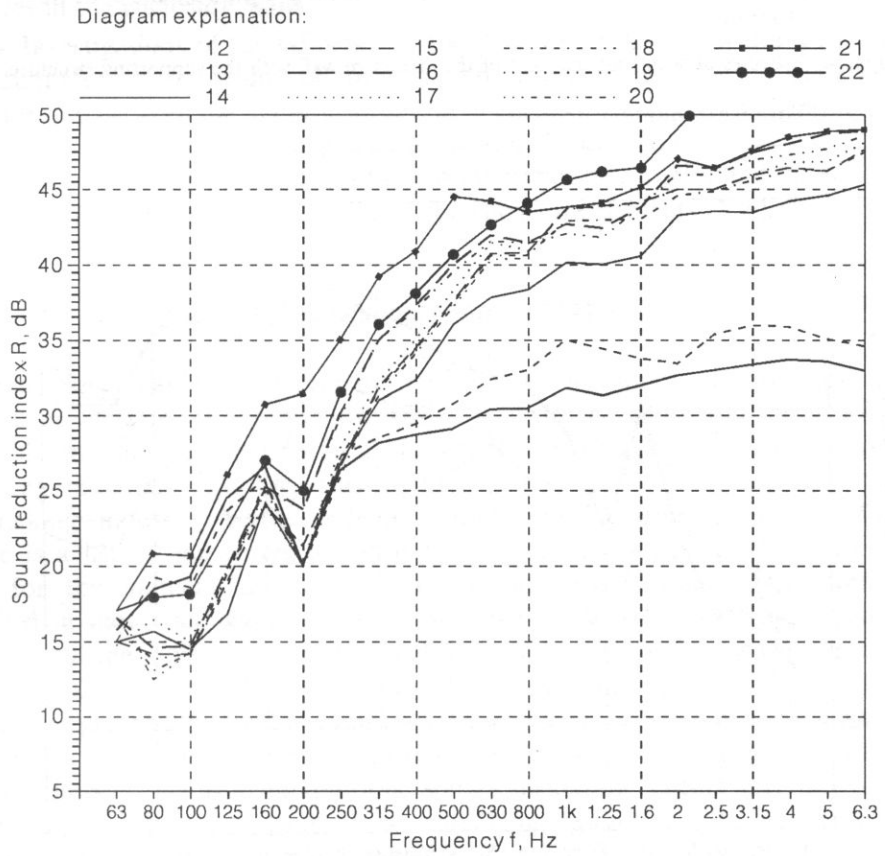

Fig. 2b. Comparison of the characteristics of sound insulation for different variants of layer walls of the enclosure.

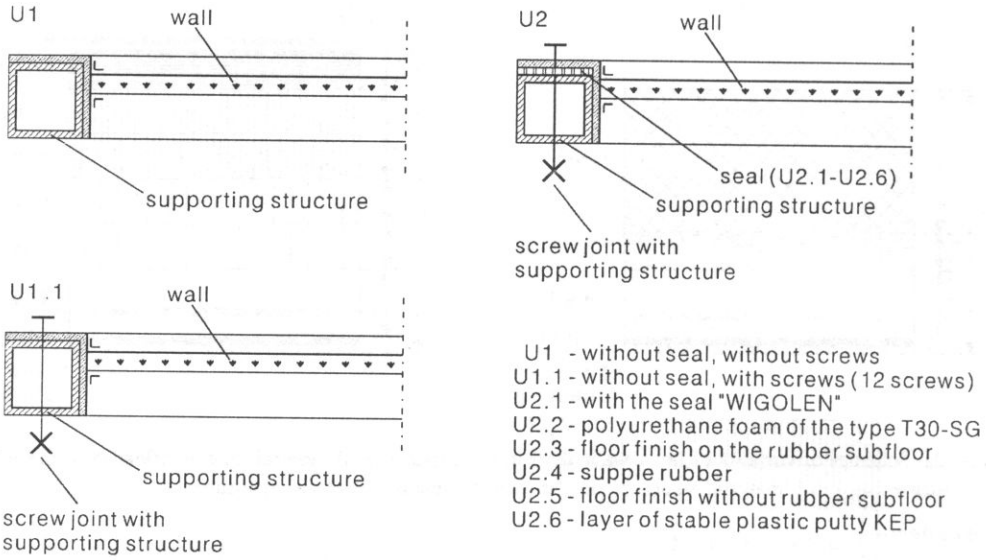

Fig. 3a. Schemes of seals and the joint of the enclosure wall with the supporting structure.

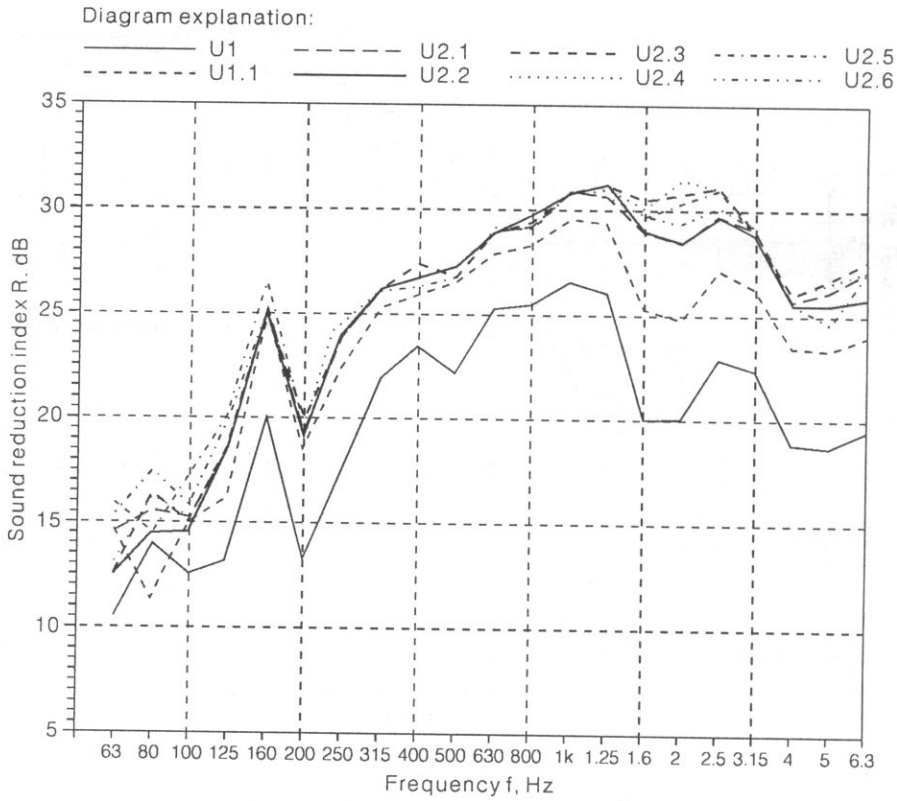

Fig. 3b. Comparison of the characteristics of sound insulation for different kinds of seals in contacts and joints of enclosure elements.

c) the influence of the fissures in the joints between the walls.

2. Investigations of the influence of seals on contacts and joints of enclosure components taking into account:

a) the influence of seals on the contacts of the enclosure wall with the supporting structure,

b) the influence of the seals in the contacts between the walls,

c) the influence of the roughness of the seal holding down in the point of the joint contact,

d) the influence of the sound transmission of the supporting structure,

e) the influence of the way of fastening the enclosure wall to the frame of the supporting structure.

3. Investigations of the influence of the constructional solutions of holes and fissures in the enclosure walls.

4. Investigations of the influence of the structure of the enclosure wall material.

Examples of the results of investigations executed in order to determine the relationship between the material structure of enclosure wall and its characteristics of sound insulation, R [3, 5], are presented in Figs. 2a and 2b.

Figures 3a and 3b present one of the results of the investigation of the effect of the seal kind on the contacts and joints of the enclosure elements [3, 4].

5. Practical appliation of enclosures

Enclosures can be applied in many noisy machines and devices situated inside or outside of production halls in different industrial branches. It is possible to apply enclosures in factories of heavy industry, chemical industry, building materials industry, glass-making industry, woodworking industry, papermaking industry, textile industry, food industry and others. In Table 2, there is a list of enclosures designed by the author as part of the work carried out for the industry of the Mechanics and Vibroacoustics Department and applied in industrial plants emitting excessive noise to the external environment caused by the noise sources situated in open air, outside or productive and technological objects. The enclosures listed in Table 2 were either the only antinoise protection applied limiting the emission of the environment up to admissible values or they entered into a complex set of applied passie protections noise dumpers, acoustic adaptation, sound insulating shields etc. the total implementation of which enabled to satisfying results in the improvement of the acoustic climate of the environment.

Figures 4 and 5 present examples of the applied enclosures.

Table 2. List of enclosures implemented in the industry in the years 1991 – 1994

No.	Noise source Kind of enclosure (Number of items)	Implementation place (Year of implementation)	Acoustic insulation of enclosure $D_{A obud}$, dB	Noise limitation effect obtained in the environment $\Delta L_{A eq}$, in dB
1	Unit of four fan water coolers Entirely closed (1)	Krakowskie Zakłady Teleelektroniczne „TELKOM-TELOS" w Krakowie (1991)	10.0	14.0
2	Unit of four pumping engines Partly closed (4)	Przedsiębiorstwo Eksploatacji Rurociągów Naftowych „PRZYJAŹŃ" w Płocku Przepompownia Ropy ST-3 w Górach k/Płocka (1993)	23.0	17.0
3	Unit of two fans of flue gas draught and dust collection plants in the boiler house Entirely closed (2)	Krakowskie Zakłady Przemysłu Owocowo-Warzywnego w Krakowie (1993)	26.0	18.0
4	Unit of three fans of flue gas draught in the boiler house Entirely closed (3)	Okręgowa Spółdzielnia Mleczarska w Pajęcznie (1993)	25.0	30.0
5	Station of two air compressors in the boiler house Entirely closed (1)	Okręgowa Spółdzielnia Mleczarska w Pajęcznie (1993)	30.0	30.0
6	Unit of two condensors in the refrigerating engine room Entirely closed (1)	Okręgowa Spółdzielnia Mleczarska w Pajęcznie (1993)	23.0	30.0
7	Unit of two equalizing tanks in the air compressor room Entirely closed (1)	Zakłady Przemysłu Lekkiego „WIGOLEN" S.A. w Czestochowie (1994)	29.0	21.0

Fig. 4. Entirely closed enclosure (with noise dumpers on the exhaust holes) protecting the unit of two condensers in the Okręgowa Spółdzielnia Mleczarska in Pajęczno.

Fig. 5. Unit for partly closed enclosures (on openwork base) protecting the pumping engines in the Przepompownia Ropy ST-3 in Góry k/Płocka.

6. Studies of acoustic effectiveness of enclosures

The value of the acoustic insulation D_{obud} [1], is a measure of the acoustic effectiveness of the enclosure. The difference between the mean value, L_{pm1} (measured in dB), of the acoustic pressure levels at all the measurement points during the work of a machine or device without enclosure and the mean value, L_{pm2} (measured in dB), of those levels at the same points during the work in an enclosure, at frequencies of the central octave bands ranging from 63 to 8000 Hz, is defined as the acoustic insulation value of the enclosure. The acoustic insulation of an enclosure can be determined also by means of a parameter D_{Aobud} (defined as the difference of A sound level L_A before and after application of the enclosure). The required effectiveness of the enclosure is directly related to the limitation of the noise emission to the external environment, i.e. to the acoustic preserved teritority in the neighbourhood of an external noise source for which the antinoise protection in the form of an enclosure was applied. Therefore, the studies of the acoustic effectiveness of enclosures are executed simulatneously with the studies of the acoustic climate in the environment. Table 2 presents the results of studies of acoustic environment at the most unfavourable point of the influence of industrial noise of the border of a factory or within the acoustic zone preserved.

7. Conclusion

As the presented review of the completed implementation works shows, enclosures still have an important application in the set of passive protections limiting industrial noise. The enclosures used in many industrial plants proved to be very useful. Enclosures can be applied as the individual protections or they can be an element of a set of several sound insulation means applied together. It is a way to considerable improve the limiting of the influence of industrial noise on the environment.

Experimental studies executed in order to elaborate new improved material and constructional solutions of enclosures proved that:

— the decrease of the assumed acoustic insulation of the enclosure D_{obud}, in spite of the choice of walls with appropriate acoustic insulation R_s, can be caused by the influence of the material and constructional factors which are formulated as a function of the parameters ΔR_i defining the increase or decrease of the acoustic insulation of the wall. The identification and determination of the parameters ΔR_i makes it possible to avoid a decrease in the acoustic insulation of the enclosure, D_{obud}, and thereby to fulfill of the requirements concerning the desired effectiveness of the enclosure.

— the knowledge of the parameters ΔR_i enables to design effective enclosures by selection of appropriate sound-absorbing and sound-insulating materials for the enclosure walls and also by the design of technical solutions of enclosure elements that are correct from the acoustic point of view.

The author is going to adress his experimental studies in the future to the elaboration of a new material and constructional solution of the barrier wall with acoustic insulation increased in comparison with the solutions applied now. The wall will be designed to construct integrated enclosures. Those enclosures, that have been rarely in use up till now, are one of the components of the frame of a noisy machine or from the entire machine frame appropriately elaborated from the acoustic point of view. The elaborated of preliminary assumptions for the design of a new generation of the frames for selected machines, characterized by an increased vibroacoustic energy absorption, will be further extension of the planned research.

References

[1] Z. ENGEL and J. SIKORA, *Enclosures* (in Polish), Wyd. AGH, Kraków 1989.

[2] Z. ENGEL and J. SIKORA, *Enclosures* (in Polish), chapter 18, p. 443–474, Podstawowe Problemy Współczesnej Techniki, T. XXVII, Wibroakustyka Maszyn i Środowiska, pod red. Z. Engela, Wiedza i Życie, Warszawa 1995.

[3] J. SIKORA, *Influence of selected material and constructional solutions on the acoustic effectivenes of enclosures* (in Polish), Ph. D. Thesis Academy of Mining and Metallurgy, Kraków 1994.

[4] J. SIKORA, *Influence of solutions of contacts and joints of the enclosure on its acoustic effectiveness* (in Polish), Mechanika, Scientific quarterly of the Academy of Mining and Metallurgy, 14, 2, 183–204 (1995).

[5] J. SIKORAa, *Study of the influence of the wall materials structure on the acoustic insulatio of enclosures* (in Polish), Mechanika, Scientific quarterlyof the Academy of Mining and Metallurgy, 14, 2, 165–181 (1995).

[6] J. SIKORA, *Enclosures: Solutions, study of acoustic effectivenes in real conditions*, Noise Control 95, Proc., Warsaw, June 1995, 295–298.

[7] H.M. BOHNY and others, *Lärmschutz in der Praxis*, München, R. Oldenbourg Verlag, 1986.

[8] I.I. BOGOLEPOV, *Sound insulation in industry*, (in Russian), Leningrad, Sudostrojenie 1986.

[9] F. FAHY, *Sound and structural vibration, radiation, transmission and response*,London, Academic Press, 1985.

[10] D.M. LIPSCOMB and A.C. TAYLOR, *Noise control handbook of principles and practices*, New York, Van Nostrand Reinhold Company 1978.

[11] R.H. MILLER and W.V. MONTONE, *Handbook of acoustical enclosures and barriers*, Atlanta, The Fairmont Press Inc., 1978.

[12] *Noise control in industry*, Sound Research Laboratories Ltd, Sudbury, Suffolk, Third edition 1991, E. and F.N. Spon, An imprint of Chapman and Hall, London–New York–Tokyo–Melbourne–Madras.

[13] J. SADOWSKI, *Principles of sound insulation of structures* (in Polish), Warszawa, wyd. PWN 1973.

[14] Ju.P. ŠČEV'EV, *Acoustical properties of heterogeneous and composed building materials* (in Russian), Moscow, Strojizdat' 1980.

ARCHIVES OF ACOUSTICS
21, 3, 299–309 (1996)

INFLUENCE OF THE EXTERNAL WALL ON THE AIRBORNE SOUND INSULATION IN BUILDINGS

B. SZUDROWICZ and A. IŻEWSKA

Building Research Institute
(00-950 Warszawa, ul. Filtrowa 1)

The external wall, just as all the other partitions in the building, takes part in the sound transmission by the flanking structural path. Depending on the construction of the external wall, its influence on the total value of the airborne flanking transmission may be different. The papers presents two different solutions of the external walls: 1) walls which may be considered as panels and 2) multi-layer partitions, where the direct sound insulation is clearly lowered near the resonance frequency existing in the range of the frequencies found in buildings. The analysis considered both the calculation formula according to the EN standard [1] as well as the results of our own measurements performed in the building.

1. Introduction

From the acoustic point of view, the external wall is treated as a construction element protecting the room the penetration of external noise. Standards depending on the level of external noise and the destination of a room determine the value of the required direct airborne sound insulation of its external wall.

The external wall, just as all the other partitions in the building, also takes part in transmitting noise in the building through the flanking structural paths. Depending on the construction of the external wall, its influence on the total value of the flanking transmission in the building may be different.

The flanking airborne insulation of some structural and construction solutions of external walls used in practice is so small that it determines the airborne sound insulation between rooms.

Such solution include certain types of multi-layer partitions where the direct airborne sound insulation is clearly lowered near the resonance frequency existing in the important range of frequencies found in the building.

The European Standard being developed at the moment gives precise and simplified methods which enable the evaluation of the influence of the external wall

on the value of the flanking sound transmission in the building. Nevertheless, these methods cannot be used directly for determination of the flanking sound transmission of many massive multilayer partitions used in practice. It is therefore necessary to evaluate this type of structures on the basis of empirical tests.

The investigation presented in this paper was financed by the Polish Committee for Scientific Research.

2. General principles

The apparent sound reduction index R' of the internal partition in the building results from its direct sound reduction index R_{Dd} and the flanking sound reduction indices R_{ij}.

The separation of the influence of the external wall in the general calculation formula may be presented as follows:

$$R' = -10\log\left[10^{-0.1R_{Dd}} + \sum_{k_{ext}}\sum_{ij} 10^{-0.1R_{ij,k_{ext}}} + \sum_{k_{int}}\sum_{ij} 10^{-0.1R_{ij,k_{int}}}\right], \tag{2.1}$$

where:

R_{Dd} sound reduction index of the separating element (direct transmission), dB
$R_{ij,k_{ext}}$ sound reduction index of the flanking path ij of the external wall, dB
$R_{ij,k_{int}}$ sound reduction index of the flanking path ij of the internal partitions, dB
ij following flanking paths ij at a given junction,
k_{ext} number of junctions at the separating partition with external walls in a given room,
k_{int} number of junctions at the separating partition with internal partitions in a given room.

In practice we usually have $k_{ext}=1$ and $k_{int}=3$. If $k_{ext}>1$, then the influence of the external wall on the total flanking transmission increases.

If we assume that the structural reverberation time of the partition in an actual field situation and in the laboratory is approximately the same ($T_{s,situ}=T_{s,lab}$) we can assume for separating elements without additional layers:

$$R_{Dd}=R_s \tag{2.2}$$

where R_s — direct sound reduction index of the separating element determined on the basis of laboratory measurements or calculations.

With assumption that $T=_{s,\ situ}=T_{s,\ lab}$ and the equivalent absorption leng one may, according to EN, determine the insulation of the flanking paths by the expression:

$$R_{ij}=\frac{R_i+R_j}{2}+\Delta R_i+\Delta R_j+K_{ij}+10\log\frac{S_s}{l_f\cdot l_0}, \tag{2.3}$$

where:

R_i sound reduction index for the element i in the source room, dB,
R_j sound reduction index for the element j in the receiving room, dB
ΔR_i sound reduction index improvement by additional layers for the element i, dB
ΔR_j sound reduction index improvement by additional layers for the element j, dB
K_{ij} junction transmission index for each transmission path ij over a junction, dB
S_s area of the separating element, m^2,
l_f common coupling length between the flanking element f and the separating one, m,
l_0 reference length, (= 1 m).

The influence of every flanking partition including the external wall on the value of flanking transmission in the building may be described on the basis of the resulting from the insulation of flanking paths at the edge "k".

If the rooms are not displaced with respect to each other, than the resultant insulation of flanking paths with the given edge k may be presented, considering formula (2.3), as follows:

$$R_{(Ff+Df+Fd)k} = -10\log\left(\frac{l_f \cdot l_0}{S_s}\sum_{ij} 10^{-0.1R_{ij,o}}\right), \tag{2.4}$$

where

$$R_{ij,o} = \frac{R_i + R_j}{2} + \Delta R_i + \Delta R_j + K_{ij}. \tag{2.5}$$

For further analysis a more useful form of formula (2.4) is the following one:

$$R_{(Ff+Df+Ed)k} = R_{(Ff+Df+Fd)k,o} + 10\log\frac{S_s}{l_f \cdot l_o}, \tag{2.6}$$

where

$$R_{(Ff+Df+Fd)k,o} = -10\log\left[10^{-0.1R_{Ff,o}} + 10^{-0.1R_{Fd,o}} + 10^{-0.1R_{Df,o}}\right]. \tag{2.7}$$

Introducing formulas (2.2) and (2.7) in (2.1), it is possible to write the latter in a form allowing for a relatively simple analysis of the influence of various partitions on the flanking transmission in the building

$$R' = -10\log\left[10^{-0.1R_s} + \sum_{k_{ext}} \frac{l_{f,ext} \cdot l_o}{S_s} 10^{-0.1R_{(Ff+Df+Fd)k,o,ext}} + \right.$$
$$\left. + \sum_{k_{int}} \frac{l_{f,int} \cdot l_o}{S_s} 10^{-0.1R_{(Ff+Df+Fd)k,o,int}}\right] \tag{2.8}$$

where

$R_{(Ff+Df+Fd)k,o,ext}$ — expressed by the (2.7) unit is the resultant sound insulation of flanking paths at the edge common for the separating partition and external wall,

$R_{(Ff+Df+Fd)k,o,int}$ — expressed by the (2.7) unit is the resultant sound insulation of flanking paths at the edge common for the separating wall and internal partitions.

Calculation of the insulation of the partition, expressed by (2.8) may be conducted for various frequency bands or by referring to the weighted indices R_w.

3. Buildings with panel structures

In the case of panel structures without additional insulation layers, the weighted direct sound reduction index from airborne transmissions of the separating partition may be presented as a function of its unit mass.

The prEN 12354-1 : 1996 gives the so-called european mass law which for partitions with an area mass $m' > 150$ kg/m², has the form:

$$R_w = 37.5 \cdot \log m' - 42, \tag{3.1}$$

where m′ — surface mass of the partition, kg/m².

In Poland such dependencies have been worked out for various construction materials. For concrete panels with a mass $m' > 100$ kg/m²

$$R_w = 27.1 \cdot \log m' - 15.6. \tag{3.2}$$

The differencies between these dependencies, (3.1) and (3.2), are relatively small. If we consider the fact that K_{ij} for panel partitions is a function of the ratio of masses (m_i/m_j) and it is not influenced by the frequency, $R_{(Ff+Df+Fd),k,o,w}$ may be presented in the form

$$R_{(Ff+Df+Fd)k,o,w} = f\left(\frac{m_s'}{m_f'}\right), \tag{3.3}$$

where m_s' — surface mass of the separating partition, kg/m²,
m_f' — surface mass of the flanking partition, kg/m².

Calculations of the dependency (3.3) were performed taking into consideration the mass law according to (3.2) and using formulas describing K_{ij} given in the draft of EN standards. The results of those calculations for the cross junction are presented in Fig.1. Similar curves may be set for the T junction.

Using data according to Fig. 1 greatly simplifies both the calculations according to formula (2.8), as well as the analysis of the influence of various flanking partitions including the external wall on the total value of flanking transmission in the building.

The curves given in Fig. 1 were verified by numerous measurements in buildings. In most cases, the results of those tests did not differ by more than ± 1 dB from the calculated values.

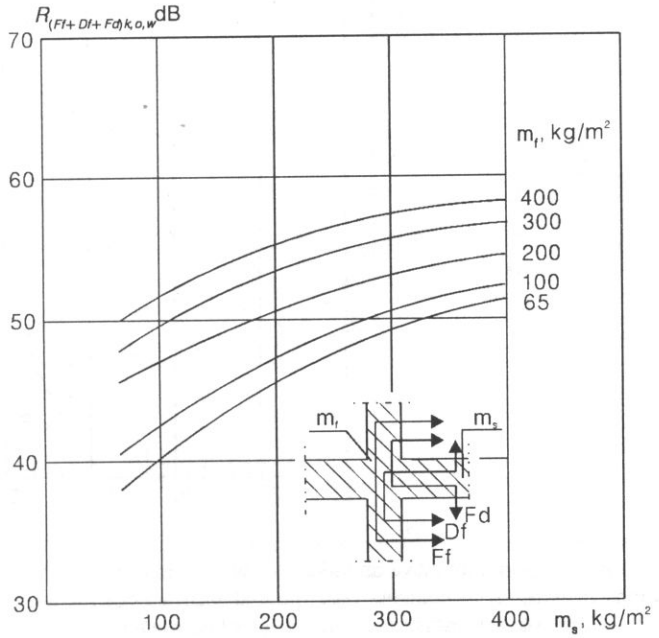

Fig. 1. Weighted index of unit flanking airborne sound insulation $R_{(Ff+Df+Fd)k,o,w}$ of panel partitions (cross junction).

4. Buildings with massive layered walls

Massive external walls are relatively frequently used in multi-family buildings. Such solutions include some types of massive layered walls, in which thermal insulation is made of foamed polystyrene.

Due to the relativity large dynamic rigidity of styrofarm panels the resonance frequency of the layered system is in the mid-frequency band. In the vicinity of this frequency there is an evident decrease of the direct sound reduction index. Examples of such walls are given in Figs. 2 and 3.

On the basis of numerous measurements in buildings, it was found that this phenomenon also causes the deterioration of airborne insulation between rooms in that such walls are used as flanking partitions. Examples of the results of tests made in two buildings are presented in Figs. 4 and 5. The airborne insulation of the ceilings R' was tested using standards methods as well as the resultant insulation of two flanking paths $R_{(Ff+Df)}$ at very edge of the ceilling with side walls, including the external wall. An evident similarity was found between the characteristics of the insulation, R' of the separating partition and $R_{(Ff+Df)}$ of the external wall.

The flanking sound insulation $R_{(Ff+Df)}$ was determined on the basis of the following formula

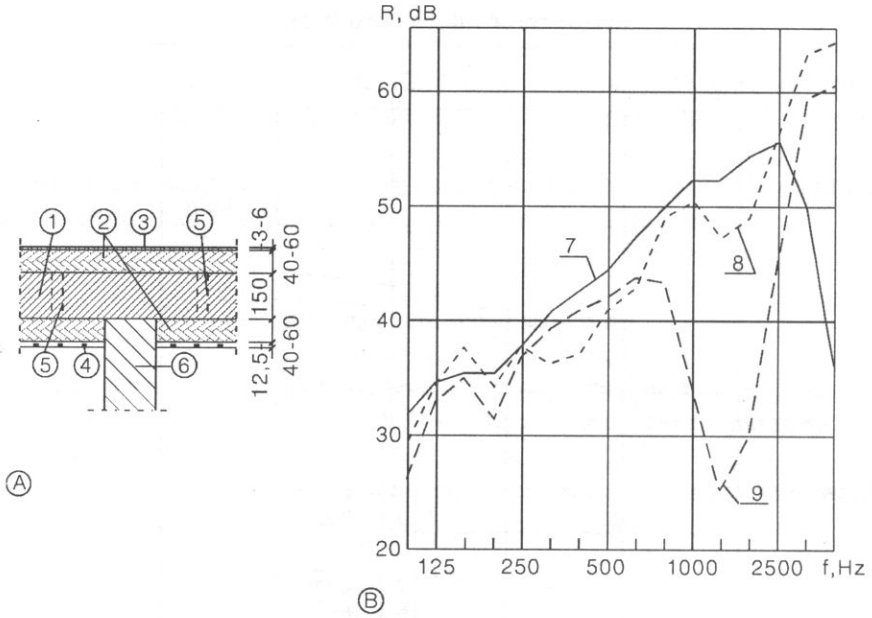

Fig. 2. External massive multi-layer wall — example no. 1

A. Diagram (dimensions in mm): *1* — concrete core (poured on the construction site), *2* — foamed polystyrene panels, *3* — thin plaster mass, *4* — plaster-cardboard panel, *5* — foamed polystyrene connections, *6* — massive internal partition.

B. Direct sound reduction index: *7* — wall without finishing layers according to the diagram, *8* — wall with finishing layers according to the diagram, *9* — wall with finishing layers on both sides made of thin plaster mass.

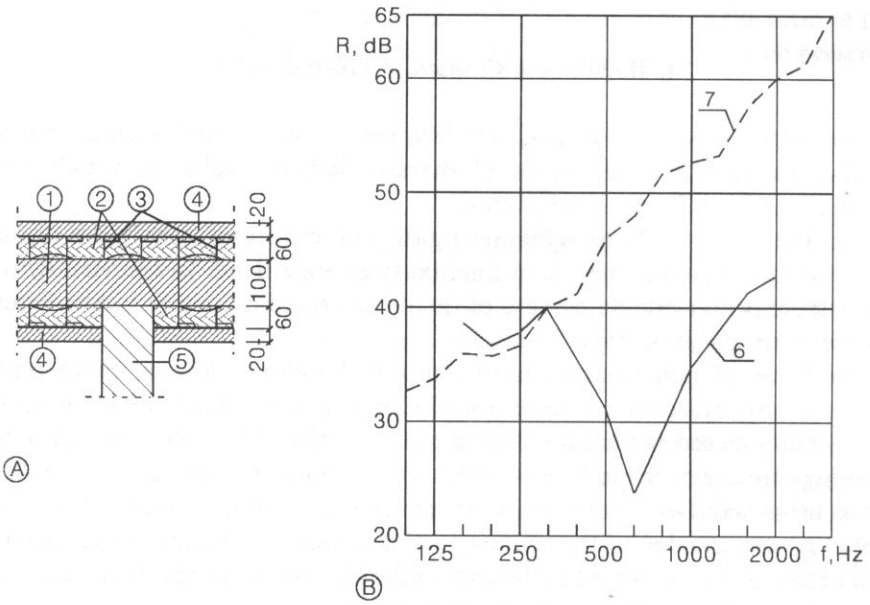

Fig. 3. External massive multi-layer wall — example no. 2

A. Diagram (dimensions in mm): *1* — concrete core poured on the construction site, *2* — foamed polystyrene, *3* — reinforcing net, *4* — gunite (concrete panel shot under presusre), *5* — internal partition.

B. Direct airborne sound insulation: *6* — wall according to diagram, *7* — concrete core.

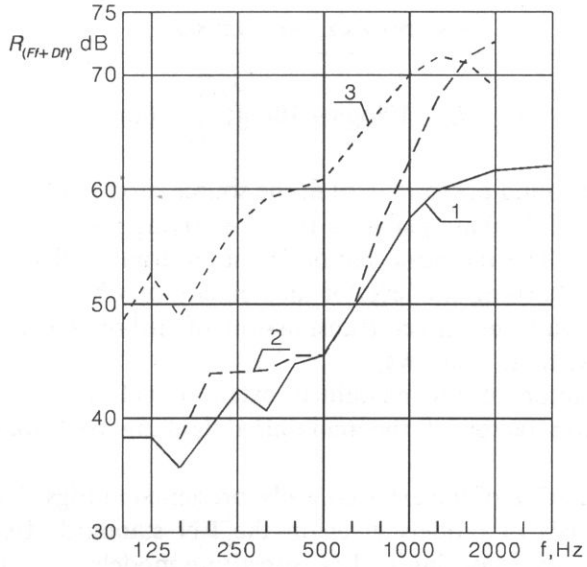

Fig. 4. Airborne sound insulation between rooms in building with an external wall according to Fig. 2. *1* — apparent sound reduction index R' of floor, $S_s=12.9$ m², measured by the standard method, *2* — flanking airborne sound insulation $R_{(Ff+Df)}$ of external wall measured according to formula (4.1), $S_f=7.2$ m², *3* — flanking sound insulation of internal wealls (brick wall of 25 cm thickness), $S_f=24.4$ m² measured according to formula (4.1)

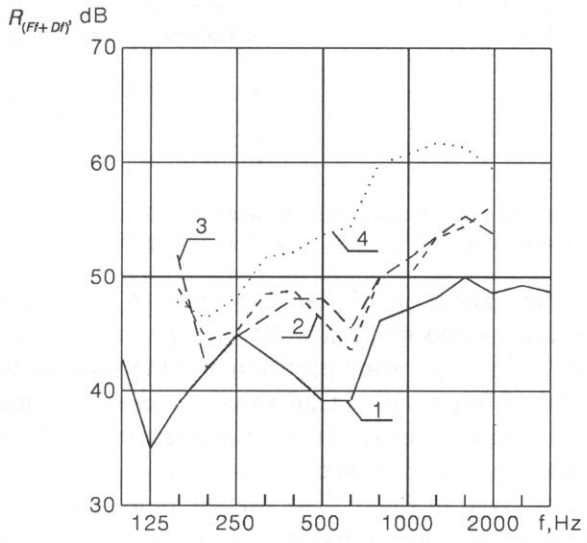

Fig. 5. Airborne sound insulation between rooms in building with an external wall according to Fig. 3. *1* — apparent sound reduction index R' of floor, $S_s=11.9$ m², measured by the standard method, *2* — flanking sound insulation of external wall $R_{(Ff+Df)}$ measured according to formula (4.1), $S_f=7.0$ m², *3* — flanking sound insulation $R_{(Ff+Df)}$ of internal cellular brick wall of 12.5 cm thickness, $S_f=16.0$ m² measured according to formula (4.1)

$$R_{(Ff+Df)} = L_1 - L_v - 10\log\sigma + 10\log\left(\frac{S_s}{S_f}\right) 10\log\frac{1}{\sigma} + 27.5, \tag{4.1}$$

where: L_1 — average sound pressure level in the source room, dB, L_v — average level of vibration velocity of flanking partition in the receiving room ($v_0 = 10^{-9}$ m/s, dB), σ — radiation factor. The radiation factor of the external wall was determined by measurement, by establishing the level of the velocity of vibrations and that of the sound intensity L_1 with the direct transmission of airborne energy through the external wall (part without windows).

The radiation factor of the examined external wall is significantly greater than 1. The radiation factor of the remaining flanking partitions was assumed to be equal to 1.

The flanking insulation of the external walls, presented in Figs. 2 and 3, cannot be calculated on the basis of models given in the EN standard. Using the general principles of calculation according to EN, substitute models were used in that was assumed that the influence of external layers on the insulation between rooms will be determined empirically. The models for the external walls presented in Figs. 4 and 5 are given in Fig. 6.

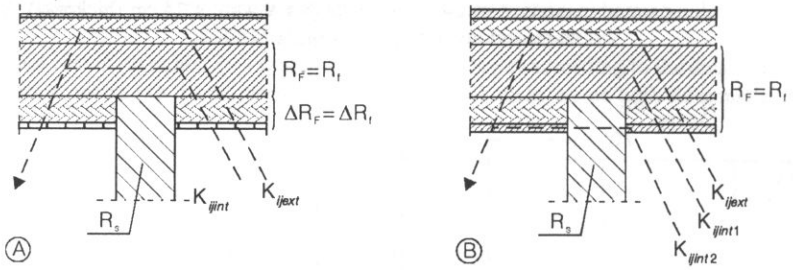

Fig. 6. Models of paths of flanking sound transmission for external walls according to Figs. 2 and 3. A. for wall according to Fig. 2, B. for wall according to Fig. 3.

Measurements of the insulation of flanking paths $R_{(Ff+Df)}$ at the edge of the external wall with the ceiling and internal walls were performed for several pairs of rooms of the same size of the separating partition and the external wall omitting the window area. Examples of test results mean values from several measurements are presented in Figs. 7 and 8. Taking into consideration the structural reverberation time T_s and assuming K_{ij} according to EN, calculations of $R_{(Ff+Df)}$ for the measured cases were made using models given in Fig. 6. The shaded areas in Fig. 7 and 8 show the influence of external layers of the external wall on its flanking insulation $R_{(Ff+Df)}$.

Analyzing the data in Figs. 7 and 8, we must take into consideration the fact that the dispersion of the results of measurements in situ of the sound insulation of flanking paths were quite large and reached ± 4 dB in the low and high frequency bands and slightly lower, (± 2 dB) in the medium one. This may be caused both by different quality of the execution, as well as by the difficulties in measuring the parameters included in formula particularly the radiatoin factor of partitions.

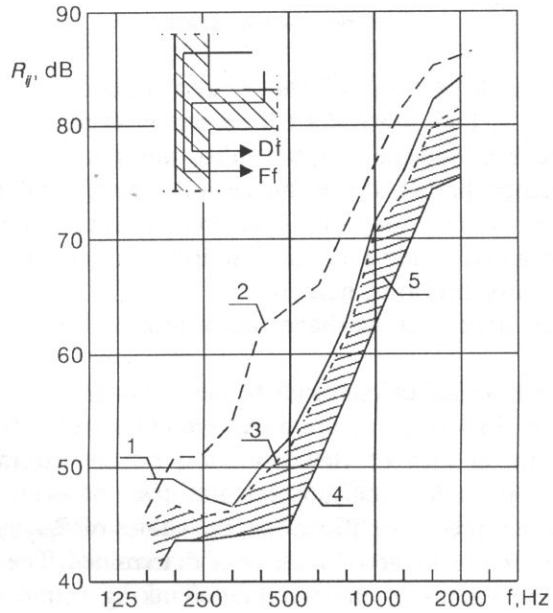

Fig. 7. Comparison of the measured and calculated flankig sound insulations $R_{(Ff+Df)}$ of the external wall according to Fig. 2. *1* — insulation R_{Ff} calculated with omission of external layers of the wall, *2* — insulation R_{Df} calculated with omission of external layers of the wall, *3* — insulation calculated as above $R_{(Ff+Df)}$, *4* — insulation $R_{(Ff+Df)}$ measured in the building (mean values), *5* — influence of external layers on flanking airborne sound insulation $R_{(Ff+Df)}$ of the external wall.

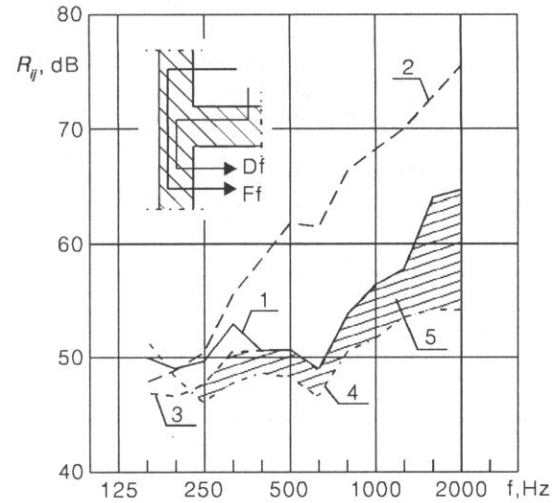

Fig. 8. Comparison of the measured and calculated flankig sound insulation $R_{(Ff+Df)}$ of the external wall according to Fig. 3. *1* — insulation R_{Ff} calculated with omission of external layers of the wall, *2* — insulation R_{Df} calculated with omission of external layers of the wall, *3* — insulation calculated as above $R_{(Ff+Df)}$, *4* — insulation measured in the building (mean values), *5* — influence of external layers on flanking sound insulation $R_{(Ff+Df)}$ of the external wall.

Significantly smaller dispersions of the results were obtained in the case of weighted indices $R_{(Ff+Df),w}$. They were ± 1 dB on the average.

On the basis of the tests and the adopted substitute model we cannot determine, for the various frequency bands, the influence of a given flanking paths on the insulation between rooms. This may be approximately determined by calculations with respect to the weighted sound reduction indices. This requires nevertheless the adoption of additional assumptions, namely:

- for the examines structures we have, according to the general assumption, $R_{Fd,w}=R_{Df,w}$,
- the error in the performed calculations of the values of the indices R_w does not exceed the value of the dispersion of the measurement results, despite the fact the difference in the characteristics of the insulation of the external wall and the saparating partition do not allow for such calculations.

Being aware of the adopted simplifications, the values of $R_{(Ff+Df+Fd),k,o,w}$ for the examined structures of external layered walls were determined. They are given in Fig. 9. For comparison, the values of the weighted flanking sound reduction indices $R_{(Ff+Df+Fd),k,o,w}$ determined on the basis of the diagram in Fig. 2, have also beenincluded. This comparison demonstrates that the discussed external walls cause a significant lowering of the weighted sound reduction index of the ceilings and the internal walls in the building as proved by direct measurements.

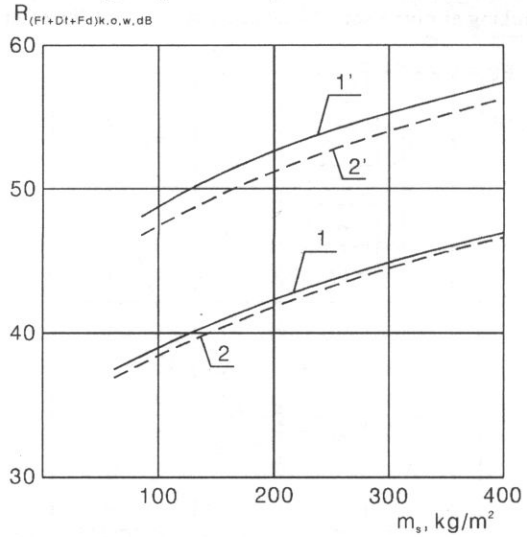

Fig. 9. Weighted unit flanking airborne sound insulation of external walls: *1* — of the wall according to diagram in Fig. 2, *2* — of the wall according to diagram in Fig. 3, *1'* — of the concrete core of the wall according to Fig. 2, *2'* — of the concrete core of the wall accoridng to Fig. 3.

The curves shown in Fig. 7 may be used for a preliminary estimation of the influence of the external walls on the value of the flanking transmission in the building in which the internal partitions may be treated as panels. If this condition is

not fulfilled e.g. the internal partitions are double structures then, depending on the structures, the connection between the external wall and the internal partitions, i.e. the values of indices $R_{(Ff+Df+Fd),k,o,w}$, differ significantly from those given in Fig. 7. We see from the tests performed that it does not refer to the case when floating floors are used on the massive ceilings.

5. Conclusions

In the sound evalution of the external wall we should consider both its direct as well as flanking airborne sound insulation.

The influence of the external panel wall on the flanking sound transmission in the building may be evaluated approximately on the basis of its surface mass.

In practice there are several solutions for external walls which clearly increases the flanking sound transmission in the building. An example of such a wall was discussed in this paper on the basis of the results of measurements and calculations.

The influence of external walls of the structure described in this paper on the value of the flanking airborne transmission in the building may be temporarily estimated on the basis of data found in Fig. 7.

References

[1] *Building Acoustics — Estimation of acoustic performance of buildings performance of products. Part 1. Airborne sound insulation between rooms* prEN-12354-1 : 1996.

[2] B. SZUDROWICZ and A. IŻEWSKA, *Flanking transmission ins building with multi-layer partitions*, Inter-Noise 94, Yokohama, pp. 1575–78.

[3] B. SZUDROWICZ and A. IŻEWSKA, *Simplified evaluation of flanking transmission based on mean mass and mean area of flanking elements*, Proceedings of CIB W-51-Acoustics Conference, Warsaw 1994, pp. 140–56.

ARCHIVES OF ACOUSTICS
21, 3, 311–316 (1996)

DISPERSION PROPERTIES OF TRANSVERSELY ISOTROPIC LAYERED SHELLS

Š. MARKUŠ and T. NÁNÁSI

Institute of Materials and Machine Mechanics
Slovak Academy of Sciences
Bratislava, Slovakia

Harmonic wave propagation in thick, cylindrical, three-layered shells of infinite length was studied. Both the outer layers and the core are composites made of short strand fiberglass resin, but the planes of isotropy in the outer layers are orthogonal to the plane of isotropy at the core. A closed form solution of the exact linear equations of elasticity was sought in terms of Frobenius power series. The influence of the core thickness on the dynamics of the wave motion is estimated from numerically computed dispersion curves. Prime consideration was given the asymmetric wave motion and the different types of waves which can occur are identified over a wide range of wave numbers.

1. Stress-strain and strain — displacement relationships

Let u_i, v_i and w_i be the orthogonal components of displacement in axial (x-wise), circumferential (φ-wise) and radial (z-wise) directions of the i-th layer, respectively. The stress-strain relationship for the outer layers made of transversely isotropic material with the plane of isotropy parallel to the $x-r$ is of the form:

$$\begin{bmatrix} \sigma_{xi} \\ \sigma_{\varphi i} \\ \sigma_{ri} \\ \tau_{\varphi ri} \\ \tau_{xri} \\ \tau_{x\varphi i} \end{bmatrix} = \begin{bmatrix} C_{11i} & C_{12i} & C_{13i} & 0 & 0 & 0 \\ C_{12i} & C_{22i} & C_{12i} & 0 & 0 & 0 \\ C_{13i} & C_{12i} & C_{11i} & 0 & 0 & 0 \\ 0 & 0 & 0 & C_{44i} & 0 & 0 \\ 0 & 0 & 0 & 0 & C_{55i} & 0 \\ 0 & 0 & 0 & 0 & 0 & C_{44i} \end{bmatrix} \begin{bmatrix} \varepsilon_{xi} \\ \varepsilon_{\varphi i} \\ \varepsilon_{ri} \\ \gamma_{\varphi ri} \\ \gamma_{xri} \\ \gamma_{x\varphi i} \end{bmatrix} \tag{1.1}$$

where $C_{55i}=1/2(C_{11i}-C_{13i})$, for $i=2$ (the core). The stress-strain relationship for the middle layer made of transversely isotropic material with the plane of isotropy parallel to the $x-\varphi$ plane is given in the form:

$$\begin{bmatrix} \sigma_{xi} \\ \sigma_{\varphi i} \\ \sigma_{ri} \\ \tau_{\varphi ri} \\ \tau_{xri} \\ \tau_{x\varphi i} \end{bmatrix} = \begin{bmatrix} C_{11i} & C_{12i} & C_{13i} & 0 & 0 & 0 \\ C_{12i} & C_{22i} & C_{12i} & 0 & 0 & 0 \\ C_{13i} & C_{12i} & C_{11i} & 0 & 0 & 0 \\ 0 & 0 & 0 & C_{44i} & 0 & 0 \\ 0 & 0 & 0 & 0 & C_{44i} & 0 \\ 0 & 0 & 0 & 0 & 0 & C_{66i} \end{bmatrix} \begin{bmatrix} \varepsilon_{xi} \\ \varepsilon_{\varphi i} \\ \varepsilon_{ri} \\ \gamma_{\varphi ri} \\ \gamma_{xri} \\ \gamma_{x\varphi i} \end{bmatrix} \tag{1.1''}$$

where $C_{66i}=1/2\ (C_{11i}-C_{12i})$ for $i=1, 3$ (inner and outer layers).

The strain-displacement relations in polar coordinates are:

$$\varepsilon_{xi}=\frac{\partial u_i}{\partial x}, \qquad \gamma_{r\varphi i}=\frac{\partial v_i}{\partial x_i}+\frac{1}{r}\frac{\partial u_i}{\partial \varphi}$$

$$\varepsilon_{ri}=\frac{\partial w_i}{\partial r}, \qquad \gamma_{xri}=\frac{\partial w_i}{\partial x}+\frac{\partial u_i}{\partial r} \tag{1.2}$$

$$\varepsilon_{\varphi i}=\frac{1}{r}\frac{\partial v_i}{\partial \varphi}+\frac{w_i}{r} \qquad \gamma_{\varphi ri}=\frac{1}{r}\frac{\partial w_i}{\partial \varphi}+\frac{\partial v_i}{\partial r}-\frac{v_i}{r}.$$

2. Governing differential equations

Consider a thick shell with homogeneous orthotropic layers. The three-dimensional equilibrium equations for each layer can be expressed as follows [1]:

$$\frac{\partial \sigma_{xi}}{\partial x}+\frac{1}{r}\frac{\partial \tau_{x\varphi i}}{\partial \varphi}+\frac{1}{r}\frac{\partial}{\partial r}(r\tau_{xri})=\rho_i\frac{\partial^2 u_i}{\partial t^2}$$

$$\frac{1}{r^2}\frac{\partial}{\partial r}(r^2\tau_{\varphi ri})+\frac{1}{r}\frac{\partial \sigma_{\varphi i}}{\partial \varphi}+\frac{\partial \tau_{x\varphi i}}{\partial x}=\rho_i\frac{\partial^2 v_i}{\partial t^2} \tag{2.1}$$

$$\frac{\partial \tau_{xri}}{\partial x}+\frac{1}{r}\frac{\partial \tau_{x\varphi i}}{\partial \varphi}+\frac{1}{r}\frac{\partial}{\partial r}(r\sigma_{ri})-\frac{1}{r}\sigma_{\varphi i}=\rho_i\frac{\partial^2 w_i}{\partial t^2},$$

Dimensionless variables have first been introduced in the form $r=zH$ and $x=\xi R_4$, with H being the total thickness, R_4 the outer radius of the cylinder, and $\kappa=R_4/H$ and $\lambda=R_4/L$, where L is the wavelength. The stress-strain and strain-displacement relationships (1.1)', (1.1)'' and (1.2) are now used to obtain the governing differential equations of the three-dimensional elasticity in terms of displacement:

$$\begin{aligned} &[C_{11i}D_{\zeta\zeta}+\kappa^2 C_{55i}(D_{zz}+D_z/z)+\kappa^2/z^2 C_{66i}D_{\varphi\varphi}]u_i+\kappa/z(C_{12i}+C_{66i})D_{\zeta\varphi}v_i+ \\ &+[\kappa/z(C_{55i}+C_{12i})D_\zeta+\kappa(C_{13i}+C_{55i})D_{z\zeta}]w_i=\rho_i R_4^2 D_{tt}u_i, \\ &\kappa/z(C_{12i}+C_{66i})D_{\zeta\varphi}u_i+[C_{66i}D_{\zeta\zeta}+\kappa^2/z^2 C_{22i}D_{\varphi\varphi}+ \end{aligned} \tag{2.2}$$

$$+\kappa^2 C_{44i}(D_{zz}+1/zD_z-1/z^2)]v_i+ \qquad (2.2)$$
$$+[\kappa^2/z(C_{23i}+C_{44i})D_{z\varphi}+\kappa^2/z^2(C_{22i}+C_{44i})D_{\varphi}]w_i=\rho_i R_4^2 D_{tt}v_i\,,$$
[cont.]

$$[\kappa(C_{13i}+C_{44i})D_{z\varphi}-\kappa^2/z^2(C_{22i}+C_{44i})D_{\varphi}]v_i+$$
$$+[C_{55i}D_{\zeta\zeta}+\kappa^2/z^2C_{44i}D_{\varphi\varphi}+\kappa^2C_{33i}(D_{zz}+1/zD_z)-\kappa^2/z^2C_{22i}]w_i=\rho_i R_4^2 D_{tt}w_i\,.$$

3. Boundary and continuity conditions

For the purpose of this treatment we assume the inside and outside surfaces of the layered cylinder to be stress free. Furthermore, at the internal interfaces of the adjacent layers there is equality of each displacement and of the shear and normal stress components. The stresses are given by the following equations [2]:

$$\sigma_{zi}(z,\varphi,\xi)=\left[C_{13i}\lambda u_i+\frac{C_{23i}}{z}(nv_i+w_i)+C_{33i}w_i'\right]\sin(\lambda R_4\xi)\cos(n\varphi)e^{i\Omega t} \qquad (3.1)$$

$$\tau_{z\zeta i}(z,\varphi,\xi)=C_{55i}(u_i'-\lambda w_i)\cos(\lambda R_4\xi)\cos(n\varphi)e^{i\Omega t}$$

$$\tau_{z\varphi i}(z,\varphi,\xi)=C_{44i}\left(v_i'-\frac{nw_i+v_i}{z}\right)\cos(\lambda R_4\xi)\sin(n\varphi)e^{i\Omega t}\,,$$

The boundary and continuity conditions are defined as follows:

$$\sigma_{z1}(R_1)=0, \quad \tau_{z\xi 1}(R_1)=0, \quad \tau_{z\varphi 1}(R_1)=0,$$
$$\sigma_{z1}(R_2)=\sigma_{z2}(R_2), \quad \tau_{z\xi 1}(R_2)=\tau_{z\xi 2}(R_2), \quad \tau_{z\varphi 1}(R_2)=\tau_{z\varphi 2}(R_2),$$
$$u_1(R_2)=u_2(R_2), \quad v_1(R_2)=v_2(R_2), \quad w_1(R_2)=w_2(R_2),$$
$$u_2(R_3)=u_3(R_3), \quad v_2(R_3)=v_3(R_3), \quad w_2(R_3)=w_3(R_3),$$
$$\sigma_{z2}(R_3)=\sigma_{z3}(R_3), \quad \tau_{z\xi 2}(R_3)=\tau_{z\xi 3}(R_3), \quad \tau_{z\varphi 2}(R_3)=\tau_{z\varphi 3}(R_3),$$
$$\sigma_{z3}(R_4)=0, \quad \tau_{z\xi 3}(R_4)=0, \quad \tau_{z\varphi 3}(R_4)=0.$$

4. Solutions of differential equations

As the system of differential equations (2.2) is singular at $z=0$, the general solution is sought in terms of generalized power series (Frobenius series):

$$u_i=\sum_{j=1}^{j=6}A_{ij}\sum_{k=0}^{k=\infty}a_{kj}z^{k+\alpha_j}[\sin(\lambda R_4\xi)\cos(n\varphi)\exp(i\Omega t)], \qquad (4.1)$$

$$v_i = \sum_{j=1}^{j=6} A_{ij} \sum_{k=0}^{k=\infty} b_{kj} z^{k+\alpha_j} [\cos(\lambda R_{4\xi}) \sin(n\varphi) \exp(i\Omega t)], \qquad (4.1)$$

[cont.]

$$w_i = \sum_{j=1}^{j=6} A_{ij} \sum_{k=0}^{k=\infty} c_{kj} z^{k+\alpha_j} [\cos(\lambda R_{4\xi}) \cos(n\varphi) \exp(i\Omega t)].$$

The coefficients a_{kj}, b_{kj}, c_{kj} and the indices α_j in the Frobenius power series are to be determined such that the differential equations (2.2) are satisfied. The procedure has been treated in paper [1] and will not be repeated here.

The purpose of this paper is to find the dispersion curves when the cylinder consists of two types of transversely isotropic materials to form a sandwich configuration. By inserting the solutions (4.1) into the set of differential equations (2.2) and the boundary conditions (3.2) and by using relations (3.1) we can accomplish the task.

The wavespeed ratio $c_w = (\Omega/\lambda)/\sqrt{(C_{55i}/\rho)}$, where λ is the actual wavenumber in the longitudinal direction and is implicitly involved in the coefficients of the Frobenius power series. For a non-trial solution, the determined of the final 18 homogenous linear algebraic equations must vanish. This results in the dispersion (or frequency) equation of the form:

$$| \beta_{ij}(n, c_w, \lambda \ldots) | = 0, \qquad \text{for } i, j = 1, 2, \ldots 18. \qquad (4.2)$$

5. Numerical evaluation and discussion of results

The dispersion equation (4.2) is a function of all the geometrical and material parameters of the layered shell. We have considered a rather thick shell in which $\kappa = R_4/H = 4$ for all computations. The only geometrical parametr varied is the ratio of the core thickness to the total thickness H of the shell, $ph2 = h_2/(2h_1 + h_2)$. Extreme values of the parameter $ph2$ are $ph2 = 0$ (corresponding to a single layered shell made of the material defined by Eq. (1a)) and $ph2 = 1$ (corresponding to a single layered shell made of material defined by Eq. (1b)). The matrices of elastic constants are given as follows:

Material according to (1.1)′:

$$\begin{bmatrix} 21 & 9 & 7 & 0 & 0 & 0 \\ 9 & 21 & 7 & 0 & 0 & 0 \\ 7 & 7 & 10 & 0 & 0 & 0 \\ 0 & 0 & 0 & 5 & 0 & 0 \\ 0 & 0 & 0 & 0 & 5 & 0 \\ 0 & 0 & 0 & 0 & 0 & 6 \end{bmatrix}$$

Material according to (1.1)″:

$$\begin{bmatrix} 21 & 7 & 9 & 0 & 0 & 0 \\ 7 & 10 & 7 & 0 & 0 & 0 \\ 9 & 7 & 21 & 0 & 0 & 0 \\ 0 & 0 & 0 & 5 & 0 & 0 \\ 0 & 0 & 0 & 0 & 6 & 0 \\ 0 & 0 & 0 & 0 & 0 & 5 \end{bmatrix}$$

These values have been kept constant in the numerical experiment. With this arrangement the dispersion equation is a function of only four nondimensional

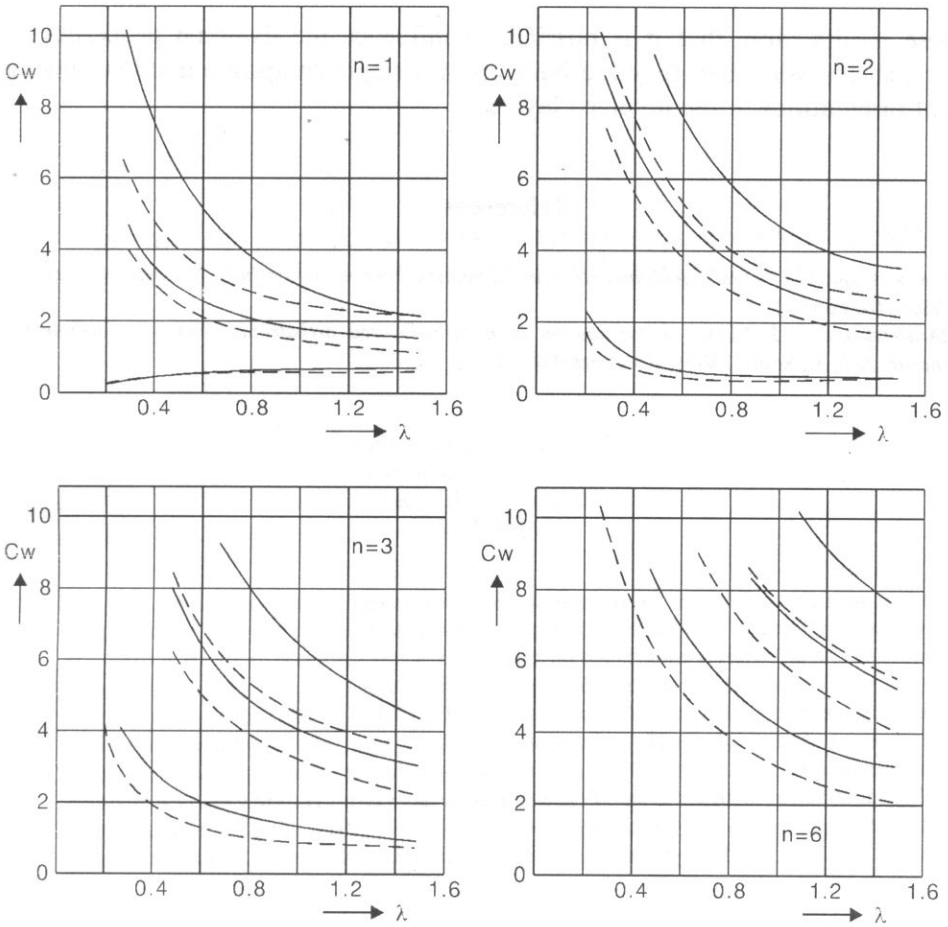

Fig. 1. First three branches of the dispersion curves c_w (λ, ph2) for n = 1, 2, 3, 6. Solid lines: ph2 = 0, dotted lines — ph2 = 1.

parameters: the circumferential wavenumber n, longitudinal wavenumber λ, wavespeed c_w and the nondimensional core thickness ratio $ph2$.

In actual calculation the left side of the dispersion equation (4.2) has been evaluated for fixed values of n, λ and $ph2$ cover a range of wavespeeds c_w. The interval have been sought in which a sign change was encountered. To identify the precise roots, the bisection method was used. In most search areas near the roots the values of the frequency determinant fluctuated violently within limits as large as $\pm 10^{99}$.

The first three branches of the dispersion curves for $n = 1, 2, 3$ and 6 are shown in Fig. 1. The solid lines correspond to ph2 = 0 (the limiting case of single layered shell made of material according to (1.1)'). Dotted lines correspond to ph2 = 1 which is the other limiting case for a single layered shell made of material according to (1.1)".

These results show that it is possible to influence the dynamic properties of sandwich shells even when they are built up of a single composite material having different orientations in the involved layers.

References

[1] Š. MARKUŠ and D.J. MEAD, *Axisymmetric and asymmetric wave motion in orthotropic cylinders*, J. Sound Vibr., (to appear).

[2] Š. MARKUŠ and D.J. MEAD, *Wave motion in a three-layered orthotropic–isotropic–orthotropic composite shell*, J., Sound. Vibr. (to appear).

ARCHIVES OF ACOUSTICS
21, 3, 317–324 (1996)

SOUND FIELD SIMULATION OF THE TRACTOR'S GEARBOX STRUCTURE USING STRUCTURAL AND ACOUSTIC INTERACTIONS

K. PRIKRYL

Institute of Mechanics of Bodies
Technical University of Brno
Technická 2, 616 69 Brno
Czech Republic

The ANSYS 5.0 finite element software was used to develop a finite element for the determination of the sound field of the driving unit of a real tractor. Generally, noise from the gearbox structure is emitted through vibration on the product surface and it is necessary to predict correctly the sound field formed by this radiated noise. The sound field exterior environment was modelled with FLUID30 acoustic fluid elements. These elements are most useful for modelling the structural and acoustic interactions. The nodal acoustic pressures of the sound field are plotted as sound pressure contours. The Figures show the sound pressure contours near the vibrating surface and in the plane at the end of the investigated sound field. The paper deal with the modelling of the whole coupled structural-acoustic system of the gearbox in order to reduce the noise emitted from the vibrating surface.

1. Introduction

Gears are sources of structural excitation in mechanical systems. Two types of excitation forces are generated: the first type are forces of gear tooth impact, the second are inertial forces caused by changes in the gear tooth deformation during meshing. Tooth impact, changeable tooth deformations are periodic and are manifested in the form of dynamic forces.

The vibration energy is transmitted to the gearbox housing through the shafts and bearings, and the gearbox housing radiates structure borne noise. The very small pressure fluctuations in the surrounding air constitute a sound field. These pressure fluctuations are usually caused by solid vibrating surfaces. As the disturbance, which produces the sensation of sound, may propagate from the source through any elastic medium, the concept of a sound field will be extended to include structure-borne as well as air-borne noise.

The aim of this paper is to model the Fluid-Structure Interaction and describe those problems in which the structural and fluid responses are strongly coupled. In

other words, it is aimed at the acoustic analysis of air-borne noise due to the real tractor's gearbox vibrations. The FEM programme system ANSYS 5.0 was used for solving the mentioned problem.

2. Modelling of the structural-acoustic system

2.1. The finite element model of the driving unit

The drive unit of a tractor is composed of many individual components. The dynamic characteristic of the fully assembled box-type structure system is a complex function of these individual components.

The individual components (Fig. 1) are box-type structures with varying thickness of the walls, flanges and diaphragms with cored holes for the bearings. The individual housings are connected by bolts. The drive unit is installed by elastic springs for simulation of the investigated structural and acoustic interactions.

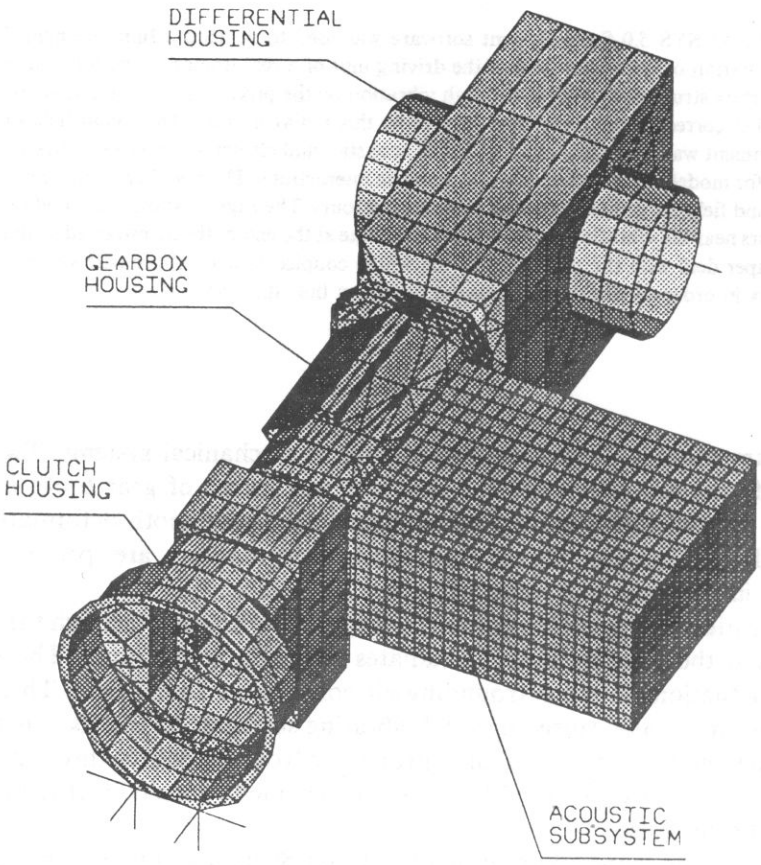

Fig.1 Body of drive unit with acoustic subsystem

The ANSYS finite element software was used to develop a finite element model for the determination of the box-type structures. For the modelling of the structures, the shell element SHELL 63 was used. The walls of the structures are relative thin and the bending moments of these walls are represented more exactly than by using volume elements. Elastic springs were modelled with COMBIN14 elements. More precise meshing was chosen on the gearbox's left side wall. The size of these elements was set at 0.03 m with regard to the acoustic space because this is the wall where the experimentally monitoring of the emitted acoustic energy was done.

2.2. Modellilng of the acoustic field

For the air-borne noise calculation of FE-model was used too. The sound field in the exterior environment was modeled with FLUID30 3-D acoustic fluid elements. They are most useful for modelling structural and acoustic interactions because they contain interfacing fluid elements that are in contact with the solid.

Interfacing fluid elements offer possibilities to represent the free acoustic field [10]. In practice it is field in which the effect of the boundaries are negligible in comparison with the region of interest. It can be, for example, in an anechoic chamber. This way we are able to model a free acoustic field. It is necessary to model the acoustic space as a close space in front of the vibrating wall. This closed space has to have properties of an anechoic chamber. The walls have to absorbe all the sound incident on them. For this reason it is necessary to choose the coefficient of absorption equal one. For a visual evaluation of the influence of the absorption coefficient of the walls in the modelled acoustic space, the 2D model has been used [6].

The size of the aocustic elements was chosen with regard to the wave length which is related to the wave motion frequency as follows:

$$\lambda = \frac{c}{f_{\max}}, \tag{2.1}$$

where $c = 343\ \mathrm{ms}^{-1}$ — speed of sound in the air space, $f_{\max} = 2500$ Hz — highest considered frequency of the sound wave.

The size of the acoustic element should be $L_{\max} = \lambda/6 = 0.03$ m.

2.3. The coupled structural-acoustic system

Both subsystems, the structure and the acoustic exterior environment are in mutual contact through the left side wall of the gearbox housing. The matrix equation of motion of the coupled structural-acoustic system is then [1]

$$\begin{bmatrix} M_s & 0 \\ \rho_0 A^T & M_a \end{bmatrix} \begin{bmatrix} \ddot{u} \\ \ddot{p} \end{bmatrix} + \begin{bmatrix} 0 & 0 \\ 0 & B_a \end{bmatrix} \begin{bmatrix} \dot{u} \\ \dot{p} \end{bmatrix} + \begin{bmatrix} K_s & -A \\ 0 & K_a \end{bmatrix} \begin{bmatrix} u \\ p \end{bmatrix} = \begin{bmatrix} f_s \\ 0 \end{bmatrix}, \tag{2.2}$$

where the index s for the structure and the index a for the acoustic subsystem or in a short form

$$\mathbf{M}\ddot{\mathbf{q}}+\mathbf{B}\dot{\mathbf{q}}+\mathbf{K}\mathbf{q}=\mathbf{f} \tag{2.3}$$

u — column vector of the structure deformations in the node points.
p — column vector of acoustic pressures in the nodal points.
A — coupling matrix of both subsystems.
M, B, K — mass matrix, damping matrix and stiffness matrix, respectively.
f — column vector of exciting forces.
q — column vector of total coordinates.
ρ_0 — density of air (1.2 kgm^{-3}).

3. Spectral and modal properties of the drive unit model

The basic dynamic characteristics of conservative mechanical systems are their spectral and modal properties.

The mentioned characteristics are derived from the homogeneous matrix equation

$$M_s\ddot{u}+K_s\dot{u}=0. \tag{3.1}$$

A modal analysis was performed using reduced modal extraction procedures with a total of 140 masters degrees of freedom. Table 1 shows some calculated natural frequencies of the drive unit housing. The first six frequencies correspond to a rigid body motion and the other ones correspond to the surface deformation on the surface vibration.

Table 1. Natural frequencies of the drive unit

Order	Frequen	Order	Frequen	Order	Frequen	Order	Frequen
1	2.29	7	164.3	31	892.6	62	2119.4
2	5.08	8	218.3	32	903.9	63	2177.8
3	6.02	9	331.5	33	913.6	64	2181.5
4	9.29	10	378.2	34	940.9	65	2199.2
5	10.56	11	436.3	35	963.9	66	2215.0
6	10.71	12	439.5	36	998.6	67	2241.7

4. Response of the acoustic subsystem to harmonic excitation

The exciting forces in the mechanical transmission originate inside the driving mechanism during running. The size of exciting forces are not known but their frequencies can be detected from a kinematic scheme of the whole driving mechanism [5]. From this point of view only their frequencies must be kept as they were.

The harmonically variable exciting force in the side direction was applied in the bearing which is positioned in a diaphragm in the gearbox. The exciting frequency

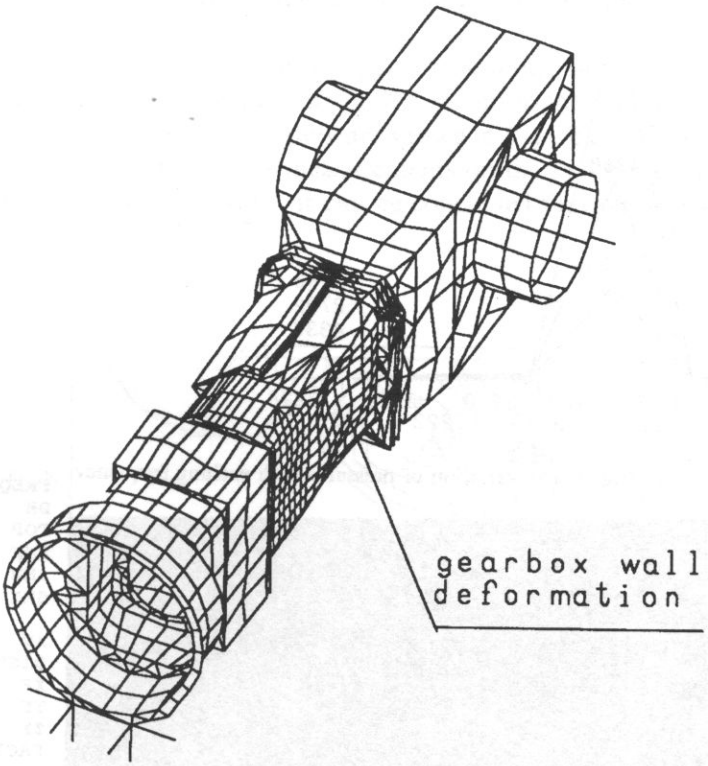

Fig. 2. Mode shape of the drive unit at $f=2215$ Hz.

was $f=2215$ Hz in order to correspond with one of the natural frequencies of the real drive unit housing 5 and the order 66 (see Table 1). If the structural motion is visualized Fig. 2, we can see that the side wall of the gearbox housing vibrates and the acoustic analysis can be performed.

4.1. Calculation of the air-borne noise

Figure 3 shows the entire frequency range that was investigated. It is a narow range in the surrounding of the natural frequency. The nodal acoustic pressures of the sound field were calculated and the sound pressure level relative to the reference pressure, Re=2.10E-5 Pa, is computed at the element's centroids. The contours near the vibrating surface and in the plane at the end of the investigated sound field i.e. at the distance 0.6 m from vibrating surface are plotted (see Figs. 4 and 5). The figures show clearly that the highest level of the acoustic pressure of 129 dB is at a close distance 0.03 m i.e near the gearbox wall. Its value decreases to 110 dB at the remote wall of the acoustic space. From Fig. 3 it can be evaluated that the noise level at points of the acoustic space selected by chance is expressively increasing in the surroundings of the natural frequencies.

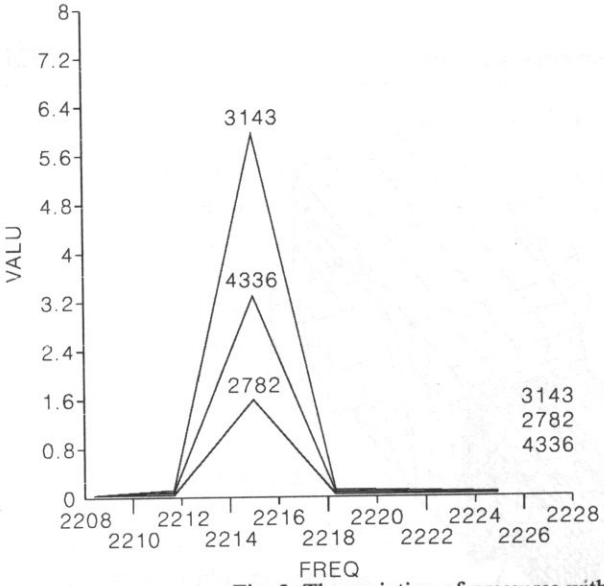

Fig. 3. The variation of pressures with exciting frequency.

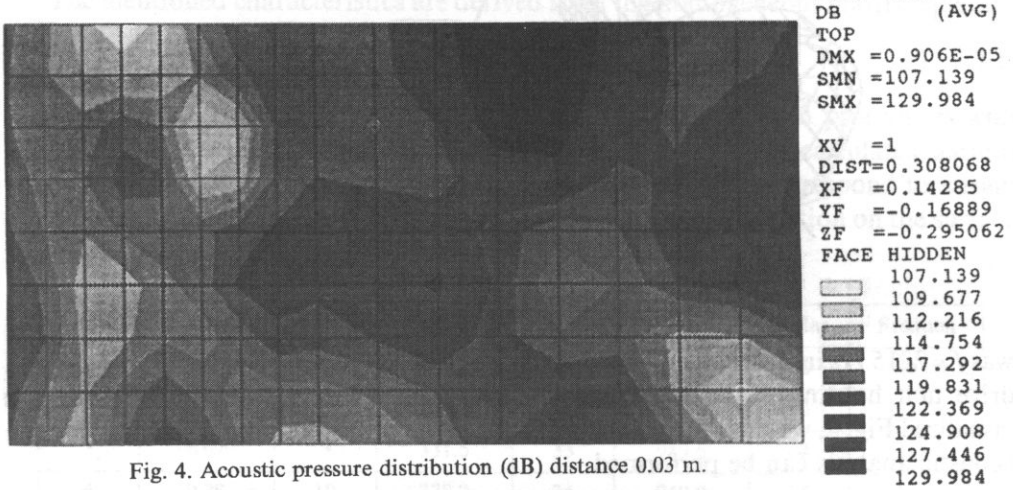

Fig. 4. Acoustic pressure distribution (dB) distance 0.03 m.

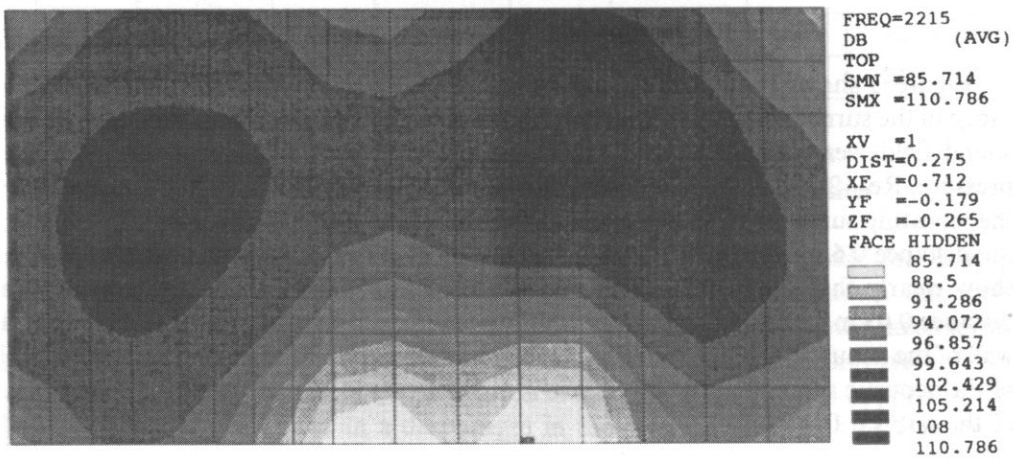

Fig. 5. Acoustic pressure distribution (dB) distance 0.6 m.

5. Model evaluation and measurements

For the comparison described in this paper, the mode shape of the real driving unit was measured by the resonance method. The coresponding mode shapes of the left side wall of the gearbox housing only are shown in Figs. 6 and 7. Here the natural frequency is $f=2222$ Hz during the measurements on the real body and $f=2215$ Hz during the calculation of the model. It can be concluded that we deal with the same mode shape of vibration.

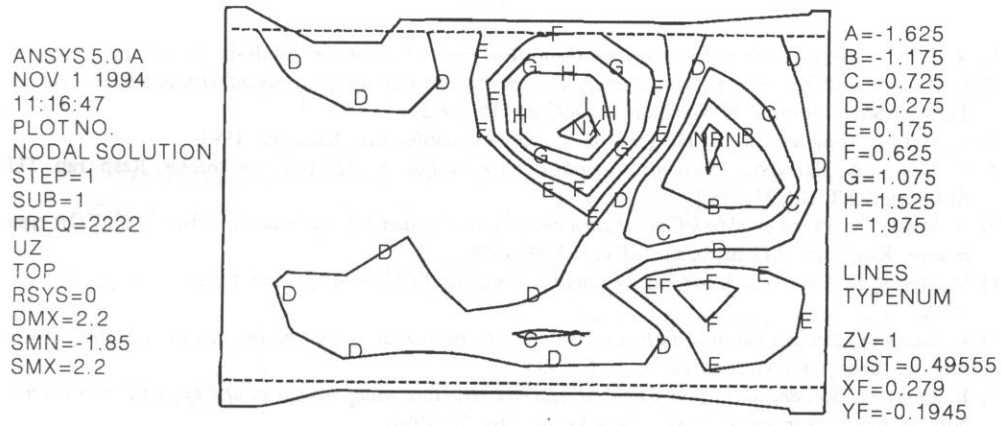

Fig. 6. Mode shape of the gearbox' side wall measurement.

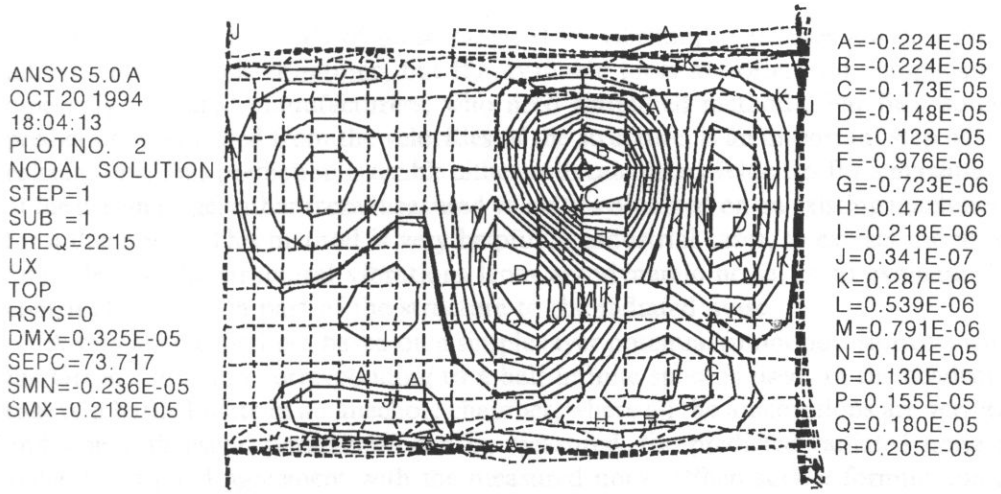

Fig. 7. Mode shape of the gearbox' side wall calculation.

6. Conclusion

Modelling of the coupled structural-acoustic system with FE-method by ANSYS 5.0 has been presented in this paper. Special attention was given to the air-borne noise. From the calculated results and the information on the surface vibration, effective changes in the individual constructional parameters for noise reduction can be found by the design optimization technique.

References

[1] *ANSYS — Engineering analysis system-theoretical manual*, Swanson Analysis System, Inc., 1989.
[2] F.K. CHOY and Z.F. RUAN, *Modal analysis of multistage gear system coupled with gearbox vibration*, Trans. ASME, Journal of Mechanical Design, 114, 1992.
[3] V. MISUN, *Noise analysis of the gearboxes*, Acoustic conference, Kocovce, 1993.
[4] V. MISUN, K. PRIKRYL, *Mechanical gearbox noise analysis of ZETOR type tractor*, Resp. rep. TU Brno, nu. ZET 101/93, 1993.
[5] V. MISUN, K. PRIKRYL, *Modelling of structure-acoustic systems of cabin and gearbox of ZETOR type tractor*, Resp. rep. TU Brno, nu. ZET 102/94, 1994.
[6] V. MISUN, K. PRIKRYL, *Modelling of sound fields using FEM*, Inzenyrska mechanika, 4, pp. 21–26, 1993.
[7] K. PRIKRYL, *Description of radiation of the noise from structures emitted through the vibration on the surface*, Inzenyrska Mechanika, 5, 3–6, 1993.
[8] K. PRIKRYL, *Simulation of sound field of gearbox structure using structural and acoustic interactions*, Numer. methods in mech. cont., Stara Lesna, 56–63, 1994.
[9] W.W. SETO, *Theory and problems of acoustic*, Mc Graw-Hill Book Company, 1971.
[10] *Tutorial ANSYS — Acoustic pressure propagation for revision 4.4, Swanson Analysis System*, 1989.

ARCHIVES OF ACOUSTICS
21, 3, 325–333 (1996)

CALCULATION OF THE ACOUSTIC RADIATION OF A PARALLELEPIPEDIC STRUCTURE BY USING ACCELERATION MEASUREMENTS

PART 1: Evaluation of inaccuracies attached to the simplifications of the model in the case of a single vibrating side

G. LOVAT, J.L. BARBRY, T. LOYAU

The determination of the acoustic pressure by a vibrating structure from velocities needs a great amount of measurements and calculations and the direct use of complete formulation is not possible in industrial situations.

The present paper proposes to calculate the radiated acoustic pressure by using velocity measurements and a simple software based on the monopoles distribution concept. The theoretical basis of the calculation is only available for a vibrating plate located in a rigid baffle. Nevertheless, this simple formulation is used in the case of a rectangular box with a single vibrating side with and without baffle.

The good agreement between experimental and theoretical results in this case allows us to use such a methodology for 3D structures with a pressure signal as reference signal.

1. Introduction

The predictive methods of noise radiated by vibrating structures are of a great interest in numerous situations, but the available tools are often too complicated, especially for small manufacturers, who need simplified methods. Far field sound prediction, performed from the velocities of the structure, is an important step of the calculations. This prediction is usable either with calculated velocities for a machinery at the design stage, either from measured velocities obtained on an existing machinery for a diagnostic. This method is very helpful in industrial cases, to extract the noise due solely to the structural vibrations from aerodynamic noise, or to evaluate the contribution of each part of the structure to the radiated noise.

A very simple method, based on a simple layer potential (monopole sources) with the Green's function corresponding to a half infinite space is used. In the academic case of a baffled plate in an anechoic chamber, where all the assumptions are verified and where all useful parameters can be measured, the predicted radiated noise is generally in good agreement with the measured noise. When such a formulation is used in a more industrial case performed for example by a vibrating rectangular box, various sources of inaccuracies are present. The lake of baffle, the spatial sampling,

the choice of the reference signal are considered in the first part of this paper. In the second part, it is shown that in spite of simplifying assumptions, this method can already be helpful to evaluate the contribution of each plate of a vibrating rectangular box to the radiated noise.

2. Calculation model

In the case of a vibrating structure (surface S) placed above a reflecting rigid baffle Σ_0, the governing equations are

$$\Delta P(M) - k^2 P(M) = 0$$

$$\frac{\partial P(M_0)}{\partial n} = \begin{cases} -j\rho_0 \omega V(M_0) & \text{if } M_0 \in S \\ 0 & \text{if } M_0 \in \sum_0 \end{cases} \tag{2.1}$$

with $P(M)$ radiated pressure (Pa), k wave number (m^{-1}), ρ_0 air density (kg/m^3), ω pulsation (rad/s), $V(M)$ velocity (m/s).
The prediction of the radiated pressure uses Green's theorem

$$P(M) = \iint_S \left((P(M_0) \cdot \frac{\partial G}{\partial n(M_0)}(M,M_0) - \frac{\partial P}{\partial n(M_0)} \cdot G(M,M_0) \right) dS, \tag{2.2}$$

where $G(M,M_0)$ is the Green's function that takes into account the boundary conditions of the problem (i.e. the reflecting surface). In the academic case, where the vibrating structure is a baffled plate, the first term of the relation (2) (dipole sources) is equal to zero and the the radiated pressure can be expressed as:

$$P(M) = -\iint_S \frac{\partial P(M_0)}{\partial n_{(M_0)}} G(M,M_0)\, dS, \tag{2.3}$$

From a practical point of view, the radiated acoustic pressure is calculated from vibrating velocities measured in several points on the plate using:

$$P(M) = \mathrm{i}\rho.\mathrm{c.k} \sum_{i=1}^{N} V(M_i)\, G(M,M_i) \Delta S_i \tag{2.4}$$

As previously specified, this formulation is only valid in the case of a baffled plate radiating in a half domain. It is however used for the determination of the acoustic radiation of the upper plate of a rectangular box, with and without baffle. Comparisons between measured and calculated pressure in the two cases are performed in the aim to evaluate the corresponding inaccuracies.

3. Experimental setup

The experimental setup included mainly a rectangular box ($600 \times 400 \times 300$ mm) whose all faces are rigid (thickness 20 mm) except the upper plate (thickness 5 mm). Each edge of this plate is fixed to the rigid frame of the box. The upper plate is excited by an electrodynamic actuator fixed inside the box and supplied by a random signal.

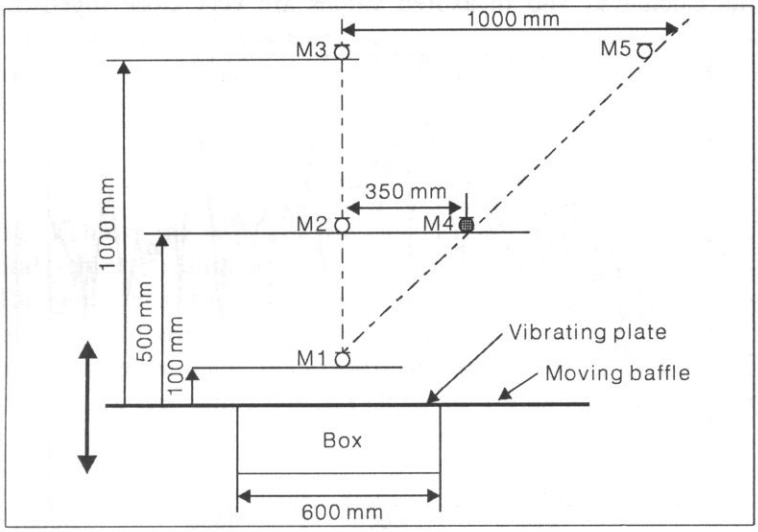

Fig. 1. Experimental setup.

The box is included in a test bench (Fig. 1) situated in a quiet room. The different parts of this test bench are:

— a plane rigid baffle which can move vertically,

— a set of five microphones BK 1/2″ located at different points (M_1 to M_5) specified on the Fig. 1 for acoustic pressure measurements,

— a laser vibrometer POLYTEC OFV 3000 including an optical probe whose displacements are automatically provided by a robot,

— a computer (MASSCOMP MC 5500) to drive the robot during the spatial scanning of the vibrating plate and to perform the acquisition and the signal processing.

4. Results

4.1. Academic case

The first tests are performed to obtain as good results as possible. In this aim, the spatial sampling of the plate needs small cells depending on the frequency range of interest (0—4000 Hz). The sound pressure levels are calculated from 117 velocities (9×13 points) measured on the vibrating plate. With this spatial sampling, the

distance between two following measurement points is smaller than the half of the bending wavelength. The calculations need a phase reference signal that is given by a force transducer located between the plate and the electrodynamic actuator. This signal contains all the frequency components and is for this reason the best possible reference. The Figs. 2 and 3 show the comparison between measured and calculated pressure in two locations: in the near field (point 1) and in the far field (point 5). In the near field, the calculated and measured values are very close together in all the

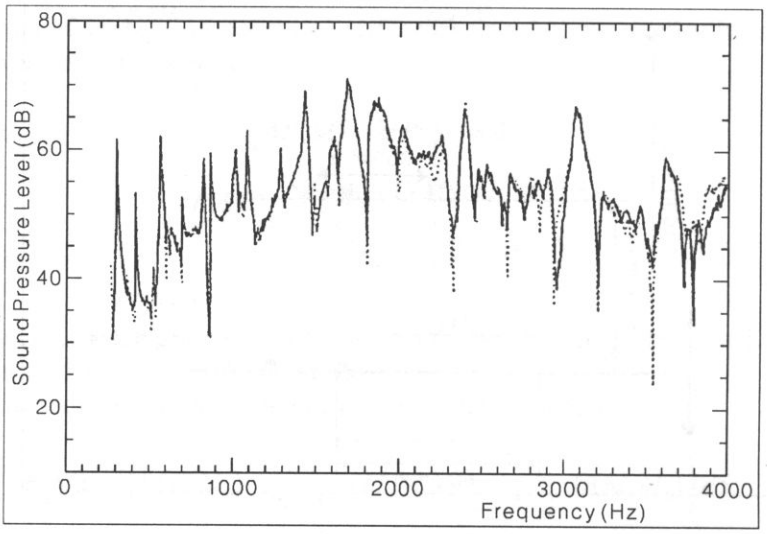

Fig. 2. Plate with baffle measured and calculated sound pressure level at point no 1 (≈ near field) ..... calculation ———— measurement.

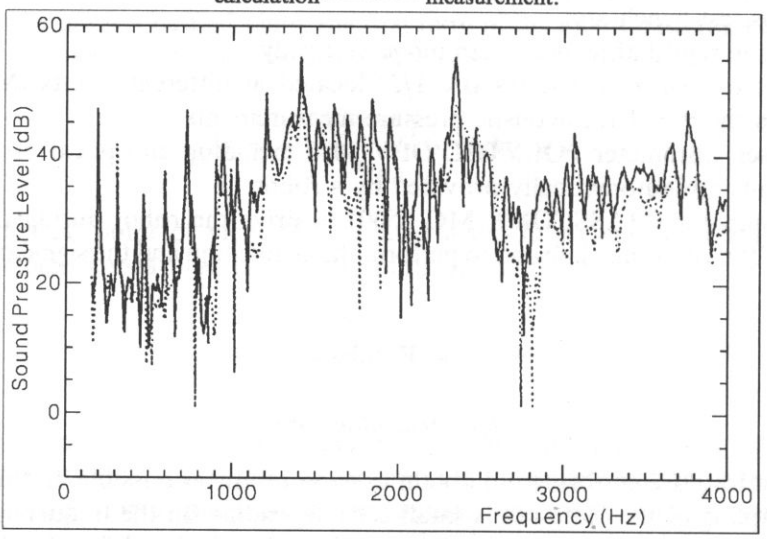

Fig. 3. Plate with baffle, measured and calculated sound pressure level at point no 5 (≈ far field) ..... calculation ———— measurement.

frequency range (above and under the critical frequency: 2400 Hz). In the far field, the agreement is very good up to 2000 Hz and the inaccuracies are weak between 2000 Hz and 4000 Hz.

In industrial conditions, such a methodology can't be used because:

— the LASER velocimetry with automatic spatial sampling device is rarely usable,

— the signal issued from a force transducer is not available and can't be used as phase reference,

— the vibrating plates are not baffled.

Consequently, the induced inaccuracies have to be evaluated, preferably in laboratory conditions.

4.2. Influence of the spatial sampling

The Fig. 4 shows the effect of the calculations size of the cells (i.e.number of experimental velocity values used for the calculation). As planed by the theory, calculated at measured acoustic pressures are in good agreement in the frequency range where the distance between measurement points is smaller than the half wavelength of the bending waves in the plate. In industrial conditions, it will be necessary to use this methodology in low frequency domain either to use an automatic scanning device.

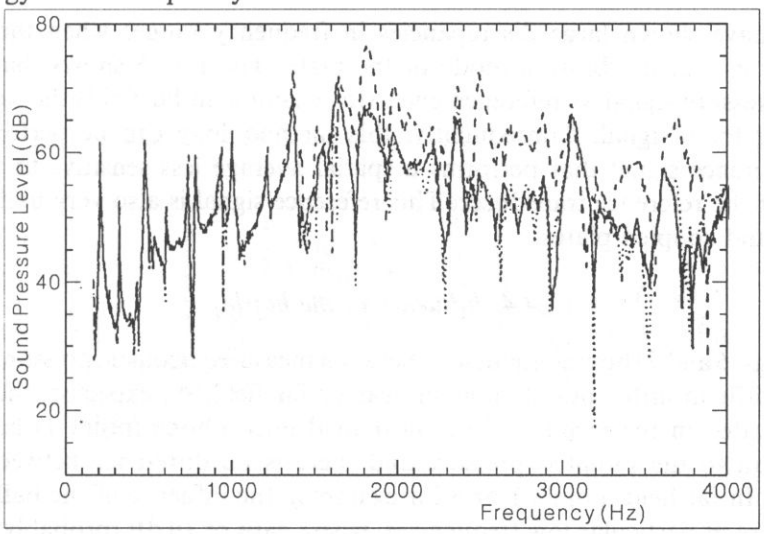

Fig. 4. Influence of the spatial sampling at point no 1. – – – – calc. with 24 points, ... calc. with 117 points, ———— measurement.

4.3. Influence of the reference signal

As shown previously, calculated and measured acoustic pressures are in good agreement with a force signal as phase reference. Unfortunately, this signal is rarely available in industrial cases and numerous tests using an acceleration signal as

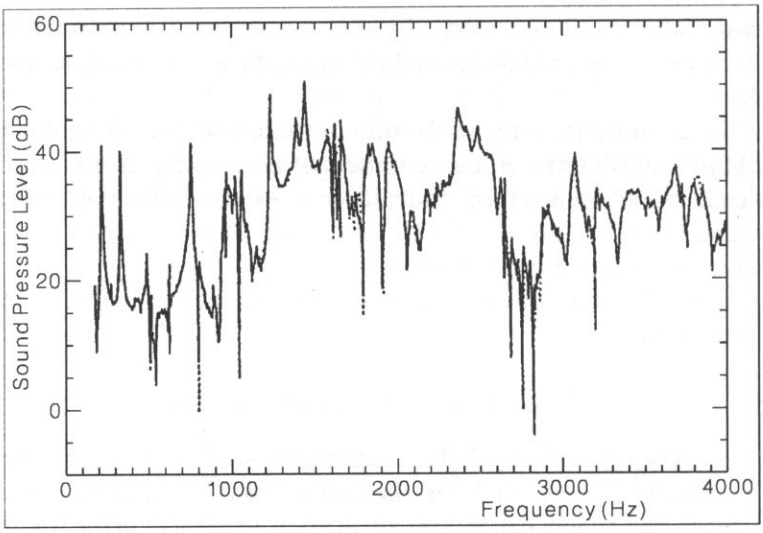

Fig. 5. Comparison between calculated acoustic pressures with force or pressure as signal reference (at point 5) .... calc. ref. = micro ——— calc. ref. = force.

reference have shown large discrepancies in frequency ranges when the reference transducer is near a vibration mode of the plate. The Fig. 5 shows that using an acoustic pressure signal as reference gives (for example in far field) the same results than using force signal. Consequently, this methodology can be performed with a such reference signal that performs a spatial average less sensitive to the spatial location of the reference transducer. This reference signal is also very useful for two vibrating and coupled plates.

4.4. Influence of the baffle

The Figs. 6 and 7 show comparisons between measured acoustic pressures with and without baffle in different locations in near or far field. As expected, the vibrating surface located in the vicinity of the near field microphone (point 1) has a major contribution to the radiated pressure and there is no difference between the two situations. In far field (points 1 or 5 for example), the infuence of the baffle is often weak, except at particular low frequencies, where gaps of 10 dB (probably due to the diffraction by the box) can arise. Generally these differences don't modify the global sound level. Nevertheless, they can be of great importance with harmonic excitation in low frequency domain. The Fig. 8 shows in far field the comparison between calculated pressure and measured pressure without baffle. From a theoretical point of view, the first term of the relationship (2), is different from zero and the radiated pressure included the contribution of dipoles sources (double layer potential). As previously shown, this term is neglected in the present calculation of the radiated pressure and the inaccuracies induced by this simplification are small in the studied case.

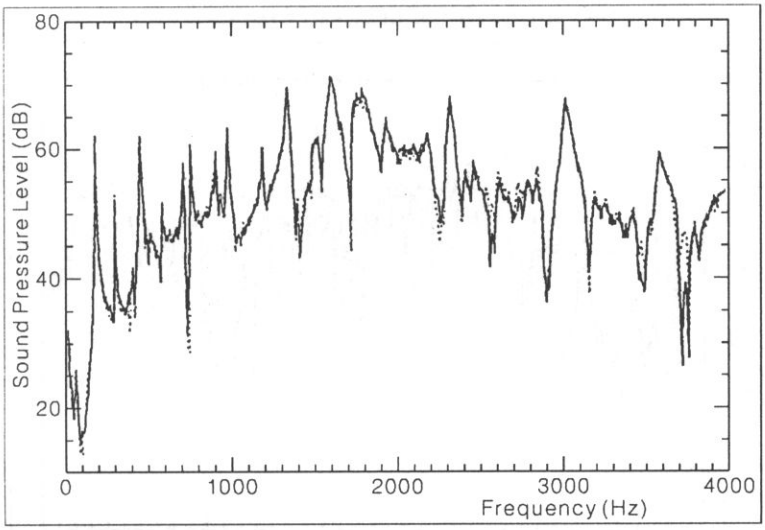

Fig. 6. Comparison between measured acoustic pressure with and without baffle (at point 1) ..... with baffle ——— without baffle.

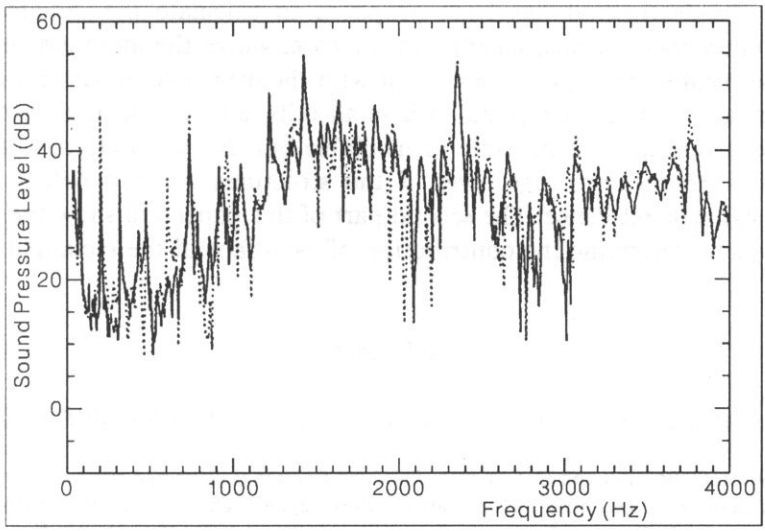

Fig. 7. Comparison between measured acoustic pressure with and without baffle (at point 5) ..... with baffle ——— without baffle.

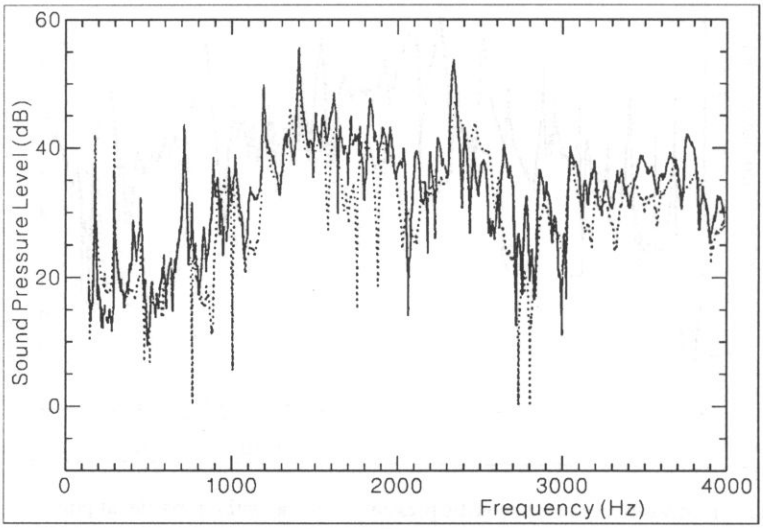

Fig. 8. Comparison between measured acoustic pressure without baffle and calculated pressures ..... calculation, ———— measurement.

5. Conclusions

A very simple method has been proposed to calculate the radiated acoustic pressure from velocity measurements. In the case, where the main assumptions are verified, the results are in good agreement with the measured acoustic pressures. In industrial cases, a spatial sampling with small cells, a force signal as reference and a baffled structure are not possible or available but this methodology can be very useful in low frequency range, even if the structures are not baffled and with a pressure signal as reference. The second part of this paper will show the use of this methodology to determine the contribution of each face of the rectangular box.

References

[1] C. Lesueur, *Rayonnement acoustique des structures,* Collections de la DER de EDF, Editions Eyrolles, 1988.

[2] N. Hamzaoui, C. Boisson and C. Lesueur, *Prévision du bruit et diagnostic vibroacoustic d'un système composé d'un rotor sur deux paliers à roulements,* 2ème Congrès Français d'Acoustique, Arcachon 1992.

[3] D. Blacodon and D. Brenot, *Estimation du champ acoustique lointain d'une plaque plane bafflé à partir de la mesure de son champ d'accélération;* Journal de Physique IV, Colloque C, supplément au Journal de Physique III, Volume 2, Avril 1992.

[4] J.P. Thomé, N. Hamzaoui, C. Millard, *Methodologie d'approche industrielle pour l'identification et la caractérisation des sources de bruit d'une machine tournante.* Modélisation et étude sur maquette, Euronoise'92, Imperial College London (UK), 14–18 Septembre 1992.

[5] G. LOVAT, J.P. THOMÉ, T. LOYAU, *Development of a vibroacoustic diagnostic software to predict sound pressure radiated by industrial machineries, from measurements of vibration levels on its body, Part 1;* Proceedings of Inter-Noise 93, Louvain, Belgium, 24–26 Aug. 1993.

[6] J.P. THOMÉ, T. LOYAU and C. MILLARD, *Development of a vibroacoustic diagnostic software to predict sound pressure radiated by industrial machineries, from measurements of vibration levels on its body. Part 2;* Proceedings of Inter-Noise 93, Louvain, Belgium, pp. 435–438, 24–26 Aug. 1993.

[7] T. LOYAU, G. LOVAT, J.L. BARBRY, M. CAFAXE, *Software for the calculation of the acoustic radiation of structures by means of vibrating measurements,* Euronoise 95, Lyon, 21–23 March 1995.

ARCHIVES OF ACOUSTICS
21, 3, 335–344 (1996)

CALCULATION OF THE ACOUSTIC RADIATION OF A PARALLELEPIPEDIC STRUCTURE BY USING ACCELERATION MEASUREMENTS

PART 2: Determination of the acoustic radiation contribution of each vibrating side

T. LOYAU, J.L. BARBRY, G. LOVAT

In the case of an existing machine, it is important to know the contribution of each part of the machine to the total acoustic radiation. One can thus identify main phenomena and estimate the gain earned by such or such way of noise reduction. A simple calculation software based on the vibrating measurements on the machine body is proposed to reply there. The theory has been presented in the first part of the article. The software has been used in the case of the radiation of a rectangular box, located on a rigid baffle, with two vibrating faces.

The calculated and measured pressure at one point is similar in the [0–3000] Hz frequency range except in some narrow frequency ranges.

The measured and calculated acoustic power does not present such zones, and the contribution of each plates to the total acoustic radiation can be obtained from the calculation of partial and total acoustic powers on the [0–4000] Hz frequency range.

In the chosen experimental case, the calculation of total and partial acoustic powers based on the only vibrating data knowledge, can be a performant tool for vibroacoustic diagnostic.

1. Introduction

The calculation of the acoustic radiation, based on the distribution of monopole sources (only vibrating measurements) solely valid in the case of the acoustic radiation of baffled plane structure, has been used in the case of a rectangular box, located on a rigid baffle, with two vibrating faces. The first part of the article has presented the calculation model and the main assumptions attached to the simplified theory (monopole sources and baffle condition) and to experimental conditions (measurement mesh, signal of phase reference).

This second part proposes to calculate radiated acoustic quantities (pressure and power) to allow to obtain a reliable tool of vibroacoustic diagnostic.

2. Experimental setup

The rectangular box studied is constituted of a rigid frame in full steel tubes (600 by 400 by 300 mm) on which them six faces are fixed. Two of steel faces (upper plate

and one of the vertical plates, Fig. 1) are considered as vibrating (thickness 5 mm). The four other faces are considered as rigid (steell plates of thickness 20 mm). The upper plate (600 by 400 by 5 mm) and the vertical one (400 by 300 by 5 mm) are each excited by an electrodynamic actuator supplied by a random signal (normal point force applied to the point $x=250$, $y=120$, $z=300$ mm and $x=0$, $y=290$, $z=150$ mm respectively). The two forces can be coherent or non-coherent.

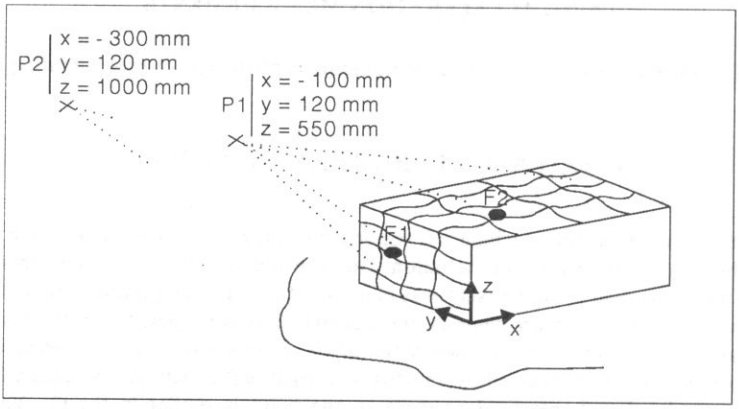

Fig. 1. Description of the box and position of the two points P1 and P2.

The vibrating velocity has been measured by a LASER vibrometer POLYTEC OFV 3000, the optical probe being placed automatically in each point of a mesh of 117 points (13 by 9) and 63 points (9 by 7) for the upper and vertical plates respectively. The distance between two consecutive points of the mesh is less than the half of the bending wavelength in the plates, this allows to cover the [0, 4000] Hz frequency range.

3. Calculation and measurement of the acoustic pressure

One proposes to test the simple calculation based on the concept of monopole sources. The acoustic pressure has been measured (microphones 1/2″ B&K 4133) and calculated at two points P1 ($x=-100$, $y=120$, $z=550$ mm) and P2 ($x=-300$, $y=120$, $z=1000$ mm) (see Fig. 1). The Figure 2 shows the superposition of the calculated and measured acoustic pressure in the case where the upper plate is excited alone (Fig. 2a and 2b respectively at point P1 and P2), and in the case where the vertical plate is excited alone (Fig. 2c and 2d respectively at point P1 and P2).

Measured and calculated results are very close up to 3000 Hz except in some particular narrow frequency ranges. Trends are respected in the [3000−4000 Hz] frequency range.

The Figure 3 shows the superpositon of the calculated and measured acoustic pressure in the case where the two plates are excited simultaneously:

a) The two forces are coherent and the complex pressure is calculated from vibrating velocity of each of plates with a common phase reference (Fig. 3a and 3b respectively at point P1 and P2).

b) The two forces are non-coherent and the calculated pressure is the sum of quadratic pressures calculated separately for each of faces (Fig. 3c and 3d respectively at point P1 and P2).

Preceding conclusions can be renewed in the case of the two simultaneously excited plates by forces coherent or non-coherent.

The contribution of each of plates to the total radiated noise can be evaluated by calculation, by comparing the total acoustic pressure and the acoustic radiated by each of plates separately. The bad results obtained in narrow frequency range raised previously could generate an erroneous diagnostic.

The calculation of the total acoustic power and the partial acoustic power radiated by each face has then been studied. The acoustic power integrates a certain number of values of pressure and smooth local calculation problems put in obviousness in the case of a single value of pressure.

4. Calculation and measurement of the acoustic power

A first test has been undertaken in the case where only the upper plate is excited to compare the acoustic power obtained by calculation and by measurement.

The measurement of the acoustic power has been obtained by the intensimetry technic. The intensity probe (12.5 mm space microphones) has been placed in a regular mesh of 165 points (15 by 11), the measurement surface being thus bigger than the plate surface.

The calculation has been undertaken by simulating an intensimeter (calculation of the complex pressure in two separate close points separated by 12.5 mm) at each points of the same regular mesh.

The Figure 4 shows the flawless superposition of the measured and calculated acoustic power.

A second test has then been undertaken in the case where the two plates are excited by non-coherent forces.

The superposition of the calculated total acoustic power and the calculated partial acoustic power radiated by the upper and vertical plates is shown respectively in Figures 5 and 6. The results obtained no longer put in obviousness the gaps located in narrow frequency range as in the case of the calculation of a single value of pressure. The useful frequency range is similarly repelled up to 4000 Hz.

The participation of each of faces to the total acoustic radiation can then be analyzed. In this precise case, the upper plate mainly contributes to the total acoustic radiation and the vertical one contributes in some few frequency narrow ranges well identified.

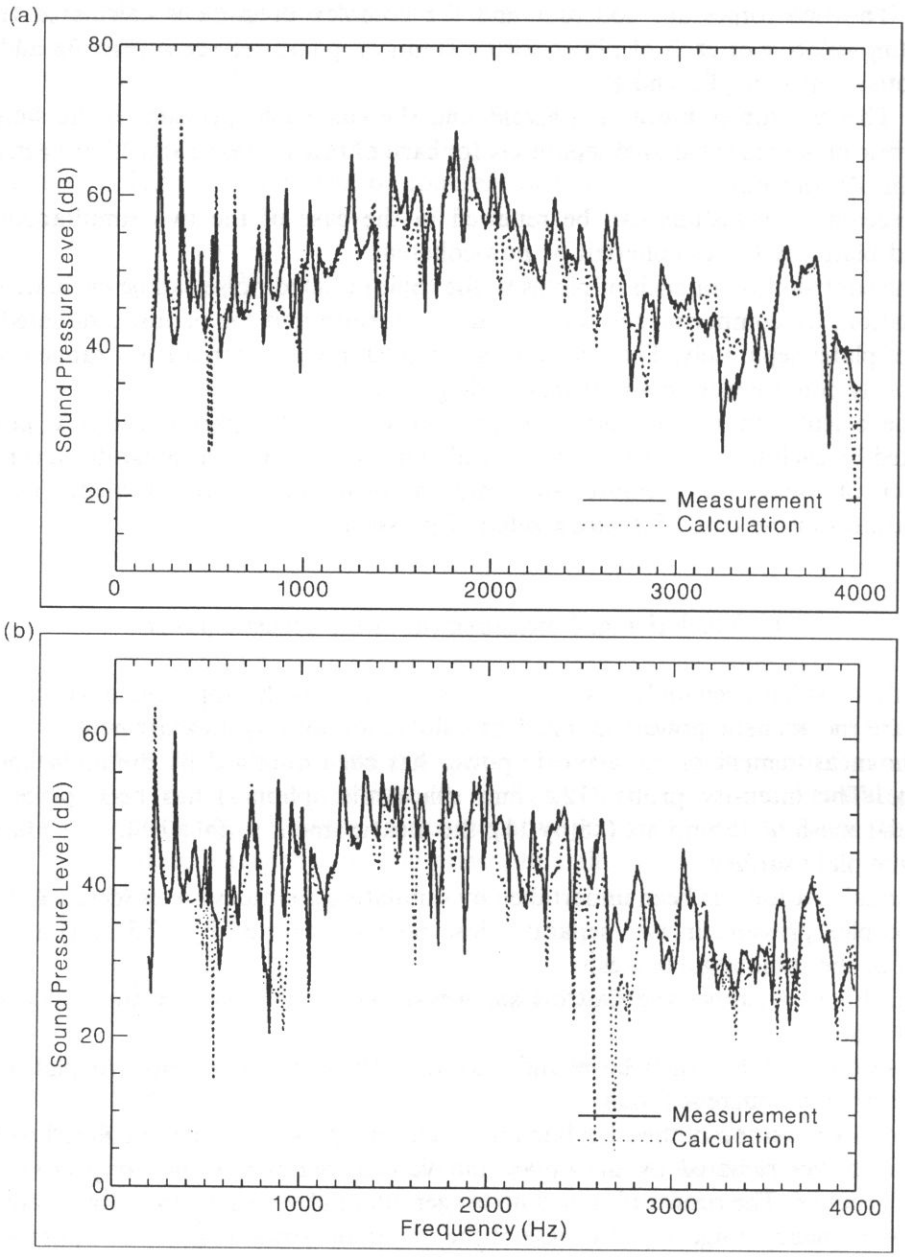
(a)
80
60
40
20
Sound Pressure Level (dB)
0
1000
2000
3000
4000
Measurement
Calculation
(b)
60
40
20
0
Sound Pressure Level (dB)
0
1000
2000
3000
4000
Frequency (Hz)
Measurement
Calculation

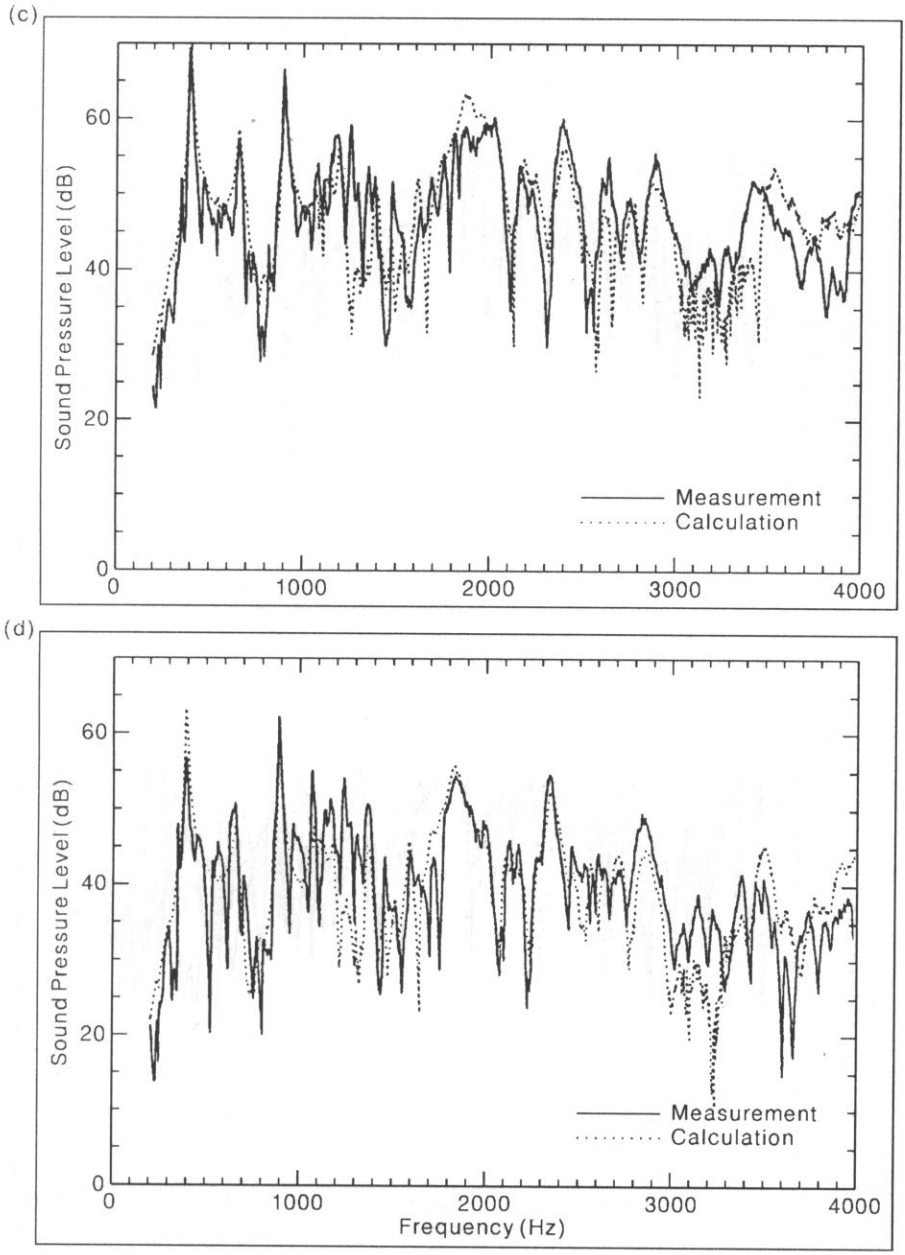

Fig. 2. Measured and calculated pressure radiated by the upper plate, (a) at point P1, (b) at point P2, and radiated by the vertical plate (c) at point P1, (d) at point P2.

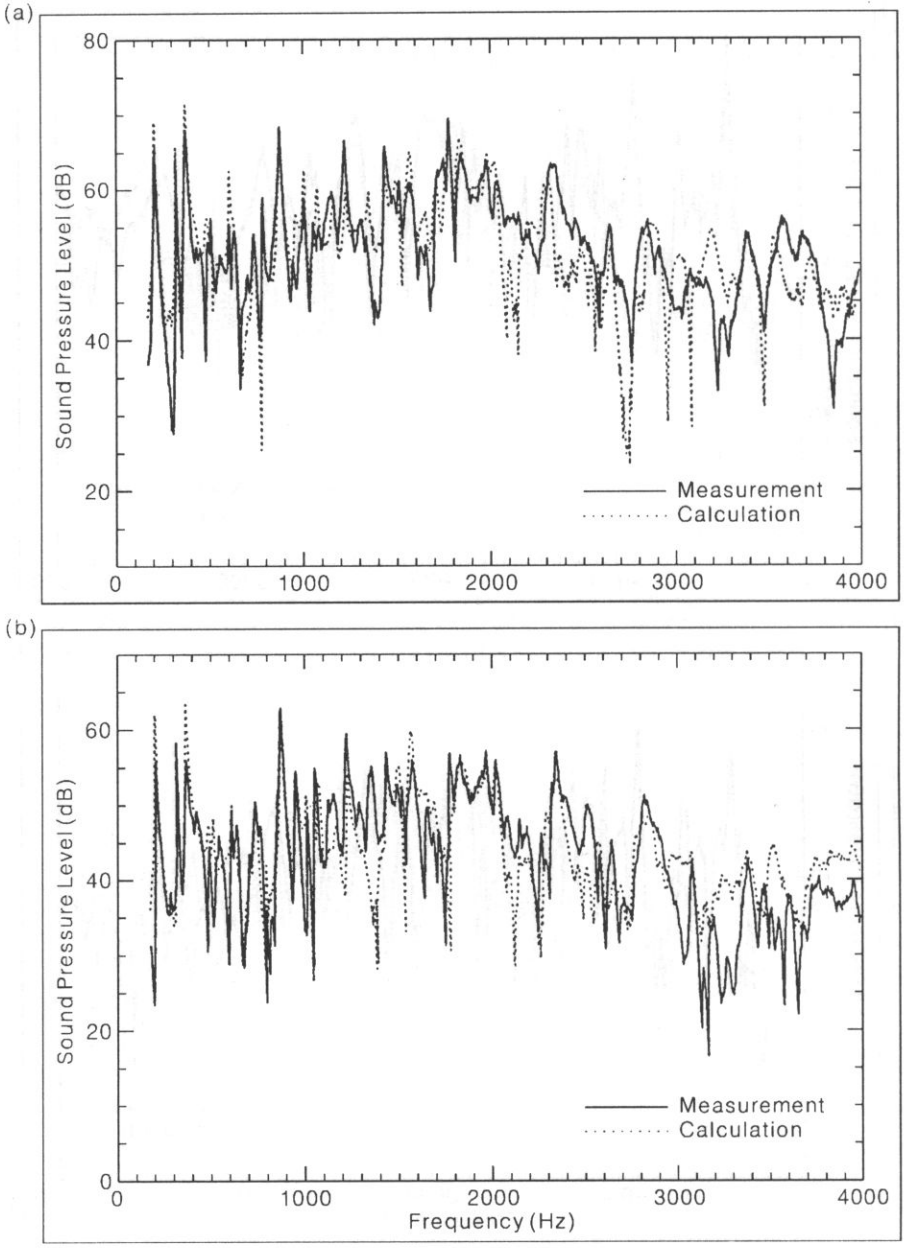
(a)
80
60
40
20
Sound Pressure Level (dB)
0
1000
2000
3000
4000
Measurement
Calculation
(b)
60
40
20
0
Sound Pressure Level (dB)
0
1000
2000
3000
4000
Frequency (Hz)
Measurement
Calculation

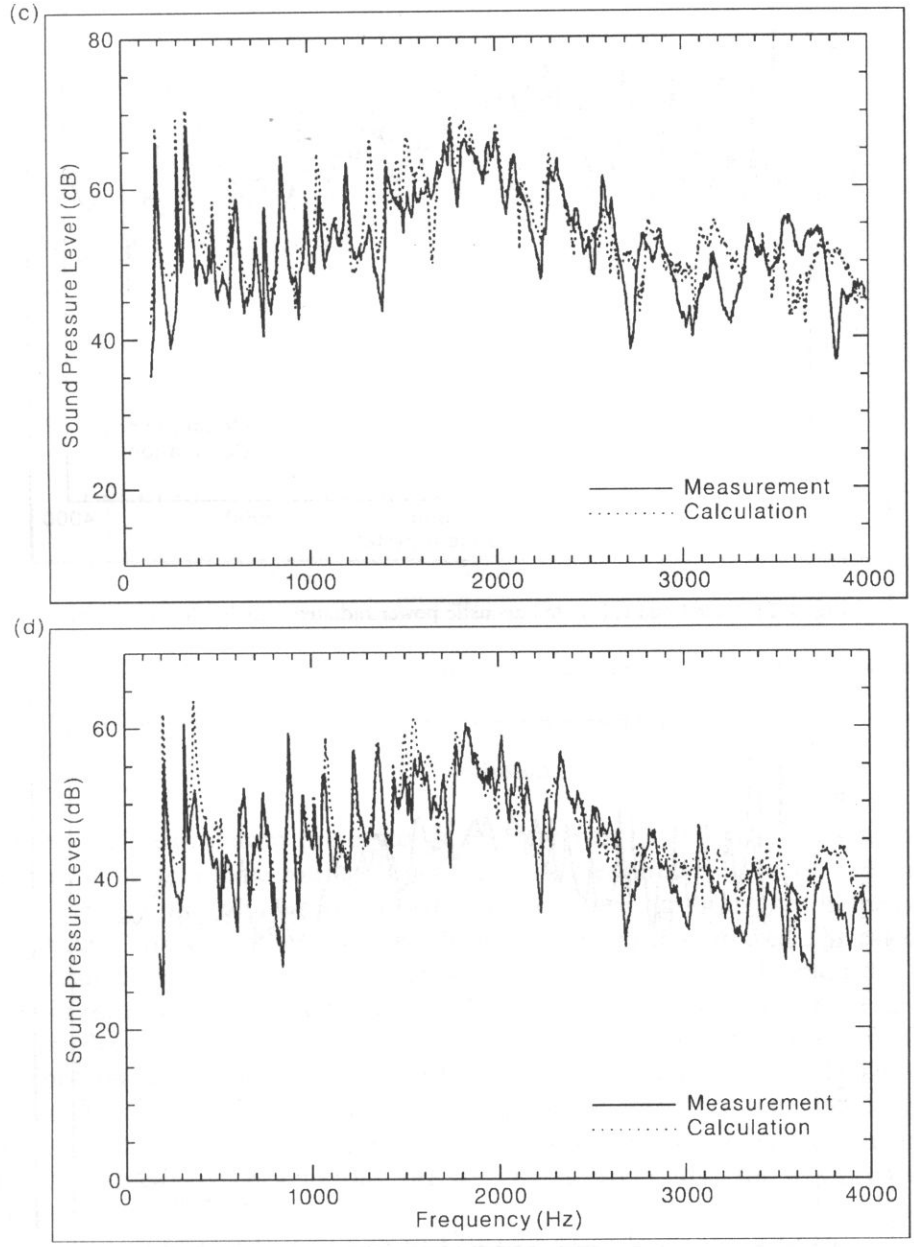

Fig. 3. Measured and calculated pressure radiated by 2 plates with coherent forces, (a) at point P1, (b) at point P2 and with non-coherent forces (c) at point P1, (d) at point P2.

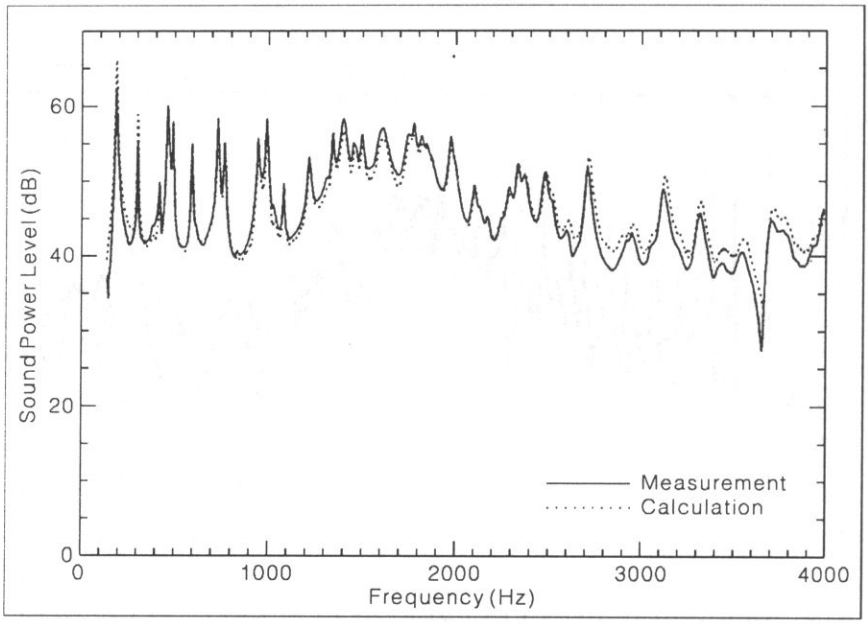

Fig. 4. Measured and calculated acoustic power radiated only by the upper plate.

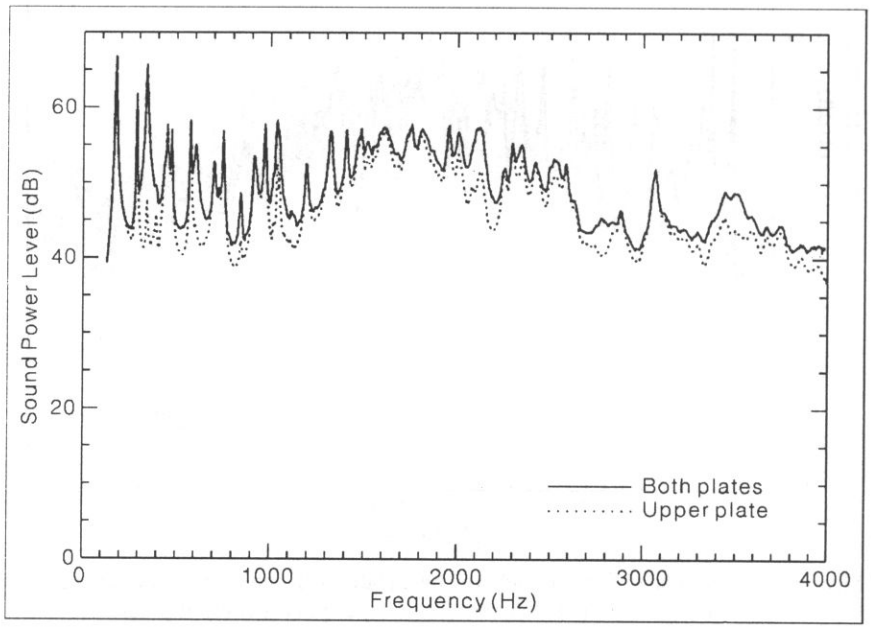

Fig. 5. Calculated acoustic power radiated by the upper plate alone and by the two plates.

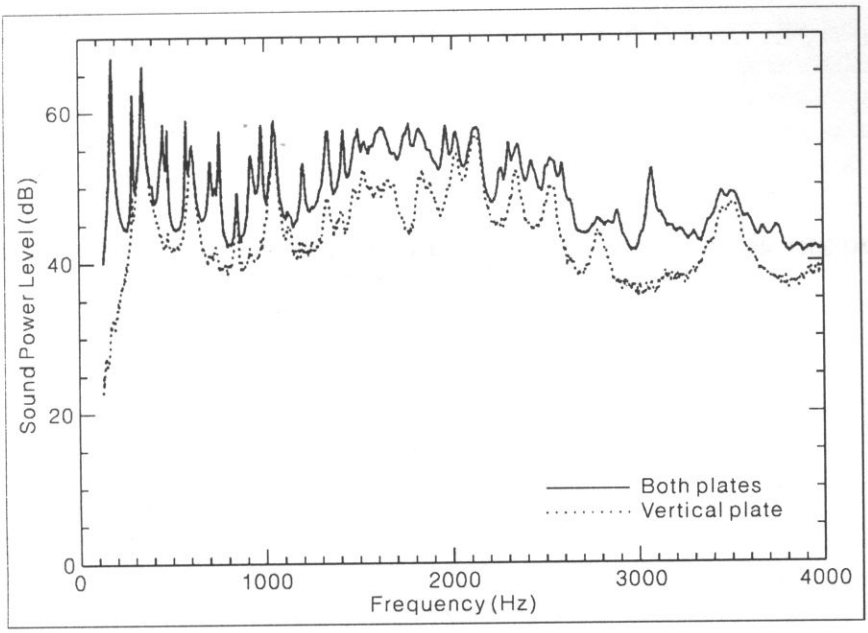

Fig. 6. Calculated acoustic power radiated by the vertical plate alone and by the two plates.

5. Conclusion

The simple calculation presented in the first part of the article, based on the distribution of monopole sources (only vibrating measurements) solely valid in the case of the aocustic radiation of baffled plane structure, has been used in the case of a rectangular box located on a rigid baffle with two vibrating surfaces. The calculated and measured pressure at a single point is similar in the [0 – 3000] Hz frequency range except in some narrow frequency ranges. The calculated acoustic power, a smoothy quantity, does not present this kind of problem and gives very good results on all the frequency range of analysis [0 – 4000] Hz. One can then obtain by calculation the total acoustic power and partial acoustic power of each face allowing to put in obviousness the each face contribution to the total acoustic radiation. The simple calculation used becomes in this precise case a good tool for a vibroacoustic diagnostic.

ARCHIVES OF ACOUSTICS
21, 3, 345–353 (1996)

AN ELECTRO-PNEUMATIC ACTIVE VIBRATION CONTROL SYSTEM FOR THE DRIVER'S SEAT OF AGRICULTURAL TRACTORS

G. J. STEIN

Institute of Materials and Machine Mechanics
Slovak Academy of Sciences
(SK-830 08 Bratislava 38, Račianska 75, P.O. Box 95, Slovak Republic)

The aim of this contribution is to present some results of the study of driver's seat with an electro-pneumatic active vibration control system applied for driver's seats of agricultural wheeled tractors. The actuator is parallel to the conventional pneumatic seat suspension and a proportional electro-pneumatic valve is used as the control element. The description of the full scale dummy system is augmented by a short theoretical description of the 1 DOF model of this system and by some results of measurements on a laboratory vibration simulator. The seat vibration control properties are evaluated according to the ISO Standard 5007:1990 pertinent to evaluation of seats for agricultural wheeled tractors.

1. Introduction

The contemporary conventional passive Vibration Control Systems (VCS) for vehicles and other transport means have reached a rather sophisticated level of vibration abatement. They cannot however, meet all the requirements of pertinent health regulations. Therefore new methods of vibration control have been developed. Some of them are already manufactured for luxury cars or subject to performance tests for special vehicles. These systems are based on the use of fast and expensive electro-hydraulic actuators and of a digital state variable control. The practical use of pneumatic elements for Active Vibration Control Systems (AVCS) is, to author's knowledge, rather limited. Much effort in the field of research of AVCS has been spent especially in Poland, e.g. [5, 6, 10–13], and elsewhere. As often reported, e.g. in [1–3, 7, 19] the effort at this Institute has been concentrated on the research of AVCS based on the compensation principle.

In the last paper on this topic [3], some advantages of such a system were shown. Some first stage experimental results were published, e.g. in [2, 19], but they were not satisfactory. It was noted later that one of the drawbacks was the wrong mounting position of the hydraulic damper in the scissors type guiding mechanism. Instead of

vibration damping it rather hampered the proper action of the active part. Hence it was decided to remove the hydraulic damper and to use the "sky-hook" damper working on the electronic principle, as described first by KARNOPP in [9]. The new system reported further below, uses artificial damping by employing the feed forward control combined with the well proven feed forward control of the compensation principle. For the theoretical description of the system the interested reader is referred to [2, 7, 16, 19]. An abridged explanation of the control system will be given below according to [17]. Furthermore some experimental results pertinent to use for driver's seats for agricultural wheeled tractors will be given together with the assesment of the required pneumatic power for proper operation of the system.

2. Description of the system

The schematic layout of the full scale dummy seat with active electro-pneumatic suspension used in the experimental research is depicted in Fig. 1. The pneumatic spring *2* with inside absolute pressure p_2 acts on the upper part *5* of a scissors type guiding mechanism *3*, which is supporting the cushion *6* with seated operator of mass M that vibrations in the vertical direction x_1 have to be controlled. This structure is mounted on the base *1* which is excited mostly in the vertical direction with the displacement x_2. A relief steal spring *4* is situated between the base *1* and the upper part *5* to hold the supposed minimal mass M at the required static height h_0 (static middle position), approximately in the middle of the possible travel of the scissors type mechanism *3*. The active part is formed by the electro-pneumatic transducer *8*,

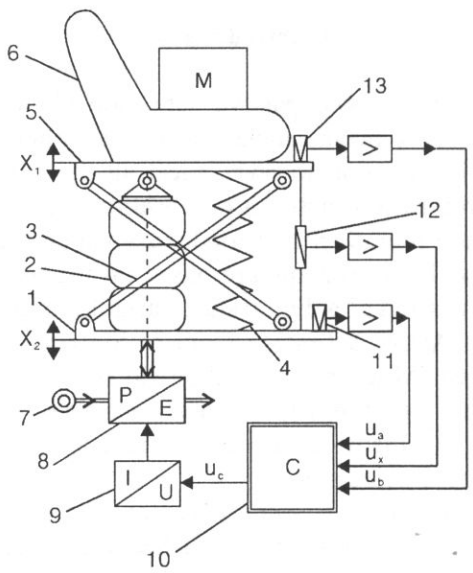

Fig. 1. Schematic lay-out of the dummy system (description in the text).

the source of compressed air 7 of absolute pressure p_1 and the outlet to the atmosphere of absolute pressure p_3. The dummy system is operated by the relative displacement sensor *12*, the base vertical acceleration sensor *11* and the upper part vertical accleration sensor *13*. The respective amplified sensor output signals are fed to the electronic controller *10* which transforms them to the output voltage u_c controlling the electro-pneumatic transducer *8* by a matched voltage-to-current converter *9*.

In the experimental realization emphasis was given to the proper design of the mechanical part in order to minimize the influence of geometrical properties of the air spring *2* and the proper choice and installation of the electro-pneumatic proportional transducer *8*. A commercially available transducer with a matched voltage-to-current converter *9* was used. To simplify further the research work, a constant mass M made of lead shots in bags was fixed to the cushion *6* in order to simulate the seated driver. The relative displacement sensor *12* was a commercially available inductance sensor with a corresponding amplifier. The vertical acceleration sensor *11* and *13* were commercially available piezoelectric accelerometers with appropriate impedance converters connected to the respective inputs of the electronic controller *10*. The electronic controller is a simple linear electronic system. It is essentially a three loop linear controller as shown in Fig. 1. It is immaterial wheather this control structure is realized by a digital computer, by a DSP with a suitable analogue input/output subsystem, by an analogue controller or by an analogue computer. In our case, after thorough tests with the MEDA type analogue computer, an analogue controller has been built of standard electronic components and used.

3. Short theoretical description

Physically the system can be treated as an oscillatory system with one degree of freedom working in the vertical direction. The simplified mathematical description of the mechanical part of the system is based on the following equation of motion [2, 17]

$$M \cdot \ddot{x}_1 + k^* \cdot (x_1 - x_2) + f = 0, \tag{3.1}$$

where k^* is the effective spring constant of the parallel combination of the steel spring *4* and the pneumatic spring *2* of Fig. 1; the mass M stands for the seated driver. The dynamic properties of the seat cushion are neglected for simplicity and only the suspension system is considered. For a more detailed analysis of a driver's seat, the interested reader is referred to the paper of RAKHEJA *et al.* [15].

The force f, generated by the air spring *2* as actuator, consists of three components:

- damping force, proportional to the isolated body absolute velocity $\dot{x}_1$ (proportionality constant b);
- compensationn force, proportional to the base vertical acceleration $\ddot{x}_2$;
- static force for maintaining the proper middle position. This static force is not further considered.

It can be shown (see e.g. [7, 16, 19]) that the relation between the output force $f(t)$, acting on the upper part *5* to control the voltage $u_C(t)$ of the combination of the voltage-to-current converter *9*, actuator *2* and the proportional transducer *8*, is linear if some strict constraints on the fluid flow in the transducer are maintained. It has an integrating character and therefore the respective Frequency Response Function (FRF) of the complex argument $p=j\cdot\omega$ has the form $G_A=H_A/p$. At the assumption of linearity and the system stability the Fourier transform of the exerted force was derived in [17] in the following form (the respective Fourier transforms are denoted by capital letters):

$$F=G_A\cdot N\cdot[R_B\cdot(A_B\cdot X_1\cdot p^2)+R_C\cdot(A_C\cdot X_2\cdot p^2)] \tag{3.2}$$

where A_B and A_C are the gains of the accelerometer preamplifiers and R_B adn R_C are the partial controllers FRF. The controllers are realized in the controller block *10*.

After subjecting Eq. (3.1) to the Fourier transform and introducing Eq. (3.2) the following equation holds (where ω_0 is the system undamped natural frequency):

$$\begin{aligned} X_1\cdot p^2+G_A\cdot N\cdot R_B\cdot A_B\cdot X_1\cdot p^2/M+\omega_0^2\cdot X_1= \\ =\omega_0^2\cdot X_2-G_A\cdot N\cdot R_C\cdot A_C\cdot X_2\cdot p^2/M. \end{aligned} \tag{3.3}$$

The left side of Eq. (3.3) would correspond to a damped linear oscillator with the corresponding mechanical damping b^* if according to the principle of the "sky hook", as described by KARNOPP [9], the middle term would correspond to $b^*\cdot X_1\cdot p/M$. On the other hand, to reach a non-trivial rest of the oscillator the right hand side of Eq. (3.3) should be zero. From these two conditions the corresponding control laws for the respective controllers R_B and R_C follow:

$$R_B=b^*\cdot(G_A\cdot N)^{-1}\cdot A_B^{-1}\cdot p^{-1}=b^*\cdot(H_A\cdot N)^{-1}\cdot A_B^{-1}, \tag{3.4}$$

$$R_C=k^*\cdot(G_A\cdot N)^{-1}\cdot A_C^{-1}\cdot p^{-2}=k^*\cdot(H_A\cdot N)^{-1}\cdot A_C^{-1}\cdot p^{-1}. \tag{3.5}$$

The term N could by looked upon as a correction term to H_A. If their combination equals to 1, then it follows that the damping controller R_B is essentially a P-controller, with gain corresponding to the damping b^*, and the compensation controller R_C corresponds to a P−I controller. The only problem, as noted by MARGOLIS [14], is the suitable design of this controller. Note that the compensation loop is fully effective only if equation (3.5) is met both in phase and amplitude in the required frequency band.

4. Test procedure

The ISO Standard 5007:1990 [21] is an international standard which describes the requirements and procedure for laboratory tests of driver's seats for agricultural tractors with unspring rear axle in a reproducible manner. It distinguishes essentially two tests:

a) **test damping**: the seat is loaded with two test masses of 40 kg and 80 kg, respectively, and a sinusoidal vibration displacement of a 30 mm pp amplitude is applied to the seat base at frequencies within the range 0.5 Hz to 2.0 Hz with a step of 0.05 Hz at maximum. The ratio V of the weighted rms vibration acceleration in the vertical direction at the seat surface a_{wfS} to that one at the seat base a_{wfB}, measured by the same method, shall be determined in the given frequency band and graphically displayed. The maximum value and the respective frequency is of interest, since it describes the damping properties of the driver's seat under standardized harmonic excitation.

b) **random vibration test**: with two test persons of 50 kg +/−1 kg and 98 kg +/−5 kg of that not more than 5 kg or resp. 8 kg could be comprised of lead balasts in a belt. The seat is subjected to a narrow band stationary random excitation in the vertical direction, with a normal amplitude probability distribution. The spectral density of the acceleration power (PSD) is defined in the Standard for the agricultural wheeled tractor classes. The vertical acceleration PSD is generated so as to describe the vibration excitation on agricultural wheeled tractors of different sizes/masses during their normal operation in reproducible manner. The most important data for those three tractor classes are given in the following Table 1, the respective vertical acceleration PSD courses are shown in Fig. 2.

Table 1. Tractor classes according to the ISO 5007:1990 Standard

Tract. class	Unbalasted mass m, kg	Centre frequency f_p, Hz	Base vertical wght. acceleration a_{wB}, $m \cdot s^{-2}$
1st	up to 3 600	3.25	2.05
2nd	3 600 to 6 500	2.35	1.50
3rd	over 6 500	2.20	1.30

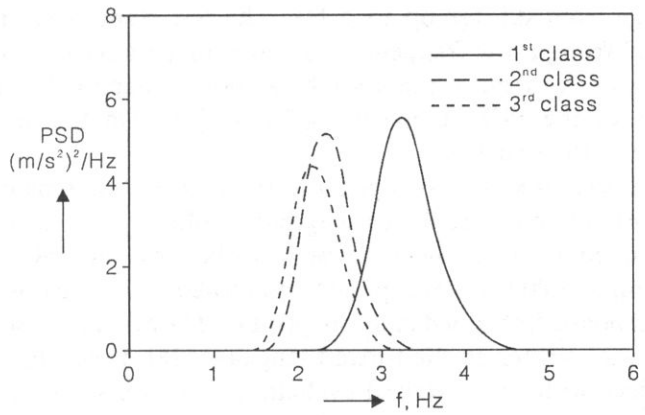

Fig. 2. Course of the vertical acceleration PSD curves for various agricultural tractor classes according to ISO 5007:1990 Standard.

The evaluation procedure is similar to that for earth moving machines as described by the ISO 7096:1982 Standard [22] (see e.g. [18, 20]). The resultant value of the so called corrected value of frequency weighted RMS acceleration transmitted to the seated operator a_c is given. This value describes the overall vibration control properties when subjected to a random vibration. The only important difference to the ISO 7096:1982 Standard is that there are no limit values given, i.e. no direct relation to the standards pertinent to the vibration influence on man such as the ISO 2631/1:1985 Standard [23] or respective national hygienic regulations. The so called SEAT Value, introduced by GRIFFIN [8], could be readily calculated from the measured data. They describe the vibration attenuation by the seat as a relative measure. For good seats this value is below 100%, but experimental evidence exists that seats with no vibration attenuation at all (i.e. with SEAT value above 100%) are sometimes used.

A further development of the procedures of standardized laboratory testing of driver's seats in the European Standard EN 30326–1:1994 [24] which is in fact the ISO 10326–1:1992 Standard. This Standard could be viewed as a "2nd generation Master Standard" describing the general requirements on seat testing in laboratory, whereas the specific conditions of application of this Standard for testing of seats for specific use (e.g. for use in earth moving machines or agricultural tractors, for passangers and crew of road vehicles, railway vehicles etc.) are dealt with in detail in the so called "Application Standards".

5. Experimental results

The model of the active vibration control system for the driver's seat for agricultural tractors was mounted on a beam of 2 m length, pivoted on one end and excited in the vertical direction by a servo-hydraulic cylinder on the other one. This laboratory test stand was able to exert an vibration amplitude up to 50 mm over a frequency range from 0.1 Hz up to 5 Hz. The test stand was driven either by a harmonic signal from a low frequency generator or by a narrow band stationary ergodic signal, generated from white noise by analogue shaping filters so as to fulfil the requirements of the ISO Standard 5007:1990 [21]. On the vertical vibration acceleration PSD at the seat base.

The test stand was fitted with two piezoelectric acceleration sensors, independent of the control sensors to measure the base a_B and cushion a_S vertical acceleration, the second one mounted in a special disk as described by the ISO Standard. The respective electrical variables were amplified, monitored on an oscilloscope and fed to a data acquisition board embedded in a 386 type PC. The evaluation was furnished by appropriate software written in the fortran language [18]. It was based on previous extensive experience with computerized evaluation of driver's seat vibration control properties.

The courses of the value V measured, according to the clause a, for both the passive and active systems, for a load of dead weight of 80 kg are shown in Fig. 3. The

solid lines represent a seat with artificial damping only for two different values ("low damping" #1 and "high damping" #2; the dashed ones represent a seat with both artificial damping and compensation engaged fo both the "low damping" #3 and "high damping" #4 as above. Note the difference between these two curves above 1.3 Hz where the most vertical vibration energy of agricultural tractors is concentrated. The pertinent values for the seat with the "sky-hook" artificial damper are as follows:

— "low damping": $V_{max}=2.60$, $f_{max}=1.10$ Hz;

— "high damping": $V_{max}=1.36$, $f_{max}=0.90$ Hz.

— no such values could be given for the combination of both vibration control systems.

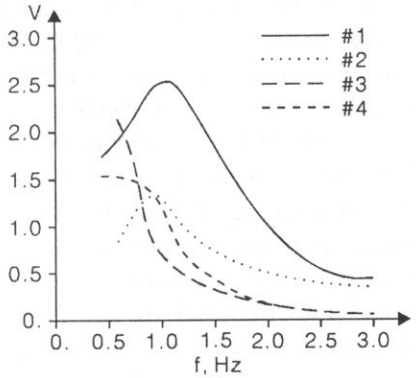

Fig. 3. Modulus of the active vibration control system response to harmonic excitation according to the clause a (description see text).

Table 2. Values of a_c measured according to the clause *b* of the ISO 5007:1990 Standard for simulated operator mass of $M=75$ kg and for the two cases of seat damping

tract. class	System: / damping:	sky hook high	sky hook low	comp.+hook high	comp.+hook low	Improvement high	Improvement low
1st	a_c, m·s^{-2}	1.23	1.46	0.55	0.64	2.3×	2.3x
	a_c, dB	122	123	115	116	7 dB	7 dB
	SEAT, %	60	71	27	31	2×	2×
	P, kW	1.45	0.44	1.45	0.84		
2nd	a_c, m·s^{-2}	1.52	1.86	0.49	0.71	3.0×	2.6x
	a_c, dB	124	125	114	117	10 dB	8 dB
	SEAT, %	77	124	33	48	2×	2.5×
	P, kW	1.47	0.93	1.47	1.14		
3rd	a_c, m·s^{-2}	1.10	1.94	0.50	0.95	2.1×	2.0×
	a_c, dB	121	126	114	120	7 dB	6 dB
	SEAT, %	84	149	39	73	2×	2×
	P, kW	1.66	1.04	1.61	0.20		

The results for random excitation, according to the clause b, for the tractor classes mentioned are given in Table 2. Note the difference in the absolute values of a_c for the two damping set. In fact, the system with "low damping" would not be suitable for practical use, since the a_c values are rather high and the SEAT value exceeds 100%, i.e. the seat would rather amplify the vibrations than to abate them. This is due to the fact that the seat resonant frequency f_{max} is close to the excitation centre frequency f_p of Table 1 and the V factor is larger than for the seat with "high damping". This is specifically valid for the 2nd and 3rd tractor classes.

An important question for all active systems is their complexity and energy consumption in comparison to common passive systems. As described by BALLO in [3, 4], the energy consumption of an active pneumatic suspension is mainly due to the need of maintaining a necessary pressure drop between the source of compressed air and the free atmosphere so as to ensure a supercritical fluid flow in the proportional flow control valve. This consideration led to using a compressed air source with absolute pressure $p_1 = 0.9$ MPa. Because no suitable flowmeter was available, an indirect method was used. The average power consumption of the compressor P kW in a certain time period was measured without taking into account the efficiency and pneumatic losses. The values measured are also given in the Table 2. Note that there is virtually no difference between the power requirement for the active system with the "sky-hook" and that for a system with "sky-hook" and compensation for the "high damping" setting, but marked improvement in the vibration control is attained. Somewhat more power is needed in the case of "low damping" setting for a similar increase in the improvement of vibration control.

6. Conclusion

The experimental resulted presents indicate the technical feasibility of the usage of an electro-pneumatic active vibration control systrem for the suspension system of a driver's seat for agricultural tractors. Despite its complexity, it performs quite well on the test stand. The improvement in the vibraton control properties by introducing the vibration compensation facility of the sky-hook damper is of the order of approx. 7 dB, i.e. twofold. In other words, by introducing the combined active vibration control, the vibrations are diminished in average to approx. 50% of the transmitted by the system with the sky-hook only. On the other hand, the better vibration control properties of the seat with both the vibration compensation and sky-hook are payed for by higher energy demand and increased complexity of the system. Note that the system employing the sky-hook with "low damping" is rather bad and would not be suited for practical use.

The author is indepted to his former supervisor — Prof. Igor Ballo, DSc. for many fruitful discussions and continuous support. The author wishes to thank Dr Marian Gajarsky, former research worker of this Institute, who made many contributions to the mechanical design of the dummy system. The author wishes to thank the Grant Agency for Science of Slovakia for supporting this research by the Grant No. 2/148/95.

References

[1] I. BALLO, *Parallel active vibration control system*, Noise Control Conference, Cracow, Poland, Sept. 1988, Proceedings Vol. 1, pp. 31–39.

[2] I. BALLO, G.J. STEIN, and M. GAJARSKY, *Electropneumatic active vibration control system for driver's seat of earth moving vehicles*, Noise Control Conference, Cracow, Poland, Sept. 1992, Proc. pp. 15–18.

[3] I. BALLO, *Active vibration control systems for dirver's seats of earth-moving vehicles*, Archives of Acoustics, **18**, 2, 183–195 (1993).

[4] I. BALLO, *Reduction of power requirements of active vibro-isolating system*, „Szkoła Metody Aktywne Redukcji Drgań i Hałasu", Cracow, Poland, May 1995, Proc. pp. 5–9.

[5] Z. ENGEL, *Nowe metody zwalczania hałasu i wibracji* (in Polish), Prace CIOP, Z. 144, 1990.

[6] Z. ENGEL and J. KOWAL, *Wibroizolacja aktywna siedziska kierowcy — operatora maszyn* (in Polish), Prace CIOP, Z. 144, 1990.

[7] M. GAJARSKÝ, *Niektore vlastnosti elektropenumatického vibroizolacného systemy* (in Slovak), Strojnícky Časopis, 35, no. 1–2, pp. 51–65, 1984.

[8] M.J. GRIFFIN, *Handbook of human vibration*, Academic Press, London 1994, p. 404.

[9] D.C. KARNOPP, *Active damping in road vehicle suspension systems*, Vehicle System Dynamics, **12**, 291–316 (1983).

[10] P. KISIELEWSKI, *Analiza i synteza układów wibroizolacji siedzisk maszynistów-operatorów lokomotyw*, (in Polish), Ph.D. dissertation AGH, Cracow 1991.

[11] J. KOWAL, *Aktywne i semiaktywne metody wibroizolacji układów mechanicznych*, (in Polish), Zesz. Nauk. AGH, Mech., 23, AGH, Cracow 1990.

[12] S. MICHAŁOWSKI, *Aktywne układy w konstrukcji maszyn roboczych* (in Polish), Monografia Z. 171 — Mechanika, Politechnika Krakowska, Cracow 1994.

[13] J. NIZOL, A. CHODACKI and S. MICHAŁOWSKI, *Aktywne hydrauliczne układu wibroizolacji*, (In Polish), Prace CIOP, Z. 144, Warsaw 1990.

[14] D. MARGOLIS, *The response of active and semi-active suspensions to realistic feedback signals*, Vehicle System Dynamics, **12**, pp. 317–330 (1983).

[15] S. RAKHEJA, Y. AFEWORK and S. SANKAR, *An analytical and experimental investigation of the driver-seat-suspension system*, Vehicle System Dynamics, **23**, 7, pp. 501–524 (1994).

[16] G.J. STEIN, *Results of investigation of an electro-pneumatic vibration isolating system*, Proceedings of the Institution of Mech. Engrs., 209, 3, Part D — Automobile Eng., pp. 227–234.

[17] G.J. STEIN and I. BALLO, *Aktiver pneumatischer Schwingungsschutzsystem fur Fahrersitze*, Congres DAGA'94, Dresden, March 1994, Preprints pp. 541–544.

[18] G.J. STEIN, R. CHMURNY, V. JINDRA, *Computerized evaluation of vibration control properties of driver's seats*, Preprint of the XIII IMEKO Congress, Torino, Italy, Sept. 1994, pp. 2184–2187.

[19] G.J. STEIN, I. BALLO nd M. GAJARSKÝ, *Active vibration control system for the driver's seat*, Proceedings of the 25th ISATA Silver Jubilee Conference, Section Mechatronics, Florence, Italy, June 1992, Proceedings pp. 183–190.

[20] G.J. STEIN and B. RUJBROVA, *Automated evaluation of vibro-isolating properties of operator's seats*, Noise Control Conference, Cracow, Poland, Sept. 1995, Proceedings po. 779–784.

[21] ISO Standard 5007:90 Agricultural wheeled tractors — Operator's seat — Laboratory measurement of transmitted vibration.

[22] ISO Standard 7096:82 Earth moving machinery — Operator seat — Transmitted vibration. (Also as STN ISO 7096 (27 7523) or DIN ISO 7096)

[23] ISO Standard 2631/1:85 Evaluation of human exposure to whole-body vibration. Part 1: General requirements.

[24] EN 30326–1:94, Mechanical vibration — Laboratory method for evaluating vehicle seat vibration — Part 1: Basic requirements (ISO 10326–1:92).

ARCHIVES OF ACOUSTICS
21, 3, (1996)

ERRATUM

TEMPERATURE INCREASE IN A TWO-LAYER OBSTETRICAL MODEL OF TISSUES IN THE CASE OF LINEAR AND NONLINEAR PROPAGATION OF A CONTINUOUS ULTRASONIC WAVE

L. Filipczyński and J. Wójcik

Archives of Acoustics, **20**, 3, 237–246, (1995)

In the Abstract on the page 127, the line 15 should be:
"the shock parameter does not then exceed the value of 1. Then the maximum temperature increase equals 1.66°C. For a radiated intensity equal to 1 W/cm²"

The first part of eqs. (3.16), (3.18), (3.21) should have the form

$$( )^{-1} \int_{-\infty}^{\infty}$$

The first left letter ζ in the terms of eqs. (3.15), (3.17), (3.18), (3.19), (3.20) should be ξ.

The letter I in eqn. (3.9) should be printed as a vector while in eqn. (3.12d) as a scalar.

The left side of eqn. (3.10) should be

$$\int \mathbf{I}' \cdot \mathrm{ds} = 0 \quad \text{where } \mathrm{ds} = |\,\mathrm{ds}\,|$$

At the vertical axis of Fig. 3 there should be printed the shock parameter σ.